CHEMICAL STRUCTURE OF A SPORINITE FROM A LIGNITE: COMPARISON WITH A SYNTHETIC SPORINITE TRANSFORMED FROM SPOROPOLLENIN

R. Hayatsu, R. E. Botto, R. L. McBeth, R. G. Scott, and R. E. Winans

Chemistry Division, Argonne National Laboratory,
9700 South Cass Avenue, Argonne, IL 60439 USA

INTRODUCTION

The maceral sporinite is thought to be derived from spores and pollen. Both sporinite and sporopollenin, the insoluble cell wall residue after chemical treatment, are considered to have a highly polymerized, cross-linked aliphatic structure with some aromatics (1-3). Many investigators have endeavored to characterize the physical and chemical nature of sporinites (4-7) and sporopollenin (8-11); however, their chemical structures have not been well defined. Furthermore, little is known about how sporopollenin transforms to sporinites during the early stage of coalification.

The aim of the present study is to compare chemical structures of an immature sporinite and its precursor, sporopollenin. In a parallel experiment, the transformation of sporopollenin into a synthetic sporinite has been carried out in the laboratory using thermal catalytic reactions under conditions of simulated catagenetic maturation.

EXPERIMENTAL

Samples

Sporinite. A sporinite material separated from a North Dakota lignite (82% sporinite by petrographic analysis) was treated with 5% HCl, and then refluxed with benzene-methanol (3:1) for 24 hrs. Total extractable material was about 10 wt% of the sample. Analysis of the extracted sporinite yields the following composition: $C_{100}H_{130}N_{0.5}O_{21}$.

Sporopollenin. Sporopollenin was isolated from *Lycopodium clavatum* spores which were refluxed with $CHCl_3$ (24 hr), and then with benzene-methanol 3:1, 24 hr). The yields of total extract and insoluble residue were 55.4 and 44.0 wt%, respectively. The organic solvent extracted residue was then hydrolyzed by refluxing with 6% KOH methanol-water (7:3) solution for 20 hrs. After removal of hydrolyzates, the residue (25 wt% from the original spore) was further treated with 72% H_2SO_4 at 0°-4°C for 12 hrs, and then was refluxed with 3% H_2SO_4 for 10 hrs, filtered, washed with water and methanol, and dried. The yield of sporopollenin, ($C_{100}H_{138}N_{0.6}O_{29}$) was 15.8 wt% from the original spore.

Synthetic Sporinite. Sporopollenin (0.5 g) and 4 g of freshly acid activated montmorillonite clay were ground together and were then placed in a 25 x 2 cm i.d. tube. After evacuation, the sealed tube was inserted to a depth of about 5 cm in a tubular furnace and was heated at 150°C for 2 months.

After the reaction, the mixture was extracted with refluxing benzene-methanol (3:1), chloroform, and finally with ether. To remove the clay, the solvent insoluble residue was treated three times with HCl-HF (1:1) by stirring at room temperature for 24 hours. The yield of synthetic sporinite was 81 wt% with a composition of $C_{100}H_{124}N_{0.1}O_{21}$.

Pyrolysis

A sample (~200 mg) was placed in a 20 x 1 cm i.d. quartz tube; after evacuation the sealed tube was inserted to a depth of about 5 cm in a preheated furnace at 600°C and was heated for 1 minute. The pyrolyzate was extracted with refluxing benzene-methanol (3:1); the yield was generally 38-55 wt%.

Oxidation

In general, a sample (0.3 g) was oxidized with a two-step, buffer-controlled permanganate oxidation (for procedure see ref. 12-13). Before the oxidation, in order to protect phenolic rings from destruction, the sample was methylated with dimethylsulfate -d_6. In general, the yields of oxidation products were about 58-79 wt% for all three samples.

Characterization and Identification Procedures

All mass spectra (GCMS, solid probe) were obtained on a KRATOS MS25/DS55 Data System. Solid probe data were obtained in a precise mass measurement mode. GC separations were made using a 60 m x 0.25 mm bonded OV-1701 fused silica column temperature programmed 50-280°C at 8°/min. Solids were evaporated and pyrolyzed in the source using a direct heating platinum filament probe designed in this laboratory.

Solid ^{13}C spectra were recorded at 2.3 T (25.18 MHz for ^{13}C) on a Bruker Instruments spectrometer, Model CXP-100, in the pulse Fourier transform mode with quadrature phase detection. The ceramic sample spinners had an internal volume of 300 µL and were spun at approximately 4 kHz. Operating parameters in cross-polarization experiments included a spectral width of 10 kHz, a 90° proton pulse width of 4.2 µs (60 kHz proton decoupling field), an acquisition time of 20 ms, a pulse repetition time of 1 s and a total accumulation of 1000 transients. In a typical experiment, 200 W of memory was allocated for data acquisition and was then increased to 4K (2K real data) by zero filling. Before Fourier transformation of the data, the interferogram was multiplied by a decreasing trapezoidal window function after the first 20 data points.

Infrared spectra were obtained by the KBr disk method using an IBM-098/4A FTIR spectrometer.

RESULTS AND DISCUSSION

FTIR and NMR

Solid ^{13}C-CP/MAS and FTIR studies indicate that sporopollenin, synthetic sporinite and sporinite are highly aliphatic. Both natural and synthetic sporinite samples showed very similar FTIR spectra: the absorption band near 1710 cm^{-1} is due to C=O stretching of carbonyl and carboxyl groups. The weak band at around 1615 cm^{-1} may be due to the presence of aromatic rings.

The ^{13}C-CP/MAS spectra of raw spores, isolated sporopollenin, synthetic sporinite and North Dakota sporinite are shown in Figure 1. The spectrum (a) of raw spores indicates the wide variety of carbon structural types which are present. The most prominent feature is the broad absorption found in the aliphatic region, ~15-50 ppm. Sharp resonances appearing at 75 ppm and 105 ppm are typical of polysaccharide structures. In addition, there are two other resonances of lower intensity found in the aliphatic C-O region, ~50-70 ppm. The low-field region consists of several unsaturated carbon resonances (110-150 ppm)

and a reasonably broad absorption centered at 175 ppm which is typical of aliphatic ester groups.

Solvent extraction of the raw spores followed by base (KOH) treatment produces an insoluble material whose solid ^{13}C spectrum (not shown) is devoid of resonances in the low-field region. Further characterization of the solubilized materials by solution ^{13}C-NMR and MS indicates that they are largely lipid structures comprised of unsaturated fatty acids. Subsequent treatment of the insoluble material with H_2SO_4 produces a solid residue which we term sporopollenin. Its ^{13}C spectrum (b) shows the additional diminution in the sharp resonances at 75 and 105 ppm, previously assigned to carbohydrate carbons. What apparently remains is a highly aliphatic polymer containing a relatively high proportion of aliphatic C-O functionalities (presumably aliphatic ether or aliphatic hydroxyl groups), and a small amount of unsaturation. These unsaturated structures are presumed to be olefins which had been formed via dehydration of -OH groups during H_2SO_4 treatment.

Sporopollenin can be readily transformed in the presence of clays at 150°C into an insoluble material whose solid ^{13}C spectrum (c) closely resembles the spectrum (d) obtained for a natural (North Dakota lignite) sporinite sample. There has been a significant reduction in the number of aliphatic C-O groups with the concomitant appearance of new resonances in the unsaturated carbon region (110-155 ppm). At present, we are not certain whether these new resonances are aromatic or olefinic in nature. The fraction of unsaturated carbon (f_u) determined for spectrum (c) and (d) is also comparable: f_u=0.21 for natural sporinite and f_u=0.23 for synthetic sporinite.

Oxidation

As shown in Figure 2, a two-step, buffer-controlled, $KMnO_4$ oxidation of both natural and synthetic sporinites gave qualitatively and quantitatively similar products. Major products were unbranched dicarboxylic acids, while branched dicarboxylic acids and tricarboxylic acids were also identified, but in much lower concentrations. Aliphatic monocarboxylic acids were not detected, contrary to previous reports on several other sporinites (4) and kerogens (14-15). This would seem to imply that our sporinite samples do not have peripheral long-chain alkyl groups. However, sporopollenin yielded only minor amounts of two monocarboxylic acids, C_{16} and C_{18}. The aromatic acids, benzene- and phenol-carboxylic acids were present in low amounts in all three samples.

It is interesting to note that after methylation with dimethylsulphate-$\underline{d}_6$, the oxidation of all three samples produced a mixture of methoxy-$\underline{d}_3$ and regular methoxy benzenecarboxylic acids. This indicates that sporopollenin and sporinite samples contain both hydroxy and methoxy benzene derivatives as structural units. The GCMS analyses of the oxidation products from all samples showed methoxy-$\underline{d}_3$ derivatives are always predominant: OCD_3/OCH_3 ratios for sporinite ~9.4, synthetic sporinite ~8.6 and sporopollenin ~2.9.

While the yields of unbranched dicarboxylic acids for sporinite and synthetic sporinite were much higher than those of branched dicarboxylic acids (see Figure 2), sporopollenin produced relatively large amounts of branched dicarboxylic acids together with some keto-dicarboxylic acids. Most of these branched acids were mono- or di-methyl derivatives, but isoprenoid acids were not detected in any of the samples.

The oxidation of synthetic sporinite produced higher yields of aromatic acids, in particular benzenepolycarboxylic acids (tri-, tetra-, and penta-),

compared with that of sporopollenin. It is obvious that the thermal catalytic reaction promoted alteration of the sporopollenin structure by dehydration, condensation, aromatization, etc. The ratio of aliphatics/aromatics in the oxidation products became close to that of natural sporinite. These trends are typically observed for the transformation of plant biopolymers to geopolymers, such as coals and coal macerals.

Pyrolysis

As expected, the major products obtained from the pyrolysis of both natural and synthetic sporinites (see Figure 3) were long chain alkanes and alkenes. Benzenes, naphthalenes, indanes/tetralins and phenols were minor components. On the other hand, pyrolyzates from sporopollenin were quite different. The most abundant products obtained were naphthalenes, while other aromatics were also found in significant amounts. However, the oxidation, NMR and FTIR studies clearly showed that the sporopollenin has a highly aliphatic structure.

Achari et al. (8) have reported that the pyrolyses of several sporopollenins show the presence of typical carotenoid degradation compounds, including ionene and various naphthalenes in the products. In contrast with the observation by Achari et al., (8) Schenck and co-workers (10) have found benzene and phenol derivatives from the pyrolysis of Lycopodium sporopollenin. However, there was very little evidence for the presence of naphthalenes.

Although we have consistently failed to detect ionene, which is the most important degradation product from β-carotene, significant amounts of various napthalenes have been identified. We do not know, at present, why our results differ from those obtained in two other laboratories. Perhaps, one reason for this discrepancy is that our sporopollenin sample was obtained using a milder isolation procedure ($KOH-H_2SO_4$) than the procedure ($KOH-H_3PO_4$) employed by others (2,10). In any case, sporopollenin, which is a highly aliphatic polymer, produces considerably more aromatics than aliphatics under pyrolysis. It is known that the pyrolysis of polyenes, including non-conjugated polyenes, produces aromatic and cyclic hydrocarbons (8,16-17). Hence, the aliphatic substructures of sporopollenin may well have a substantial number of olefinic double bonds and/or alcoholic OH groups. During pyrolysis, such alcoholic OH groups could easily dehydrate to form polyenes which rapidly aromatize prior to their thermal fragmentation.

SUMMARY

Thermal reactions of sporopollenin with clay minerals produced a geopolymer-like material which closely resembles an immature sporinite in composition, pyrolysis and oxidation products, and spectroscopic properties. Both natural and synthetic (transformed sporopollenin) sporinites have highly polymerized, cross-linked aliphatic structures containing some benzene and phenol ring systems. Several organic oxygen groups also have been identified in these polymeric materials; they are alcoholic and phenolic OH, methoxyl, carbonyl/carboxyl and ether. Among these, alcoholic OH groups appears to be predominant.

Sporopollenin is presumably transformed into immature sporinite by chemical reactions such as dehydration, hydrogen disproportionation, aromatization, etc. Indeed, it is known that these reactions occur during natural evolution (18). For example, conversion of alcohols to olefins and to alkanes, or of cycloalkenes to cycloalkanes and to aromatic hydrocarbons, is known. Polymerization or condensation of olefins involves the formation of aromatic rings. Many of these reactions are promoted by acidic catalysts such as natural clay minerals.

The present study gives some insight into the chemical structures of an immature sporinite and its precursor, sporopollenin, and the chemical transformations leading to sporinite during the early stage of coalification.

ACKNOWLEDGEMENT

The authors thank Harold Schobert and Edward N. Steadman of the University of North Dakota Energy Research Center for their generous gift of the North Dakota sporinite sample. The elemental analysis was provided by P. C. Lindahl and I. Koi of the Argonne Analytical Chemistry Laboratory.

This work was performed under the auspices of the Office of Basic Energy Sciences, Division of Chemical Sciences, U. S. Department of Energy, under contract number W-31-109-ENG-38.

REFERENCES

1. Stach, E., Mackowsky, M.-TH., Teichmüller, M., Taylor, G.H., Chandra, D. and Teichmüller, R., "Coal Petrology", p. 247, Gebrüder Borntraeger, 1982.
2. Brooks, J. and Shaw, G., Chem. Geol. 10, 69, 1972.
3. Given, P.H., "Coal Science" (M. Gorbaty et al., eds.) Vol. 3, p. 63, Academic Press, 1984.
4. Allan, J. and Larter, S.R., Adv. Org. Geochem. 1981, p. 534, John-Wiley, 1983; preprint ACS Div. Fuel Chem. 26, No. 1, 26, 1981.
5. Winans, R.E., Hayatsu, R., Scott, R.G., and McBeth, R.L., ACS Symp. Series 252, p. 137, 1984.
6. Wilson, M.A., Pugmire, R.J., Karas, J., Alemany, L.B., Woolfender, W.R., Grant, D.M., and Given, P.H., Anal. Chem., 56, 933, 1984.
7. Meuzelaar, H.L.C., Happer, A.M., Pugmire, R.J., and Karas, J., J. Coal Geol. 4, 143, 1984.
8. Achari, R.G., Shaw, G., and Holleyhead, R., Chem. Geol. 12, 229, 1973.
9. Brooks, J. and Shaw, G., Trans. Bose Res. Inst. 40, 19, 1977.
10. Schenck, P.A., de Leeuw, J.W., van Graas, G., Haverkamp, J., and Bouman, M., "Organic Maturation Studies and Fossil Fuel Exploration (J. Brooks, ed.), p. 225, Academic Press, 1981.
11. Given, P.H., Rhoads, C., Painter, P.C., Spackman, W., and Ryan, N.J., Proc. Int. Conf. Coal Sci. 1983, p. 389, 1983.
12. Hayatsu, R., Scott, R.G., and Winans, R.E., "Oxidation in Organic Chemistry" Part D (W. Trahanovsky, ed.) p. 279, Academic Press, 1982.
13. Hayatsu, R., Winans, R.E., Scott, R.G., and McBeth, R.L., Fuel 60, 158, 1981.
14. Simoneit, B.R. and Burlingame, A.L., Geochim. Cosmochim. Acta 37, 595, 1973.
15. Djuricic, M.V. and Vitorovic, D., Adv. Org. Geochem. 1971, p. 305, Pergamon Press, 1972.
16. Edmunds, F.S. and Johnstone, R.A.W., J. Chem. Soc. 2892, 1965.
17. Johnstone, R.A.W. and Ouan, P.M., J. Chem. Soc. 2221, 1963.
18. Hunt, J.M., "Petroleum Geochemistry and Geology" p. 112, Freeman Co., 1979.

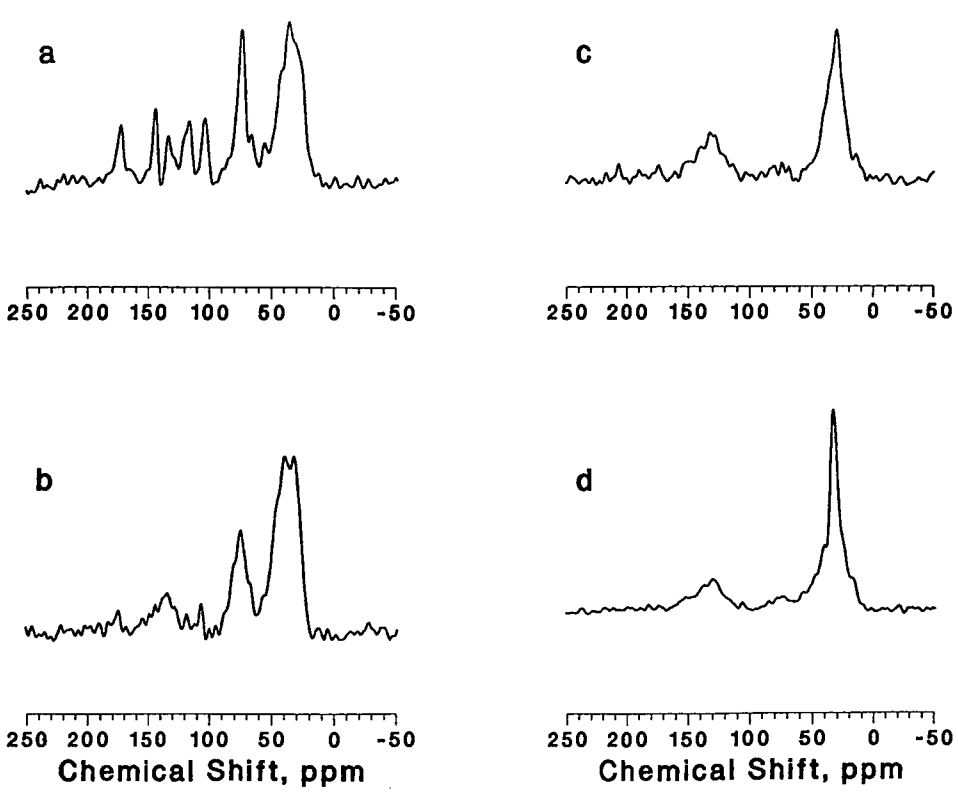

Figure 1. Solid ^{13}C-NMR spectra of (a) raw spores, (b) sporopollenin, (c) synthetic sporinite and (d) North Dakota sporinite.

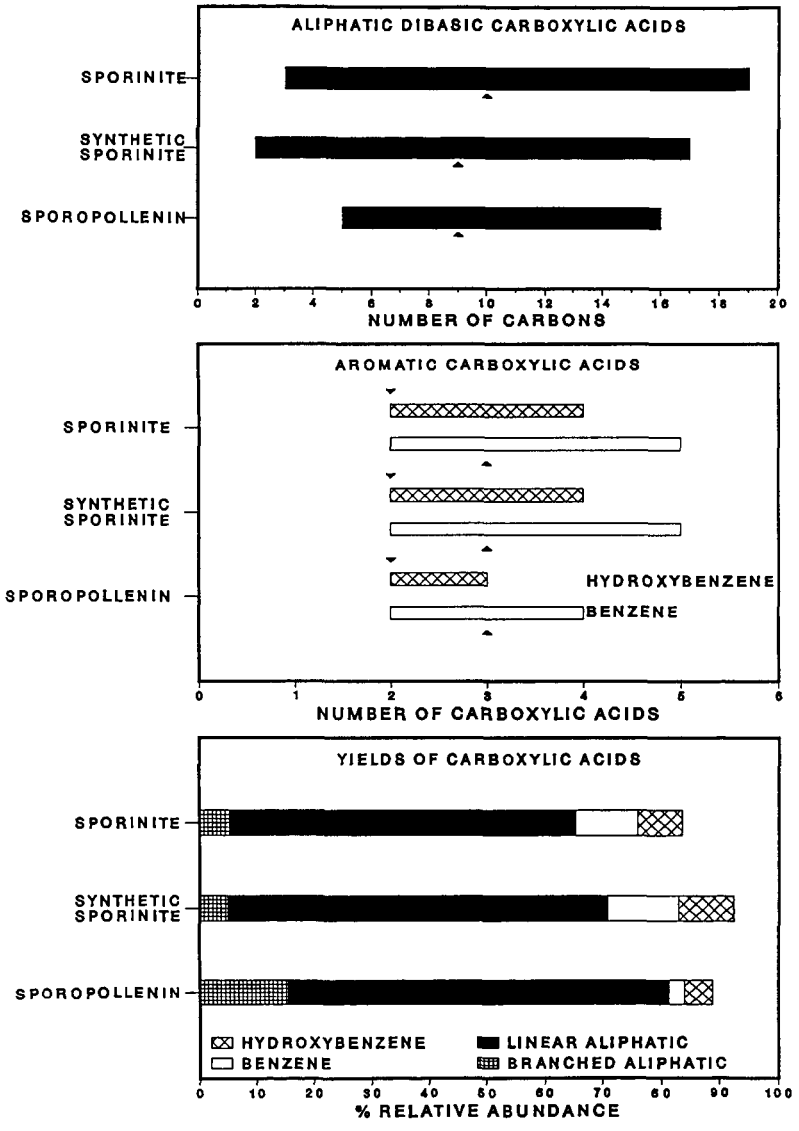

Figure 2. Relative abundances of $KMnO_4$ oxidation products: symbol (▲) indicates most abundant product.

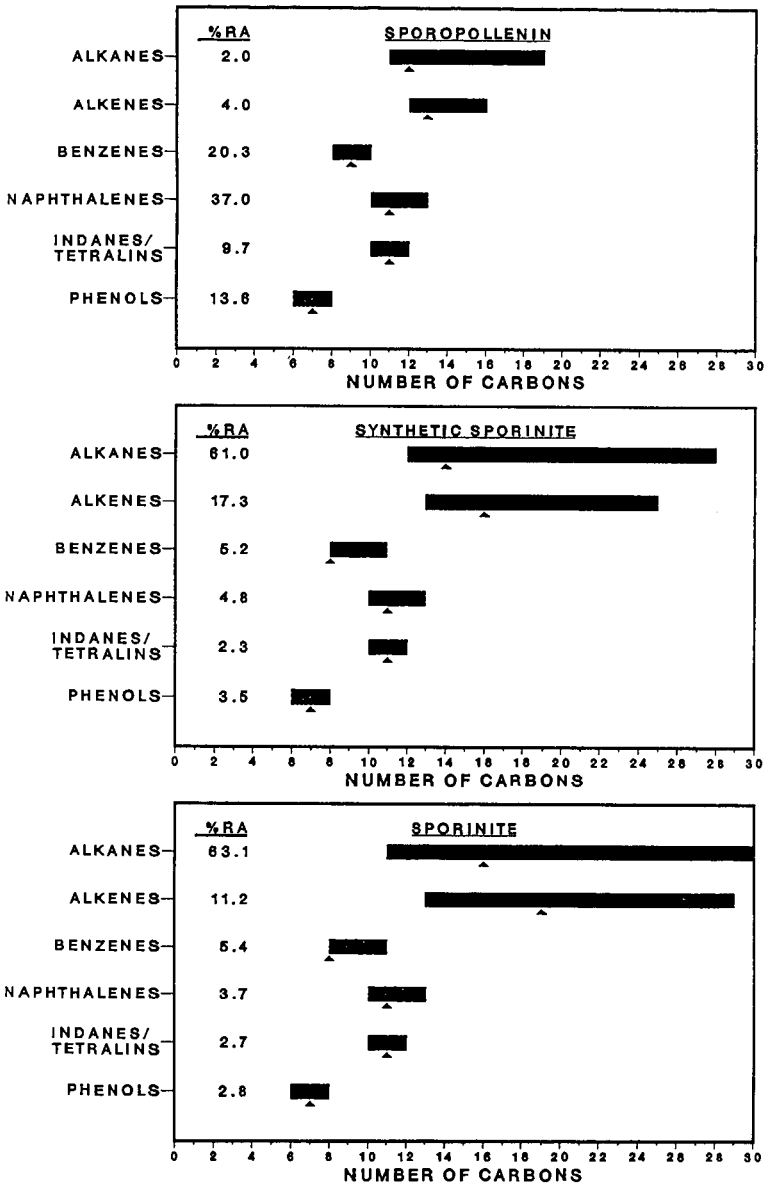

Figure 3. Relative abundances of pyrolyzates: symbol (▲) indicates most abundant product.

THE EFFECT OF SOLVENT EXTRACTION ON THE REFLECTANCE OF COAL AND COAL-OIL MIXTURES

By

B. Kybett, J. Potter, M. Etter and M. Krahe

Energy Research Unit, University of Regina, Regina, Saskatchewan S4S OA2 Canada

INTRODUCTION

The commercial classification of coal is often based upon its rank. Technological properties, such as the potential for liquefaction, also vary with the rank of the coal since this is a measure of the average chemical composition. Coal rank can be determined from the reflectance of the coal using a microscopic method.

In many coal liquefaction processes the coal is co-processed with heavy oil or pitch. The solid residues from the process can contain unreacted coal, partially reacted coal intermediate products and semicoke. The semicoke could have been formed from the coal, the oil or pitch or from the liquid products of the process. A detailed petrographic analysis of these solid products can provide useful information about their nature and source.

Petrographic analysis is done by mounting crushed coal or residues in epoxy resin, polishing the surface and examining it microscopically using reflected light and oil immersion objectives. Any oil or pitch present in the sample will dissolve in the oil used to coat the objective lens and both obscure the image and more importantly, prevent accurate measurement of the reflectance of the sample. The oil is usually removed by Soxhlet extraction; pentane, tetrahydrofuran (THF) and toluene are the most common solvents.

One way to determine whether coal found in the solid residues is unreacted, or partially reacted is by measuring its reflectance and comparing this with the reflectance of the coal feedstock components from which they are derived. Changes in reflectance are related to changes in the composition (rank) of the coal. A major problem (1) with this approach is that changes in reflectance may have occurred while the coal was stored as a slurry with the oil and/or during the solvent extraction.

The solvent extraction process does not appear to affect the reflectance of bituminous coals. Some previous observations seem to indicate that the reflectance of the coal was affected by the oil or by the solvent extraction, but this was not conclusive. A series of experiments was done to directly determine the effect of soaking in oil and subsequent solvent extraction on the reflectance of low rank coals (4).

RESULTS AND DISCUSSION

Two lignites from southern Saskatchewan were used, from the Boundary Dam Mine (BDM-8) and the Coronach Mine (CM-8). They were of rank lignite B, and were chosen as they contained relatively large amounts of inertinite and exinite (Table 1) so that measurements of reflectance on all three major maceral groups could be made. The coals were ground to less than 20 mesh and separated, by riffling, into seven samples. Three samples were mixed with heavy oil (Lloydminster) and stored for 24 days at room temperature and 30°C for 7 days. They were extracted with a solvent (Soxhlet method) until the filtrate, after the coal had stood overnight, with stirring, in solvent, was colourless. Three solvents were used, pentane (168 hours extraction time), toluene (76 hours) and tetrahydrofuran (52 hours). Three coal samples that had not been treated with oil were solvent extracted with the same solvents for the same time. One coal sample was left untreated.

The loss in mass of the coals during the extraction process was determined for each sample. It was about 20%, which is high (3), but since some of this loss was due to handling there is no quantitative significance to the differences in the loss of mass.

TABLE 1

PETROGRAPHIC ANALYSES (%)

	BDM-8	CM-8
Huminite	72	56
Exinite	9	4
Inertinite	25	21
Mineral matter	10	3

Reflectances

The coals were set in epoxy resin and polished. Reflectances, at 546 nm, were measured against optical glass standards using a Leitz Orthoplan-pol, MPV compact microscope/photometer system. A total of 100 random measurements were made for each type of huminite and 75 for the other, rarer, macerals. The mean random reflectance, rather than the maximum reflectance, is usually determined for low rank coals because huminites and liptinites are isotropic.

The reflectance of huminite is usually measured since it is the most common, and the most uniform, maceral. The results for dark huminite (eu-ulminite A) in the CM-8 coal are given in Table 2. The reflectances are quoted to 3 figures, but are statistically valid to two figures only. The reflectance of CM-8 has not been affected by either extraction with a solvent or by soaking in oil followed by extraction.

TABLE 2

MEAN RANDOM REFLECTANCES, DARK HUMINITE

	BDM-8	CM-8
Feedstock	0.253	0.246
Pentane	0.262	0.252
Oil/pentane	0.274	0.254
Toluene	0.292	0.263
Oil/toluene	0.286	0.265
THF	0.289	0.246
Oil/THF	0.285	0.247

There does seem to be a pattern of increasing reflectance with severity of extraction (temperature of extract on and solvating power of solvent) with the BDM-8 coal, but the variations are within the average standard deviation of 0.03. There is some evidence from the reflectance data that the dark huminite in BDM-8 feedstock consisted of two subgroups, with mean random reflectances of 0.18 and 0.27. The amount of the lower reflectance subgroup decreased after solvent extraction, but again these differences, while consistent, are well within the statistical error.

Measurements were also made on light huminite, exinite and inertinite. Solvent extraction or soaking in oil had no discernable effect on the mean random reflectance of any of these macerals. There is a general relationship between reflectance and aromaticity (5). Solvent extraction with pentane, toluene or THF, while it removed some coal material (up to 20%) from the low rank coals had no effect on the overall degree of aromaticity of the coal.

CONCLUSIONS

The solid coal residues from coal liquefaction processes often show a change in reflectance. This change is, with low rank coals, not due to soaking in oil or sub-

sequent solvent extraction to remove the oil. It is a measure of the chemical changes in these coal particles during the liquefaction process and can be used as a measure of the severity of the reaction that these particles have undergone.

LITERATURE CITED

(1) International Committee for Coal Petrology, Full Minutes of Commission 111 Meeting, Dubrovnik, Sept., 1985.
(2) Energy Research Unit, University of Regina, "Characterisation of solid residues from coal liquefaction processes", Chapter 9, CANMET Report OST 84-00019, June 1985.
(3) Given, P.H., "Organic geochemistry of coal" in Coal Science, Volume 3, ed. M.L. Gorbaty, J.W. Larsen and I. Wender, Academic Press, New York, 1984.
(4) Etter, M., "The effect of solvent extraction on the reflectance of lignite", Honours Thesis, University of Regina, March, 1986.
(5) van Krevelen, D.W., "Coal", Elsevier, New York, 1981.

^{1}H NMR EVIDENCE TO SUPPORT THE HOST/GUEST MODEL OF BROWN COALS

Richard Sakurovs, Leo J. Lynch and David S. Webster

CSIRO Division of Fossil Fuels, P.O. Box 136, North Ryde, N.S.W. 2113, Australia

ABSTRACT

Many groups have proposed a two-component molecular structure for brown coals. This hypothesis has been investigated by in situ ^{1}H NMR measurements during heating (to 875 K) of a suite of Australian and New Zealand brown coals, a set of Morwell brown coal lithotypes, and extracts and extract residues of some of these coals. The variation in the behaviour of the coals during heating and pyrolysis, although significant, was not particularly sensitive to lithotype ranking but showed a strong correlation with atomic H/C ratio. The extracts were found to be fully mobilized in the temperature range 470-700 K whereas the residues essentially remained rigid molecular lattices throughout the heating and pyrolysis. This behaviour was independent of the lithotype and H/C ratio of the source coal. The much higher H/C ratios of the extracts compared to the residue materials allow these observations to be explained (to a first approximation) in terms of the host/guest hypothesis whereby the coals are composed of extract (guest) and residue (host) materials in differing proportions.

INTRODUCTION

Morphological variation in brown coal seams has led to 'lithotype' classification schemes. The classification for Victorian brown coals is based on the colour of the dried, weathered coal and ranges from 'pale' to 'dark' in five steps. A number of studies (1-4) have sought to establish relationships between lithotype and the composition, structure and properties of the coals. Although these studies have established that major chemical (2) and physical (3) differences do exist between the extreme pale and dark lithotypes within a given seam, it has not been demonstrated that basic coal properties are significantly ranked by the lithotype classification.

Palaeobotanical analysis of a lithotype suite (5) has led to the suggestion that the principal factor in producing lithotype variation was the prevailing depth of the water table during deposition and has shown that the content of woody material and the extent of gelification decreases along the sequence from dark to pale lithotype. Maceral analysis of this lithotype suite (from the LY1276 core, Latrobe Valley, Victoria) showed that the principal differences in the maceral composition were in the distribution of huminite, which was much greater in the three lighter lithotypes, and in the liptinite content, which was significant only for the lighter lithotypes (5).

NMR and infrared spectroscopic analysis of the same lithotype suite and a set of light lithotypes giving a depth profile of the same core revealed that the main chemical variations between lithotypes were higher aromatic and lower carbonyl/carboxyl contents in the darker lithotypes, but correlation of these criteria with lithotype ranking was poor (6). By contrast, other studies (7,8) have shown that dark lithotypes have greater polar functionality, including carbonyl/carboxyl content, than the corresponding pale lithotypes. Moreover, Hatswell et al. (4), who studied the liquefaction properties of a range of lithotypes (also from the LY1276 core) with similar elemental compositions (to remove any effect of H/C), found no variation with lithotype. It would therefore appear that correlations between lithotype classification and maceral analysis or chemical properties are poor.

Several groups (1-3, 9) have considered brown coal structure at the molecular level and have suggested that brown coals have a two-component molecular structure. Hatcher's proposal (1), based mainly on ^{13}C cross-polarization magic angle spinning

NMR and infrared studies of peats and a range of other materials at different stages of coalification, is that coals are derived from a mixture of highly aliphatic sapropelic material of aquatic origin on the one hand and vascular plant-derived lignin residues on the other.

Lynch and Webster (3), in a preliminary study of the pyrolysis behaviour of brown coal lithotypes, found a correlation between the thermal behaviour and H/C ratio of the coals and also noted a close identity between the proportion of the hydrogen mobilized during heating and that lost by volatilization below 800 K. It was argued that these observations were consistent with Hatcher's two-component structural model.

Redlich et al. (9) separated a suite of brown coals with a wide range of H/C values into two fractions by heating the dried coal under nitrogen in the presence of decalin at 593 K for 1 h and, after cooling, extraction with dichloromethane. These apolar, non-hydrogenating conditions were thought to be sufficiently mild to avoid major decomposition of the coal and, essentially, to result in the extraction of physically bound aliphatic materials, although even at temperatures as low as 600 K some decarboxylation did occur. The decalin used in the dichloromethane extraction process could not be easily separated from the total extract, therefore the pentane-insoluble or 'asphaltene' part of the extract was studied. This treatment excluded the decalin together with the less polar species from the extract. The pentane insolubles accounted for 1/3 of the total extract. In all cases, the properties of the extracts and residues were found to be mostly independent of the source coal. The residue fraction, or 'host', was described as a phenolic, macromolecular material, probably lignin-derived, while the 'guest' (the dichloromethane-soluble fraction) was always predominantly aliphatic (f_a ~0.3) (9). This lack of variation led to the conclusion that the differences in brown coal properties depend to a first approximation on the ratio of these fractions present in the coal.

Verheyen et al. (6), as part of their study, separated lithotype specimens into alkali soluble 'humic acids' and insoluble 'kerogen'. The 'humic acids' accounted for ~20% of the dark to ~50% of the pale lithotypes, the actual quantities depending on the severity of the treatment. However, in contrast to the fractions separated by the method of Redlich et al. (9), which yielded similar proportions of extract and residue, the properties of both the 'humic acid' and 'kerogen' fractions varied with lithotype and the H/C of the source coals.

The preliminary study by Lynch and Webster (3) using the proton nuclear magnetic resonance (^{1}H NMR) thermal analysis (PMRTA) technique (10), which supported the host/guest model, is extended here to a wider selection of brown coals (Table 1) including some New Zealand coals and the lithotype set from the LY1276 core studied by Hatswell et al. (4). The residues and pentane-insoluble extracts of some of the coals prepared by the method of Redlich et al. (9) were also examined.

EXPERIMENTAL

Whole coal samples were predried at 378 K under nitrogen. Samples of ~200 mg were pyrolysed in open glass tubes, under flowing nitrogen, at a heating rate of 4 K/min to temperatures of 875 K in an NMR furnace-probe (11). Solid echo measurements of the proton NMR transverse relaxation signal, I(t), were made on the specimens at regular intervals during pyrolysis. The intensity of the signals was empirically corrected to account for the temperature sensitivity of the NMR measurement. (See Lynch et al. (10) for a more detailed description of the techniques used.)

Residues and extract specimens were supplied in a predried state and measured under the same conditions as the whole coals. Yields of residue obtained (wt% basis) are given in Table 1, together with elemental compositions and lithotype classifications for the brown coals and lithotypes.

TABLE 1. DATA FOR BROWN COAL SUITE

Sample		H/C	C[a]	O[a]	Lith[b].	Resid. (wt%)	%mm	Coal M_{400} (kHz^2)	Coal M_{600} (kHz^2)	Resid. M_{600} (kHz^2)
Victorian and New Zealand coals										
1	Bacchus Marsh	1.22	70.5	20.6	1	50	62	24.5	9.5	24.8
2	Roxburgh (NZ)	1.11	69.8	23.0	-	60	55	19.5	11.6	25.4
3	R5	1.08	70.9	21.8	1	59	58	21.7	10.2	24.7
4	H1317	0.99	71.4	22.0	1	67	48	26.1	13.8	25.2
5	Idaburn (NZ)	0.95	68.4	25.5	-	72	39	19.5	15.7	25.6
6	Newvale (NZ)	0.91	67.6	26.6	-	77	28	24.7	19.7	26.4
7	R30	0.89	69.5	24.5	4	80	26	24.8	20.3	25.9
8	H1317	0.85	70.6	24.4	5	-	21	26.8	22.9	-
9	LY1276/Morwell	0.79	68.4	26.2	5	88	15	25.4	24.2	26.1
Lithotype suite										
a	LY1276/Morwell	0.83	66.8	27.0	1	-	33	23.0	18.0	-
b	LY1276/Morwell	0.78	66.1	28.0	2	-	27	25.0	19.6	-
c	LY1276/Morwell	0.80	66.5	27.2	3	-	23	25.2	20.8	-
d	LY1276/Morwell	0.81	66.2	26.6	4	-	23	25.7	20.5	-
e	LY1276/Morwell	0.75	67.0	27.2	5	-	23	24.2	21.3	-

[a]Expressed as wt% on a dry, mineral matter and inorganic ion free basis.
[b]Lithotype ranking 1 = pale, 5 = dark.

RESULTS

Figure 1 shows stacked plots of the ^1H NMR transverse relaxation signals obtained during PMRTA of a Bacchus Marsh brown coal and its extract and residue specimens. Analysis of such data provides parameters that semi-quantitatively describe aspects of the composition and molecular dynamics of the specimens during heating. Thus, (i) the initial intensity, I(0), of the transverse relaxation signal (taken as the peak of the solid echo, Fig. 1) gives an estimate of the residual hydrogen content of the specimen; (ii) in general each of the ^1H NMR signals can be resolved into a slowly relaxing exponential component fitted at longer times (the 'mobile' component), and a rapidly relaxing Gaussian-like residual signal(the 'rigid' component). Because resolution of these components is somewhat subjective and sensitive to the details of the curve fitting procedure used, care was taken to use a consistent procedure to analyse all the data. The initial intensities of the fitted components are taken as measures of the fraction of hydrogen in 'mobile' and 'rigid' (on a time scale of $\sim 10^{-5}$ s) molecular structures of the specimen; (iii) each recorded NMR signal, I(t), is characterized by an empirical second moment, M_{2T}, of a truncated (at 10 kHz) frequency absorption spectrum obtained by its Fourier transformation (10). For a rigid organic solid the magnitude of M_{2T}, which is an intensive property, is directly related to the average short range (~1 nm) proximity of hydrogen atoms to each other. However, importantly, the contribution of a particular molecular unit within a structure to this quantity rapidly decreases with the onset of its molecular mobility so that M_{2T} is inversely related to the average molecular mobility of the structure.

The temperature dependences of the residual hydrogen content and the percentage of the initial hydrogen content that is defined as mobile are plotted in Fig. 2a for the high H/C Bacchus Marsh pale lithotype coal and its extract and residue specimens. The corresponding pyrograms for the empirical second moment are compared in Fig. 2b. The residual hydrogen content pyrograms define the region of main pyrolytic decomposition and loss of volatiles, and the second moment and remaining

mobile hydrogen pyrograms reflect changes in the molecular mobility of the specimens. Data for the LY1276 lithotype suite are presented in Fig. 3 and results for the suite of brown coals are shown in Fig. 4. The second moment pyrograms for residues of samples 1-7 and 9 and pentane-insoluble extracts of samples 1,3 and 4 are compared in Fig. 5.

The M_{2T} values at 400 K (M_{400}) and at 600 K (M_{600}) and %mm (the greatest remaining mobile hydrogen value achieved during the pyrolysis, which occurs at about 600 K for all the brown coals) are secondary parameters derived from the pyrograms. The values of M_{600} and %mm for the coals and M_{600} for the residues are plotted against H/C in Fig. 6, and in Fig. 7 %mm for the coals is plotted against the yield of residue.

DISCUSSION

The Bacchus Marsh, R5 and H1317 (sample 4, pale lithotype) brown coals gave high enough yields of extract to allow PMRTA of their extracts. PMRTA data for the Bacchus Marsh coal, which had the highest H/C and extract yield of the brown coals, its 'asphaltene' extract and its residue material are compared in Figs 1 and 2. Although their M_{2T} values (Fig. 2b) indicate that these materials are not totally rigid molecular lattices on the time scale of 10^{-5} s at room temperature, the absence of a significant slowly relaxing exponential signal shows that none of these materials contains highly mobilized components. The similarity of the three M_{2T} values at room temperature (Fig. 2b) is unexpected. The common value of 30 kHz^2 is typical of a rigid aromatic lattice (e.g. bituminous coal) but much lower than that for a rigid aliphatic lattice. This indicates a degree of molecular mobility within the aliphatic structures to give lower M_{2T} values which are fortuitously similar to the value for the (presumed) rigid aromatic structures in the coals.

The extract became fully mobilized on heating above 460 K whereas the residue acquired a maximum of only 15% mobile structure near 600 K. The whole coal specimen also passed through a well defined maximum of 60% mobile structure near 600 K. In each case it can be seen that as heating proceeded beyond 600 K there is a parallel between 'devolatilization', indicated by the decline in residual hydrogen, and the rapid loss of the mobile component of the remaining sample (Fig. 2a). The pyrograms in Fig. 2 clearly distinguish the different thermal behaviour of the Bacchus Marsh coal, residue and extract specimens and qualitatively display the intermediate or composite nature of the whole coal.

There is considerable variation in the thermal properties of the individual brown coals (samples 1-9) as shown in Fig. 4. These coals exhibit a strong correlation between the yield of residue and hydrogen content but none with carbon content (Table 1), therefore the residue and extract materials must have vastly different hydrogen contents but similar carbon contents. A weaker but significant positive correlation between the yield of residue and oxygen content suggests that the residue would be more oxygen-rich than the extract.

In the light of the two-component hypothesis, the great difference between the H/C values of extract (1.4) and residue (0.6) materials from this suite of coals (9) suggests a strong correlation between thermal properties and H/C ratio of the brown coals. This is seen to be the case at higher temperatures (Figs 4 and 6). In particular the maximum extent of mobilization, as indicated (inversely) by M_{600} and (directly) by %mm, increased with increasing H/C of the coals (Fig. 6). However below 500 K the coals showed some individual variations which were not H/C dependent.

The fact that the PMRTA parameters near 600 K correlate strongly with H/C whereas below 500 K they do not is probably the result of variations in the interactions between the extract and residue in the source coals. The low molecular weight molecules may not be uniformly dispersed and may range from those that are

intimately interacting with the 'host' so that their thermal properties are those of a sorbed phase to those that are clustered and behave similarly to the bulk extract. Therefore the observed variations of M_{400} (Table 1) may reflect variations in the dispersion of the 'guest' molecules in the coals. Alternatively there is some evidence that the extracts from coals that show relatively lower M_{400} values are richer in straight-chain aliphatic materials (P. Redlich, unpublished data). Both these physical and chemical distinctions would be lost at higher temperatures where the 'guest' molecules are fully mobilized.

In contrast, the second moment pyrograms of the residues from these coals (Fig. 5) show that the residues all behaved similarly and acquired little molecular mobility during the pyrolysis. This close similarity is consistent with the host/guest hypothesis and is in agreement with earlier work (9) which showed that the properties of the 'host' varied little between the brown coals. It is possible that the minor degree of structural mobility acquired by the residue specimens was a consequence of their incomplete extraction and/or the retention of some of the extraction solvent. The latter possibility is supported by the noticeably earlier loss of (hydrogen) volatiles by the residue than by the coal or extract (Fig. 2a).

The temperature variation of the NMR signals of the extracts (e.g. Fig. 1c) and the second moment values calculated from them (Fig. 5) show that the extracts remain fully mobilized in the temperature range 470–700 K. At higher temperatures, the rapid increase in M_{2T} values reflects the rapid loss of volatiles and indicates that the material left after volatile evolution, containing 10% of the original specimen hydrogen (Fig. 2a), is a rigid coke at its temperature of formation.

Variations are apparent in the M_{2T} pyrograms (Fig. 5) of these extracts. For example, H1317 coal extract (from sample 4) softened at a higher temperature than the extracts of the other two coals. In addition, a secondary M_{2T} maximum at 630 K was observed for this extract, which suggests that rapid crosslinking reactions may have been occurring, leading to a reduction in structural mobility with increase in temperature/time.

Redlich et al. (9) have emphasised the direct linear relationship between the yield of extract and H/C ratio in support of the host/guest model for brown coals. They have also demonstrated that hydroliquefaction reactivity is closely correlated to atomic H/C (9) and Brookes et al. (12) have shown strong linear correlations between the intensity of infrared aliphatic C-H stretching bands and the H/C content of these coals. The good linear relationships between the maximum extent of thermally activated molecular mobility (%mm) and yield of extract residue on the one hand and H/C ratio on the other (Figs 6 and 7) are further strong support for this two-component model of brown coal structure. The identification of the extractable material as the component that is thermally mobilized in the whole coal structure, suggested by the PMRTA results, also supports the contention that the method of extraction used by Redlich et al. (9) does not chemically degrade the coal structure to any great extent.

Comparison of the PMRTA pyrograms (Fig. 3) of the five LY1276 lithotypes, which were chosen to give as wide a lithotype range as possible with minimum variation in elemental analysis (4), establishes that the thermal behaviour within this lithotype set was very similar and hence relatively insensitive to lithotype ranking.

CONCLUSIONS

1. The thermal behaviour under pyrolysis conditions of a suite of brown coals and their extracts and residues, as revealed by PMRTA, lends further support to the host/guest model of these coals. Although the residues and extracts showed very different thermal behaviour, the results within each group were similar and independent of the H/C value of the source coals. On the other hand the thermal behaviour of the coals varied significantly and there was a strong positive

correlation between the maximum extent of molecular mobilization during heating and both H/C and extract yield. The much higher H/C ratio of the extract compared to the residue material allows these observations to be explained in terms of the host/guest hypothesis whereby the coals are composed of extract and residue materials in differing proportions.

2. The thermal behaviour of brown coals of similar H/C is insensitive to lithotype.

3. Hydrogen content or atomic H/C ratio gives a much better correlation with PMRTA parameters at temperatures above 500 K than lithotype.

4. The molecular structure of the residues was largely immobile and hence relatively unreactive during heating to ~ 875 K. The pentane-insoluble 'asphaltene' extract softened at ~380 K and devolatilized rapidly above 700 K leaving some rigid coke residue.

ACKNOWLEDGEMENTS

Thanks are due to Neil Thomas and Zenta Lauks (CSIRO) for the NMR measurements; Peter Redlich (Monash University, Victoria) for the samples of extract and residue of the brown coals; and Melville Carr (University of Otago, New Zealand) for the New Zealand coal samples.

REFERENCES

1. Hatcher P.G. (1980), Ph.D. Dissertation, University of Maryland, USA.

2. Jackson W.R., Larkins F.P., Redlich P.J. (1984), Proc. Aust. Coal Sci. Conf., Churchill, Victoria, 17-25.

3. Lynch L.J., Webster D.S. (1984), Proc. Aust. Coal Sci. Conf., Churchill, Victoria, 60-67.

4. Hatswell M.R., Hertan P.A., Jackson W.R., Larkins F.P., Marshall M., Rash D. (1981), Fuel, 60, 544-547.

5. Verheyen T.V., Johns R.B., Bryson R.L., Maciel G.E., Blackburn D.T. (1984), Fuel, 63, 1629-1635.

6. Verheyen T.V., Perry G.J, Cookson D.J., Smith B.E., Brockway D.J. (1984), Proc. Aust. Coal Sci. Conf., Churchill, Victoria, 50-59.

7. Drohan P.J.A. (1978), M. Eng. Sci. Thesis, University of Melbourne, Australia.

8. Lynch L.J., Webster D.S. (1982), Fuel, 61, 271-275.

9. Redlich P.J., Jackson W.R., Larkins F.P. (1985), Fuel, 64, 1383-1390.

10. Lynch L.J., Webster D.S., Bacon N.A., Barton W.A. (1984), in 'Magnetic Resonance: Introduction, Advanced Topics and Applications to Fossil Energy' (eds L.Petrakis and J.P.Fraissard), Reidel, Dordrecht, 617-628.

11. Webster D.S., Cross L.F., Lynch L.J. (1979), Rev. Sci. Instrum., 50, 390-391.

12. Brookes N., Larkins F.P., Thomas R. (1984), Proc. Aust. Coal Sci. Conf., Churchill, Victoria, 26-31.

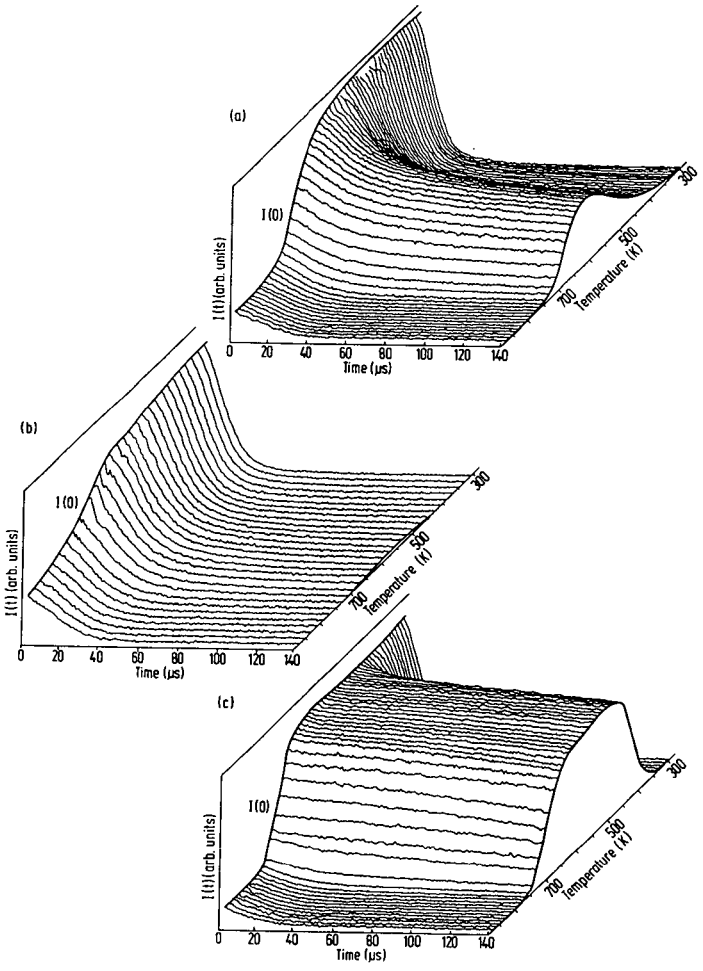

Figure 1. Stacked plots of signals obtained from ^{1}H NMR thermal analysis of (a) a Bacchus Marsh brown coal, (b) the residue after treatment at 593 K with decalin, followed by room temperature extraction with dichloromethane (9) and (c) the dichloromethane-soluble, pentane-insoluble fraction of the 593 K extract (9). The signals have been interpolated to 10 K intervals.

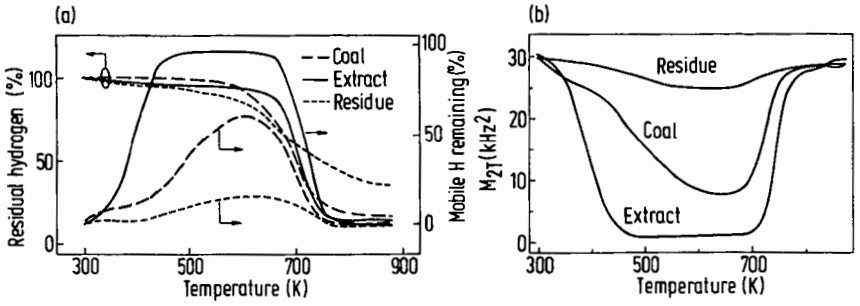

Figure 2. Plots of (a) residual hydrogen content and remaining mobile hydrogen content and (b) M_{2T} (10 kHz truncation) for a Bacchus Marsh coal, its residue and its extract during pyrolysis at 4 K/min.

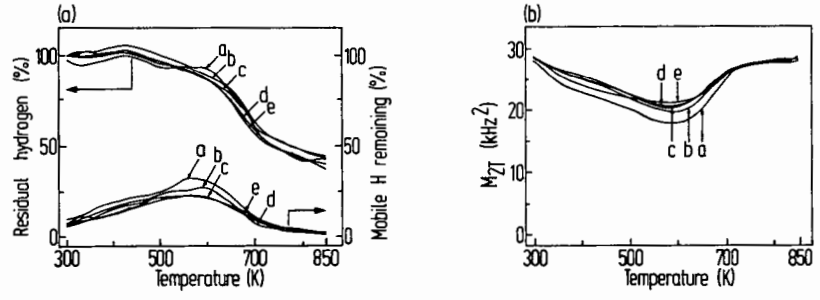

Figure 3. Plots of (a) the residual hydrogen content and remaining mobile hydrogen pyrograms and (b) the M_{2T} pyrogram for the LY1276 suite.

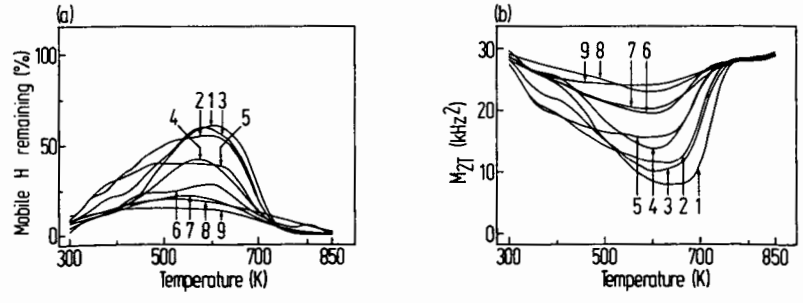

Figure 4. Plots of (a) the remaining mobile hydrogen pyrogram and (b) the M_{2T} pyrogram for the brown coals (samples 1-9).

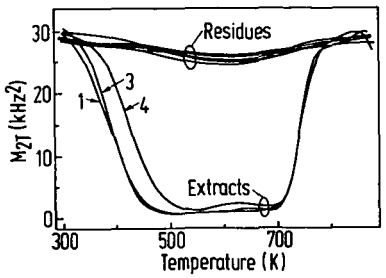

Figure 5. M_{2T} pyrograms for the residues of samples 1-7 and 9 after extraction, and the extracts of samples 1, 3 and 4.

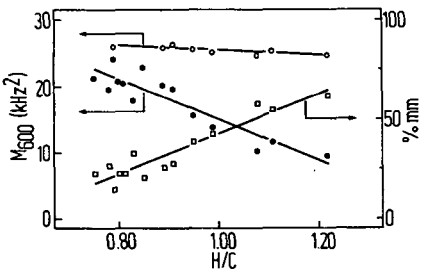

Figure 6. Variation with H/C of the extent of maximum mobility (%mm, □) and M_{2T} at 600 K (M_{600}, ●) for all samples, and M_{2T} for the residues at 600 K (o).

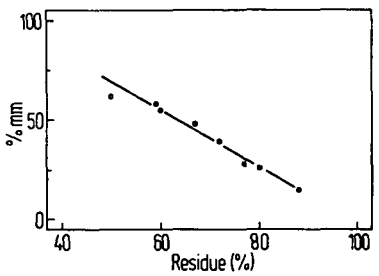

Figure 7. Plot of the extent of maximum mobility (%mm) vs yield of residue after treatment at 593 K and extraction with dichloromethane.

CHANGES IN THE CHEMICAL STRUCTURE OF LOW RANK COAL AFTER LOW TEMPERATURE OXIDATION OR DEMINERALISATION BY ACID TREATMENT . ANALYSIS BY FTIR AND UV FLUORESCENCE .

Jacky KISTER * , Michel GUILIANO , Gilbert MILLE and Henri DOU.

CNRS UA 126 - Laboratoire de chimie organique A
Equipe Analyse et évolution des systèmes chimiques complexes
Université d'AIX-MARSEILLE III
Centre de St Jerome
Avenue Escadrille Normandie-Niemen
13397 Marseille Cedex 13

The studies have been conducted on low rank coal: Flambant de Provence, France, PRV=0.44
FTIR and UV synchronous fluorescence spectroscopy are used to study structural changes in low rank coal after natural oxidation or acid (HCl/HF) demineralization.
The observed variations deal mainly with a decrease in aliphatic structures and an increase in the oxygenated species.
A quantitative oxidation study of the effect of temperature, time, mineral matter and oxygen concentrations has been conducted by FTIR.
An attempt to describe the oxygenated species by FTIR and to compare their evolution has been conducted. Various oxidation mechanisms are proposed according to the results.
The UV Fluorescence allows to show in these conditions a change in the polyaromatic ring absorptions , mainly in the 2, 3 range. This correspond to an oxidation or even loss of some aliphatic substituents.
The results are compared to those obtained by C13 NMR of solid coal, and also to the coking and caking values of oxidized coals.

INTRODUCTION

This study investigates the utility of Fourier Transform InfraRed spectroscopy(FTIR) and synchronous excitation-emission UV fluorescence as a means of measuring increases in the degree of coal oxidation with exposure time in an air atmosphere at various temperatures and for various particle sizes . This multitechnique approach shows much promise in identifying specific changes during coal oxidation or demineralization (1).
These chemical structural changes occurring in a laboratory aerial oxidation experiment are observed on French Gardanne coal , "flambant de Provence" (Subbituminous A) .
It is well known that coal weathering at various temperatures is accompanied by changes in the chemical and physical properties and therefore significantly alters the utilization potential of coals (2-7) .

EXPERIMENTAL

The coal used was from the "ETOILE N°9" seam of the Gardanne mine located in Provence , near Marseille FRANCE and was sampled directly just before these studies . Characteristics are presented in table 1
The coal used was crusched and sieved in a IKA-VERK A 10 and a IKA-VIBRAX-VXR under controlled atmosphere .
At various temperatures (from 20°C to 200°C) , samples were taken at regular intervals and stored in Nitrogen flushed vials to prevent further oxidation before analysis .

TABLE 1 .
Characteristics of "Gardanne coal"

Ultimate Analysis/DFB	%wt	Proximate Analysis	%wt	Petrographic Analysis	%wt
Carbon	60,20	Moisture	7,99	Vitrinite	60,06
Hydrogen	4,30	Ash	20,10	Exinite	6,73
Nitrogen	1,63	Volatile		Inertinite	14,86
Sulphur	4,57	matter /DFB	44,80	_Inertodetrinite	6,40
Oxygen	10,55	FSI(ASTM)	0,50	_Semifusinite	6,13
Ash	18,32	.....	.....	_Fusinite	2,33
.....	.....	.....	.....	Mineral matter	18,32

Coals demineralized by acid treatment (HCl/HF) (8) were studied and we observed the structural modifications which induced disturbances in maceral separations (9,10) .
FTIR spectra were measured on 5DX and 20SX NICOLET spectrometers using the classical halide pellet IR transmission method (11-13) .
UV fluorescence spectra were measured on a PERKIN 3000 and synchronous excitation-emission technique was used to study solid coals and coal extracts $\Delta\lambda$=23mm (14) .

FTIR STUDIES

In a recent work in our laboratory , we noted the high reactivity of "Gardanne coal"in weathering and oxidation reactions and the capacity of FTIR spectroscopy to follow quantitatively the small changes in carbonyl and aliphatic ranges (12) . It is possible that coal oxidized by exposure for long time periods at the edge of a seam differs in structure from a coal oxidized at various temperatures in the laboratory (15) . In a preliminary work , we observed the similar reaction of coal in natural oxidation of a stockpilled coal and in a laboratory aerial oxidation experiment (Tp<60°C) (12) .
Demineralized coals were studied but the demineralization reaction by prolonged acid treatment (HCl/HF) induced itself many parasite oxidation reactions (14 , 16-18) . We observed in all cases significant spectroscopic changes by FTIR difference spectra and we used the area integration method to quantify these modifications .

SAMPLE PREPARATION

The coal was oxidized by spreading about 3g uniformly in a ceramic boat which in turn was placed in a regulated oven. The samples were prepared for infrared analysis by forming standard KBr disks . Spectra were recorded and one hundred co-added interferograms were used to obtain spectra with a resolution of $2cm^{-1}$. Only the 400 - 3300 cm^{-1} region was examinated , so that the OH stretching region of the spectrum was not observed (interferences from water absorbed on the KBr) .

RESULTS AND DISCUSSION

The infrared spectra (plotted in absorption) of oxidized and fresh coal are compared in fig.1 . Major changes in the two spectra appear in the 1676 -1900 cm^{-1} range (weak shoulder near $1695cm^{-1}$) and 2760 - 3000 cm^{-1} range (aliphatic C-H stretching) . These changes were only revealed after subtraction of the fresh coal sample spectrum from the spectra of the oxidized samples (fig.1) . A correct degree of subtraction is obtained by using the kaolinite bands (1035 - 1010 cm^{-1}) as a subtraction standard , since this clay should be relatively unaffected by low temperature oxidation (15) .
After subtraction , the aliphatic C-H stretching mode appears negative , demonstrating a loss in CH_2 - CH_3 groups upon oxidation (area 2760-3000cm^{-1}) and the carbonyl and carboxylic bands appear positive (area 1676-1815 cm^{-1}) . The area integration method used to quantify the oxidation reaction is presented in fig.2 . The same technique was used for maceral separation characterization (9,10) .

The ratio of the integrated peak areas to the total area B+C were calculated (with C area limits : 1885-1839 to 900-892 cm^{-1})

The FTIR study corresponds to a study of the temperature effect (20- 110 - 200°C) for a definite granulometry (<0.125mm) followed by a study of the particle size effect (<0.500 , 0.250 , 0.125 , 0.090 , 0.063 , 0.005mm) at various temperatures . Coal demineralized with HCl/HF is studied at 20°C for a particle size <0.125mm .

a) Definite granulometry (<0.125mm) .

The results from this analysis _ disappearance of aliphatic groups (B/B+C) and formation of carbonyl or carboxylic compounds (A/B+C) as a fonction of temperature and time - are given in figures 3a and 3b .

Upon examination , the curve in fig.3a reveals that the disappearance of aliphatic groups at room temperature occurs mainly during the first few days of oxidation and then seems to level off or at least strongly slow down . At 110°C this disappearance is more important , very significant in the first days and continuing steadily until the end of the experiment . At 200°C , aliphatics disappearance happens very quickly, since the first hours of oxidation - the same remark can be made with regard to the formation of carbonyl or carboxylic compounds (fig.3b).

The "Gardanne coal" studied here presents a relatively low aromaticity level . The corresponding IR spectrum does not clearly show the characteristic adsorptions of aromatic hydrogens (3100 - 3000 cm^{-1} and (900 - 700cm^{-1}) (9-13) . A study using NMR ^{13}C as well as FTIR reveals that aromaticity is not hardly affected by oxidation (16-19) , whereas a previous study indicated an increase in aromaticity upon oxidation (17).

After evidencing the formation of carbonyl and carboxylic compounds , we tried to determine the nature of the formed oxidation products , and the best technique seems to be the spectrum subtraction method - (oxidized coal - starting coal).

We must be careful , particularly when the oxidation products are obtained in very small quantities (oxidation at 20°C) . The difference spectra obtained in these cases may be controversial as shown by the comparaison of the work of LIOTTA et al. (20) and that of RHOADS et al. (21) (signal to noise ratio too low , mineral matter nature and content slightly different from one to another sample (22)) .

At 110 and 200°C difference spectra evidence without ambiguity the formation of the various oxidation compounds (figures 4a and 4b) . The broad band between 1900 and 1500cm^{-1} shows mainly four different absorptions located at 1569_1596 , 1725_1710 , 1778_1770 and 1850_1840cm^{-1} . Furthemore , a prominent new band near 1575_1600 cm^{-1} is now revealed in the difference spectrum. This band is not detectable in the original spectrum and can be assigned to an ionized carboxyl group COO^- - the major product of oxidation (23,24). On the broad band 1500 _ 1900cm^{-1} , we used the second derivative spectroscopic technique which revealed all the absorptions (figures 5a and 5b) . Attributions are given in table 2 . Some of them are corroborated by NaOH and $NaHCO_3$ selective chemical reactivity (25).

TABLE 2

Coal oxidation
Absorptions in 1900 - 1500 cm^1 range .

Wavelength cm^{-1}	Attributions
1850	
1837	
1818	. Anhydrides
1779	
1760	. Esters type O=C-O-Aryl
1739	. Esters type O=C-O-Alkyl
1725	. Carboxylic acids Aryl-$(CH_2)_n$-COOH
1709	. Carboxylic acids Aryl-COOH
1675	. Quinones
1600 -1540	. COO^- carboxylates

Upon examination , figures 5a and 5b at 20°C and 200°C reveal that the nature and repartition of oxidized species is not the same . This poses the problem of comparison of natural ageing (weathering) of coals and laboratory oxidation at high temperatures.
Weak broad residual absorption between 1200 - 1300cm^{-1} in the difference spectrum could possibly be due to C-O bands , as in phenols or ethers , but these bands would be difficult to identify .
This phenomenon is more significant at 20°C and 60°C than 110°C and 200°C . From a purely mechanistic point of view , this observation calls for confirmations, , since it allows to suggest different mechanims .
A number of studies have concluded that the formation of ether cross-links is critical to loss of coking ability (2 4) .

b) Particle size effect.

We can see (figures 6a and 6b) the appearance of oxygenated groups (A/B+C) and disappearance of aliphatics (B/B+C) as a function of time for different grindings .The study presented here corresponds to an utmost oxidation at 200°C .Upon examination , the curves reveal that the appearance of oxygenated groups is proportional to the inverse of particle size , as well as the disappearance of aliphatics , since the two phenomena are linked chemically .This is a logical result , as the specific surface likely to react is larger for a coal of lower granulometry . In order to estimate the role played by the initial grinding , the areas a and b were integrated immediately after grinding and the "zero points" were thus obtained (table 3) .

TABLE3

"Zero points" , area integrations
Grinding effect , initial state

Granulometry < à	0,063	0,090	0,125	0,250	0,500
Ratio A.10^3/B+C	4,8	4,7	3,9	2,8	2,5

In this manner , we verified that when the particle size decreases (longer grinding times) , the oxidation increases - Even coals ground under demineralized and cooled water give "zero points" characteristic of an oxidation (12,16) . It is then problematic to present comparison studies when the initial products are not strictly identical . It must be noted that grinding effect affects minerals and macerals specifically with a proper reactivity . Therefore grinding results in organic-mineral mixtures with a reactivity to oxidation different from that of the initial heterogenous mixture . This observation let us to leave the selective sieving in favor of the notion of grinding time .

c) Demineralized coal .

The acid demineralization technique , as well as the grinding technique , results in chemical disturbances in the coal , mainly by oxidation (12,16) . If we observe the natural evolution of a demineralized coal (figure 7) , we can see that the appearance of oxygenated species corresponds to two curves , which are considerably different in the early stage of oxidation and become later identical . The shifting of the curves in figure 7 corresponds to a shifting of the "zero point" due to the initial effect of demineralization technique by oxidation (12,14,16) and the fact that for fresh coal the ratio A peak area / total area B+C is calculated with remaining traces of mineral matter (evolution by oxidation and non homogenous sampling) . Whereas for the demineralized sample the ratio A / B+C is calculated without interference . It seems that mineral matter affects oxidation particularly in its early stages

UV FLUORESCENCE STUDIES

UV fluorescence by synchronous excitation - emission technique allows the approach of the polyaromatic structure of coal before and after treatment (1,14) . This treatment may correspond to a natural or induced oxidation (12) or a demineralization treatment before a maceral separation study (9,10) or a reactivity study .

Most often in order to be analyzed by UV fluorescence , coal must be treated - either by chemical treatment transforming for exemple a solid in to liquid (hydroliquefaction and pyrolysis) ; in this case the reaction products are characterized (26) and the initial coal structure may be estimate by the knowledge of the reaction mechanisms - or a treatment with a solvent , in which case a coal fraction is characterized more or less important depending on the coal , solvent and technique used (27) .

a) Analytical technique.

Different types of spectra may be obtained by UV fluorescence - Emission spectra are obtained by exciting the compound with a fixed wavelength and determining the definite fluorescence intensity proper to that particular wavelength . In the case of complex mixtures , this method does not prove satisfactory , as the definite excitation wavelength chosen cannot correspond to the maximum extinction coefficient of each of the mixture components , and this induce for certain compounds a decrease in fluorescence intensity .

Synchronous excitation - emission spectra are the result of the technique which consists in recording the emission spectrum of a mixture and varying the excitation wavelength , while maintaining $\Delta\lambda$ optimum at 23nm . This technique clarifies the emission of each of the mixture components and results in a better resolved spectrum (28,29) .

b) Solvent coal extract study.

Several methods of solvent extraction may be used in the case of "Gardanne coal" , dissolution at refluxing , Kumagawa , soxhlet , sonication... They all give extraction yields close to 15% but extraction by sonication is more rapid (45min.). It is carried out at a low temperature (<50°C) , which prevents from a too long contact period and also significant parallel oxidation reactions . Fluorescence spectra of extracts obtained by the various extraction techniques reveal the presence of the same aromatic compounds (emission peaks at 371 and 393nm charasteristic of aromatic derivatives with 3 and 4 condensed rings (fig.8) .Further differenciation can be made by examining hexane , THF and pyridine fractions obtained from the initial extract . However this differentiation is fastidious as there is a "levelling" of the extracts directly linked to the solvent selective extraction power towards the polyaromatic species in the coal (14) .

In order to try to better evidence the spectrum differences between fresh , demineralized and oxidized coal , multiple steps fractioning has been adjusted . Four successive extractions are carried out with hexane , toluene , THF , and then the last residue is dissolved in pyridine . Each fraction thus obtained is analyzed for the three types of coal . The obtained spectra show that it is possible to compare coals (fig 9 , table 4) by emphasizing the characteristic signs . For "Gardanne coal" we notice that the oxidation (200°C , 34days) as well as demineralization affects the repartition of polyaromatics with 3 or 4 condensed rings by causing a bathochome shift ,characteristic of a loss of substituents(28 , 30) .

c) Study of solid state coal.

The analysis of the extracts allows the characterization of only a fraction of the coal . In order to obtain a more complete characterization we studied uv fluorescence on sample in powder(particle size <0,125mm) .

The obtained fluorescence profile are clearly different (14,30) from those of the extracts . The maxima characteristics of aromatic compounds with 2 , 3 , 4 condensed rings are no longer present and maxima between 440 and 550nm are observed which correspond to more condensed aromatic structures (5 or more rings) : the basic structural units (BSU) or basic squeleton .

In reference to the structural pattern of DRYDEN coal (31) , the solvent swells the miceral mesh and the small units are transported by diffusion through the matrix pores . In the case of the"Gardanne coal" , we observe that the small units have a significant extraction facility , since this coal has a very open porosity . Therefore oxidation and demineralisation affect mainly these small units and UV fluorescence is particularly adapted for evidencing this phenomenon . In contrast , in the coal matrix itself , the general structure of the basic structural units (BSU) common to all the coal samples is found (polyaromatics with 5 to 8 piled condensed rings) .

TABLE 4

UV Fluorescence characteristics
Comparison between _ coal extract
_ demineralized coal extract
_ oxidized coal extract

Emission wavelength (nm) of the main bands.

Fractions .	Fresh coal λ(nm)			. Demineralized coal λ(nm)			. Oxidized coal λ(nm)			
Hexane	315	318		. 310	318		. 318			
Toluene.....	322	339	401	. 325	349	401	. 325	349	381	401
THF.....		354	404	. 327	345	404	. 327	345	383	404

CONCLUSION

FTIR , UV fluorescence and NMR lead to the same conclusion with regard to oxidation and demineralization of "Gardanne coal" - loss of aliphatic groups attached to polyaromatics with 3 or 4 rings - appearance of oxygenated species , mainly carbonyls and carboxylic acids - no change in the BSU pattern .
The observed particle size effect seems to show that there is a surface reticulation effect (destroyed on re-grinding and determined by measuring of the Gieseler index). This reticulation might be favored by the increase in the number of hydrogen bridges available resulting from the loss of cumbersome alkyl substituents and the appearance of many oxygenated sites . The nature and evolution of the species formed at low temperatures as well as higher temperatures may allow to suggest different mechanisms revealing an influence of the mineral matter in the first stage of oxidation .

ACKNOWLEDGEMENT

All these results have been conducted in the frame of CNRS - GRECO "hydroconversion et pyrolyse du charbon " and the ATP CNRS - PIRSEM N°2051 "structure et réactivité des charbons" .

LITERATURE CITED .

1 . Kister J. and Dou H.
Fuel processing technogy , 1986 ,12 , 19-29 .
2 . Crelling J.C. , Schader R.H. and Benedict L.G.
Fuel , 1979 ,58 , 542-546
3 . Wachowska H.W. , Nandi B.N. and Montgomery D.S.
Fuel , 1974 , 53 ,212-219
4 . Ignasiak B.S. , Szadow A.J. and Montgomery D.S.
Fuel , 1973 , 53 , 12-15
5 . Cox J.L. and Nelson C.R.
ACS , Div. Fuel Chem. Preprint , 1984 , 29 , 102-107
6 . Wachowska H.W. and Pawlak W.
Fuel , 1977 , 56 , 422-426

7 . Herring J.R.
Proc. Int. Coal Science conference . Pittsburgh , 1983 , 753-756
8 . Bishop M. and Ward D.L.
Fuel , 1958 , 37 , 191-194
9 . Kister J. , Guiliano M. , Totino E. and Muller J.F.
C.R.Acad.Sciences Paris , 1986 , 302C ,II8 , 527-532
10. Totino E.
These Sciences Metz , 1986
11. Guiliano M. , Mille G. , Kister J. and Dou H.
Spectra , 1985 , 103 , 13 , 35-39
12. Guiliano M. , Kister J. , Mille G. and Dou H.
C.R.Acad.Sciences Paris , 1986 , 302C ,II9 , 621-626
13. Guiliano M. , Mille G. , Kister J. and Dou H.
Analusis , 1984 , 12 , 201-204
14. Mille G. , Lopez N. and Kister J.
C.R.Acad.Sciences Paris , 1986 in press Oct 1986
15. Painter P.C. , Coleman M.M. , Snyder R.W. , Mahajan O., Komatsu M. and Walker P.L.
Applied spectroscopy , 1981 , 35(1) , 106-110
16. Tekely P. , Nicole D. , Delpuech J.J. , Totino E. and Muller J.F.
Fuel Processing Technology in press Janv. 1987 , Rolduc Symposium 1986.
17. Mac Phee J.A. and Nandi B.N.
Fuel , 1981 , 60 , 169-170
18. Haven J.R. , Koenig J.L. , Kuehn D. , Rhoads C. , Davis A. and Painter P.C.
Fuel , 1983 , 62 , 936-941
19. Fredericks P.M. , Warbrooke P. and Wilson M.A.
Org. Geochem. 1983 , 5(3) , 89-97
20. Liotta R. , Brons G. and Isaacs J.
Fuel , 1983 , 62 , 781-791
21. Roads C.A. , Senftle J.T. , Coleman M.M. , Davis A. and Painter P.C.
Fuel , 1983 , 62 , 1387-1392
22. Kister J. , Guiliano M. , Reymond H. , Mille G. and Dou H.
Intern. J. Environ. Anal. Chem. , 1985 , 22(3/4) , 297-318
23. Bellamy L.J.
The infrared spectra of complex molecules
Methuen London 1954
24. Colthup N.B. , Daley L.H. and Wiberley S.E.
Introduction to infrared and raman spectroscopy
Academic press New York 1964
25. Speight J.G. and Moschopedis S.E.
ACS Symp. Charac. Heavy ends in petroleums
1981 , 907-911
26. Delpuech J.J. , Nicole D. , Cagniant D. , Cleon Ph. , Fouchere M.C.
Dumay D. , Aune J.P. and Genard A.
Fuel Processing Technology , 1986 , 12 205-241
27. Cagniant D. and Dumay D.
Bull.Soc.Chim.Fr , 1985 , 3 , 435-447
28. Mille G. , Kister J. , Guiliano M. and Dou H.
Spectra 2000 , 1985 , 13(106) , 27-31
29. Vo Dinh R.
Applied Spectroscopy , 1982 , 36(5) , 576-581
30. Mille G. and Kister J.
Rapport d'ATP CNRS-PIRSEM N°2051 ,1985-1986
"Structure et réactivité des charbons .
31. Dryden J.G.C.
Chemistry of coal utilisation , Supplementary volume
John Wiley , Lowry H.H. 1963 .

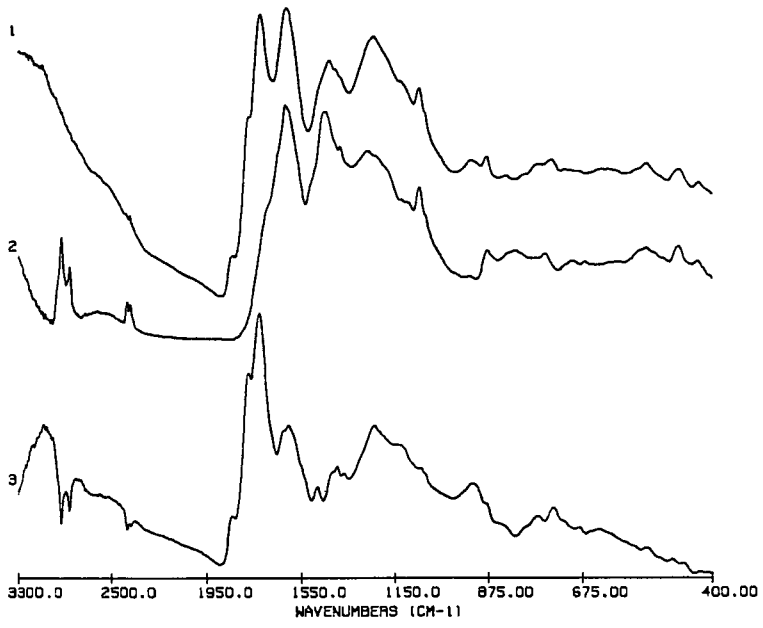

FIGURE 1

1 . Infrared spectrum of fresh coal
2 . Infrared spectrum of oxidized coal
3 . 2 – 1 difference spectrum

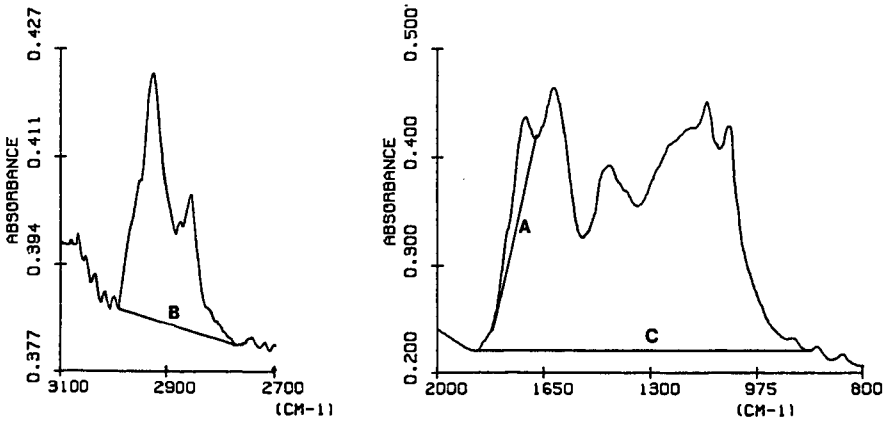

FIGURE 2

Areas integration method used
1 . 2700 – 3100 cm^{-1}
2 . 800 – 2000cm^{-1}

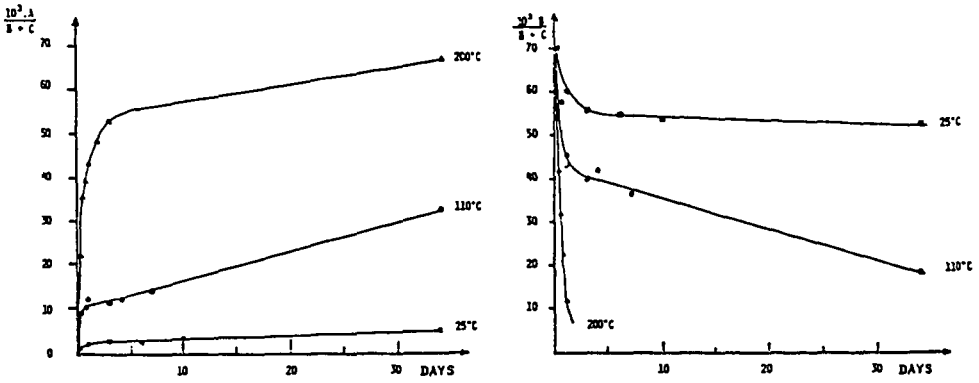

FIGURE 3a and 3b

3a . Aliphatic groups decrease : B/B+C ratio versus oxidation time at 25 , 110 and 200°C
3b . Carboxylic and carbonyl groups increase : A/B+C ratio versus oxidation time at 25 , 110 and 200°C

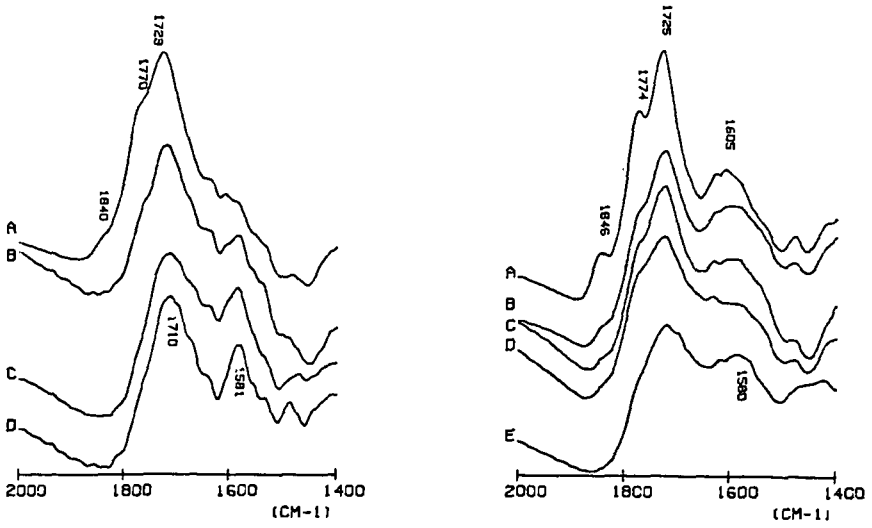

FIGURE 4a and 4b

4a . Difference spectra between 2000 and 1400 cm^{-1} of oxidized coals at 200°C ,(a , 34 days ; b , 4 days ; c , 18hrs ; d , 6hrs .)
4b . Difference spectra between 2000 and 1400cm^{-1} of oxidized coals at 110°C , (a , 34 days ; b , 4 days ; c , 18hrs ; d , 6hrs.)

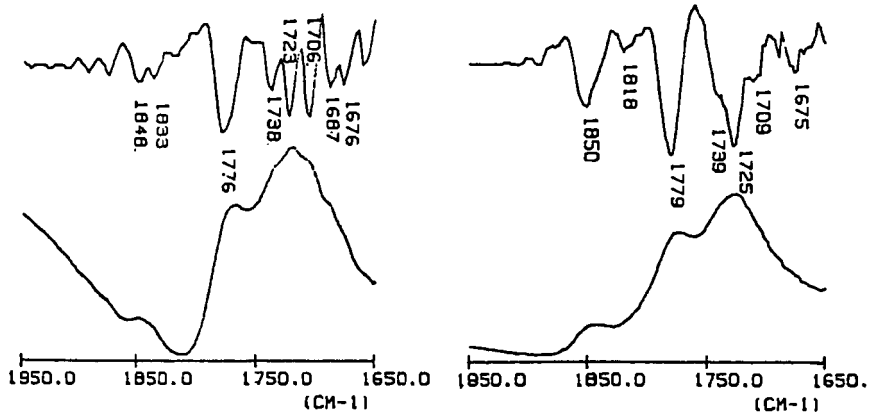

FIGURE 5a and 5b

5a . Infrared spectrum of oxidized coal at 20°C after 78 days and the corresponding derivative spectrum
5b . Infrared spectrum of oxidized coal at 200°C after 34 days and the corresponding derivative spectrum

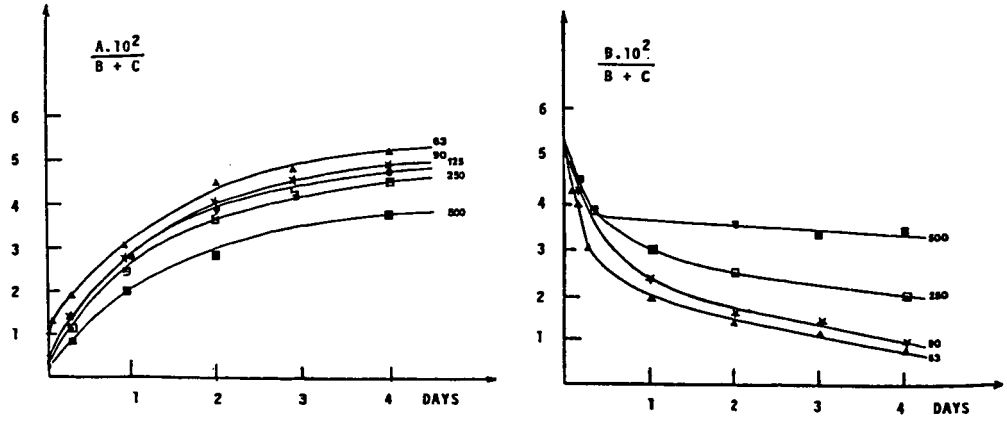

FIGURE 6a and 6b

6a . Aliphatic groups decrease : B/B+C ratio versus oxidation time at 200°C and particle size effect .
6b . Carboxylic and carbonyl groups increase : A/B+C ratio versus oxidation time at 200°C and particle size effect .

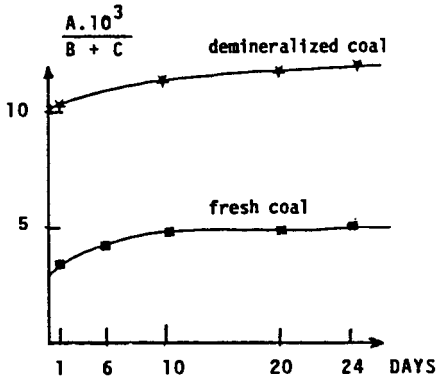

FIGURE 7

Comparison of aerial oxidized raw coal at 20°C and demineralized coal
Carboxylic and carbonyl groups increase : A/B+C ratio versus oxidation time .

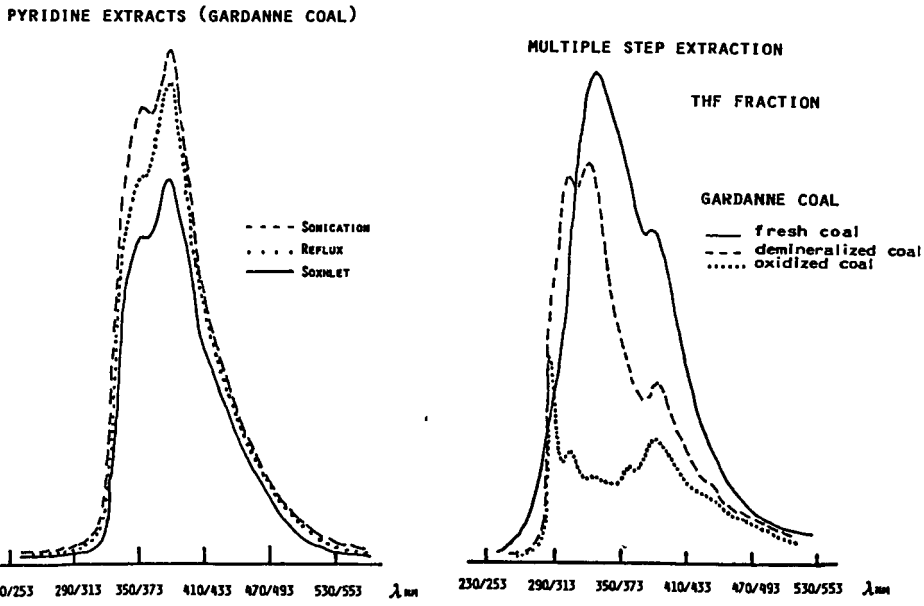

FIGURE 8 and FIGURE 9
UV fluorescence spectra of coal extracts (pyridine) obtained by different extractive methods : sonication , dissolution and soxhlet
UV fluorescence spectra of coal extracts (THF) obtained from a fresh coal , demineralized coal and oxidized coal .

STRUCTURE AND REACTIVITY OF A WYODAK SUBBITUMINOUS COAL

Shuyen L. Huang and Ramani Narayan

Laboratory of Renewable Resources Engineering
and
Coal Research Center
A. A. Potter Engineering Center
Purdue University
West Lafayctte, IN 47907

INTRODUCTION

The linkages in coal which arc susceptible to attack and cleavage are the ether, thioether, and diaryl alkane linkages (1-3). Most approaches to cleavc linkages in coal involve reacting coal under severe conditions of temperature and pressure. These severe processing conditions often result in non-specific bond cleavages and retrogressive (bond-forming) reactions. In this paper, we report on the reaction of a Wyodak subbituminous coal with a powerful site-specific reagent, namely potassium-crown ether (K-CE) under thermally mild conditions of *room temperature* and *atmospheric pressure*. The selective cleavage of ethers (4-6), sulfides and sulfones (7) by solvated electrons is documented. The solvated electrons generated by K-CE in THF can transfer onto the aromatic substrates in coal. This results in the formation of aromatic radical anions or dianions which undergo cleavage reaction at aryl ether and diaryl alkane linkages (8,9,10). The crown ethers also function as phase transfer catalysts and promote the electron transfer to the coal. The cleavage of ether linkages can render coal soluble with the formation of "coal oligomer" fragments. In this paper, the solubility of K-CE treated Wyodak coal in THF and aqueous alkali solution is reported. The analysis of thc solubilized coal by IR, ^1H and ^{13}C NMR is also described.

EXPERIMENTAL

Reaction of Wyodak Coal with K-CE Reagent

A 500 ml round bottom flask was flame dried and flushed with nitrogen. Potassium metal (12 g, 307 mmole) was transferred into the flask in a glove box under nitrogen atmosphere. 350 ml of THF solution of crown ether (16.2 g, 61 mmole) was added to the potassium metal via a double-ended needle at 0°C when a dark blue solution was obtained. Four gram of Wyodak coal (C = 70.29%; H = 4.69%; 0 = 23.76%; N = 0.86%; S = 0.39%; 100 mesh; prewashed with methanol, pentane and dried under vacuum at 105°C for 24 hrs) was added to the K-CE/THF solution. The reaction mixture was stirred for 24 hours (or 5 days in some runs) at room temperature under nitrogen atmosphere. It was then cooled to 0°C and quenched with water. The THF was removed by rotoevaporation and the remaining aqueous slurry of coal was freeze dried to remove the water. The work up of the reacted coal is shown in Figure 1.

NMR Spectroscopic Analysis

^1H NMR spectra were obtained with a Nicolet NTC-470 spectrometer (470 MHz) at ambient temperature. Coal samples (15 mg) were dissolved in 0.5 ml of chloroform-d or DMSO-d_6. Proton decoupled ^{13}C NMR spectra were obtained with a Nicolet NTC-200 at 50 MHz at ambient temperature (or 40°C) using a 12 mm probe. The sample concentration was 100 mg/ml of NMR solvent. For the THF-1 fraction chloroform-d was used, for the THF-2 fraction and the alkali-methylated coal DMSO-d_6 was used, and for the alkali-soluble fraction NaOD/D_2O was used.

Infrared Spectra

Figure 2 showed the infrared spectra of various extracts obtained from the K-CE reaction with the coal. IR spectrum of the THF-1 fraction shows sharp aliphatic C-H stretching bands below 3000 cm^{-1}, and aliphatic C-H bending bands at 1450 and 1375 cm^{-1} suggesting that this extract contains predominantly aliphatic material. In addition to the C-H stretching bands below 3000 cm^{-1}, the spectrum of the THF-2 fraction shows a broad OH stretching vibration in the 3100-3200 cm^{-1} region and two vibration bands at 1410 cm^{-1} and 1375 cm^{-1} corresponding to the C-O stretching vibrations. Thus, the THF-2 extract also contained aliphatic material which may be attached to a hydroxy aromatic ring system.

Except for the untreated Wyodak coal, the IR spectra of all the extracts showed absorption bands for carbonyl at 1725 and 1710 cm^{-1}. Using β-naphthol as a model compound to react with K-CE, the results showed that β-tetralone, 5,8-dihydro-2-naphthol and 5,6,7,8-tetrahydro 2-naphthol were the major products. This indicated that in addition to cleavage reactions, reduction of the coal phenolic units to carbonyl units is occurring. This explains the observed 1725 cm^{-1} carbonyl bands in the IR spectra of the K-CE treated coal fractions. In the alkali-soluble fraction an additional carbonyl band at 1710 cm^{-1} along with the broad stretching vibration extending from 3500 cm^{-1} suggested the presence of -COOH groups. The IR spectrum of the methylated product of the alkali-soluble fraction (spectrum not shown here) showed the carbonyl absorption was shifted to 1730 cm^{-1} corresponding to the carbonyl of ester groups. This supported the presence of carboxyl groups in the alkali-soluble fraction. The carboxylated coal fragments may have arisen by cleavage of ester linkages in the coal by the K-CE reagent. In fact, it has been suggested that as much as 58% of the oxygen in this coal is present as ester linkages (11). However, more work needs to be done to quantify how much of the -COOH groups in the alkali fraction arise from ester cleavage and how much were originally present. Interestingly, 10% of Wyodak coal can be solubilized in aqueous NaOH at room temperature and the IR spectrum of the solubilized product showed carboxyl absorption bands, suggestive of ester linkages being hydrolyzed.

^1H and ^{13}C NMR Spectra

Proton NMR spectra of the soluble fractions are shown in Figure 3. The spectrum of THF-1 (Figure 3A) confirmed the presence of predominantly aliphatic material in this extract. The dominant sharp signal at 1.3 ppm is characteristic of methylene protons of long chain polymethylenes. The sharp signal at 1.0 ppm corresponds to parafinic CH_3 or CH_3 groups gamma or further from an aromatic ring. The spectrum of THF-2 also showed the presence of long-chain polymethylene. The group of signals in the 2-3 ppm region can be assigned to dihydro aromatic protons or protons α to an aromatic ring. Based on the mechanism of the K-CE reaction, reduction of aromatic rings to dihydro and even tetrahydro aromatics was expected and the NMR evidence nicely corroborates it.

The phenolic proton (5-7 ppm or 8.5-11 ppm) and carboxylic proton signals (8.5-11 ppm) were found in the spectrum of the alkali-soluble fraction (Figure 3C). The spectrum of the methylated product of the alkali-soluble fraction (Figure 3D) showed the disappearance of the phenolic or carboxylic protons. Instead, a broad signal appeared at 3.8-4.2 due to the $-OCH_3$ protons of methoxyl ester or phenolic methyl ester. The ^{13}C NMR spectrum of the methylated product (spectrum not shown) also showed two distinct signals at 52 ppm and 56 ppm corresponding to methoxyl of phenolic and aromatic esters, respectively. The broad signal at 12 ppm in Figures 3B, 3C and 3D, could probably be due to strongly intramolecular H-bonded -OH groups.

Proton decoupled ^{13}C NMR spectra of the THF-1 fractions from three successive K-CE reactions are shown in Figure 4. The ^{13}C NMR spectra also strongly support the presence of long chain polymethylene groups in the extract. The most intense signal is at 30.2 ppm which is generally assigned to the internal methylene carbons of straight-chain alkanes (an average carbon chain length of approximately 8). The presence of a broad spectral envelope in the 15-50 ppm region in addition to the sharp alkane lines is indicative of the extract's complexity arising out of the presence of only small amounts of these polymethylene-type compounds. The broad band on the 120-140 ppm region is due to the aromatic and polycyclic aromatic species of the extract.

RESULTS AND DISCUSSION

Solubility of Wyodak Coal

After the reaction with K-CE, the Wyodak subbituminous coal was fractionated into THF soluble fractions (THF-1 and THF-2) and an alkali-soluble fraction according to the work-up shown in Figure 1. Due to the limitation of diffusion of solvated elections into the coal, the insoluble coal residue after each K-CE reaction was subjected to second and third K-CE reactions. The successive K-CE reactions with coal solubilized additional coal. It was expected that the analysis and comparison of soluble fractions among each successive K-CE reaction may indicate whether or not coal is composed of some common major structural fragments (coal oligomers) which are linked together to form the coal network.

Using conditions described in the experimental section, for each K-CE reaction, 20-30% of the coal was solubilized into the THF and aqueous alkali fractions. However, it was found that the solubility of coal depends on the amount of potassium and crown ether used and the length of the reaction time. Table 1 summarizes the results of various K-CE and coal reactions using different reagent stoichiometries and reaction times. The results show the alkali-soluble fraction increased significantly with a long reaction time. This suggested that more of the phenolic-type ether linkages were cleaved, thus increasing the alkali-soluble materials. When the amount of crown-ether was increased, the THF-1 soluble fraction increased 3- to 6-fold. The increase in the concentration of solvated electrons, due to the presence of more crown-ether, increased the amount of aromatic ring systems and phenolic or naphthol-type structures, being reduced, thus increasing the THF solubility. When the ratio of potassium to coal was decreased, by using a large quantity of coal, the solubility of coal decreased significantly. This could be attributed to limitations in diffusion rates and availability of sufficient solvated electrons.

Table 1. Solubility of Wyodak Coal

Reaction	Ratio of k/coal (g)	Ratio of K-CE (mole)	Reaction Time	THF-1 (%)	Alkali-Soluble (%)	THF-2 (%)
One K-CE Reaction	3	5	4 days	2	47	3
Total of two K-CE Reactions	3	5	4 days	2	59	5
Total of two K-CE Reactions	3	3	20 hr	6	40	3
Total of two K-CE Reaction	3	2	20 hr	12	35	4
Total of three K-CE Reaction	1	5	2 days	2	34	10

Microanalysis

Elemental compositions of the soluble fractions, the insoluble fraction and the original Wyodak coal are shown in Table 2. The results show that after each K-CE reaction of coal there was an increase in the number of hydrogen atoms. The THF-1 fraction showed high H/C ratio indicating the fraction is rich in aliphatic material. IR and NMR spectra of the THF-1 fraction demonstrated the presence of long chain methylene groups. The hydrogen uptake is due to reactions such as Birch-Huckel-type reduction, and cleavage of aliphatic bridges and ether linkages occurring during the K-CE reaction with coal.

Table 2. Results of Elemental Analysis of Wyodak Coal

Coal Samples	C	H	O	N	S	Ash	H/C
Wyodak Coal	70.29	4.69	23.76	0.86	0.39	5.68	0.80
THF-1 Fraction	77.63	9.78	11.68	0.36	0.54	0.58	1.51
Alkali-Soluble	68.38	4.95	25.50	0.93	0.33	0.39	0.87
Insoluble Fraction	71.68	5.36	21.95	0.59	0.42	2.87	0.90

The similarity between the spectrum of the THF-1 fractions from each successive K-CE reaction, strongly suggest that the major components of THF-1 solubles are a integral part of the coal network and not just "trapped molecules". The results also indicated that coal is composed of some common structural fragments (coal oligomers). Upon each K-CE reaction, some part of the coal network was being snipped releasing these soluble coal oligomer fragments.

Figure 5 shows the ^{13}C NMR spectra of alkali-soluble fractions. The broad signals in the spectra again shows the complexity of the compounds in the extracts. Broad signals at 0-50 ppm correspond to aliphatic carbons. Aromatic carbons bonded to oxygen appeared between 150 and 160 ppm (aryl ethers and phenols). The region between 100 and 130 ppm corresponds to protonated aromatic carbons. Olefinic carbons are also observed.

SUMMARY

The K-CE reagent has provided a way to dismantle the coal network and release soluble coal oligomer fragments, without recourse to any thermal or pressure effects. Up to 50% of Wyodak coal can be solubilized into THF and the alkali-soluble fractions with the alkali-soluble fraction accounting for 90% of the total solubles. The THF-1 fraction is rich in aliphatic material, and polymethylenes were shown to be the predominant component. Alkali-soluble fraction contained primarily phenolic and carboxy groups due to the nature of the extract. In addition to ether cleavage reactions, a major reaction pathway in the coal/K-CE reaction was the reduction of phenolic groups to carbonyls. The results of successive K-CE/coal reactions showed that the structural components of the extracts from each reaction are very similar, suggesting common building blocks for the coal network.

FIMS and MS/MS analysis of the extracts are under investigation to reveal more details about the structural features of the coal.

ACKNOWLEDGMENTS

Funding for this work was provided by the Electric Power Research Institute under Contract No. RP8003-1. We are grateful to the Purdue University Biomagnetic Resonance Laboratory supported by NIH Grant No. RR01077 for the NMR spectra reported here.

REFERENCES

1. D.D. Whitehurst, in "Organic Chemistry of Coal," ed., J.W. Larsen, ACS Symp. Ser., *71*, 1 (1978).
2. W. Wiser, preprints Fuel Division ACS Meeting, 20(2), 122 (1975).
3. HW. Sternberg, C.L. DelleDone, P. Pantages, F.C. Moroni, and R.E. Markbly, Fuel, *50*, 432 (1971).
4. B. Weinstein and A.H. Fenselan, J. Org. Chem., *34*, 126 (1969).
5. J.A. Marshall, and N.H. Anderson, J. Org. Chem., *30*, 1291 (1965).
6. D.H. Eargle, Jr., J. Org. Chem., *12*, 1918 (1967).
7. H.O. House, in "Modern Synthetic Reaction,"W.A. Benjamin, Inc., Ch. 3, p. 145 (1971).
8. L. Schanne and M.W. Haenel, Tet. Letters, *44*, 4245 (1979).
9. C.J. Collins, H.P. Hombach, B.E. Maxwell, N.C. Woody, and B.M. Benjamin, J. Amer. Chem. Soc., *102*, 851 (1980).
10. S. Huang, K. Wood, and R. Narayan, Amer. Chem. Soc., Div. Fuel Preprints, *32* (1986).
11. K. E. Chung, I. B. Goldberg, and J. J. Raltto, Proceedings: Ninth Annual EPRI Contractors Conference on Coal Liquefaction, p. 381, March (1985).

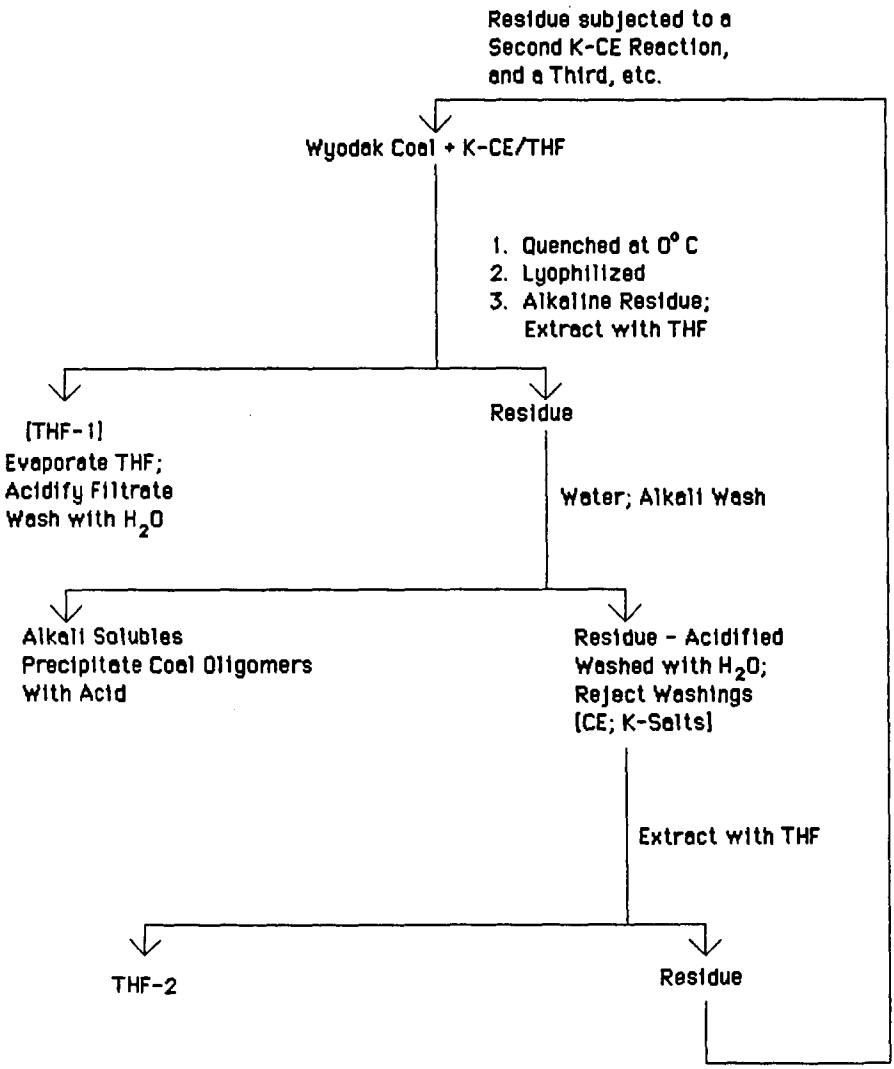

Figure 1. Work-Up of the Coal/K-CE Reaction.

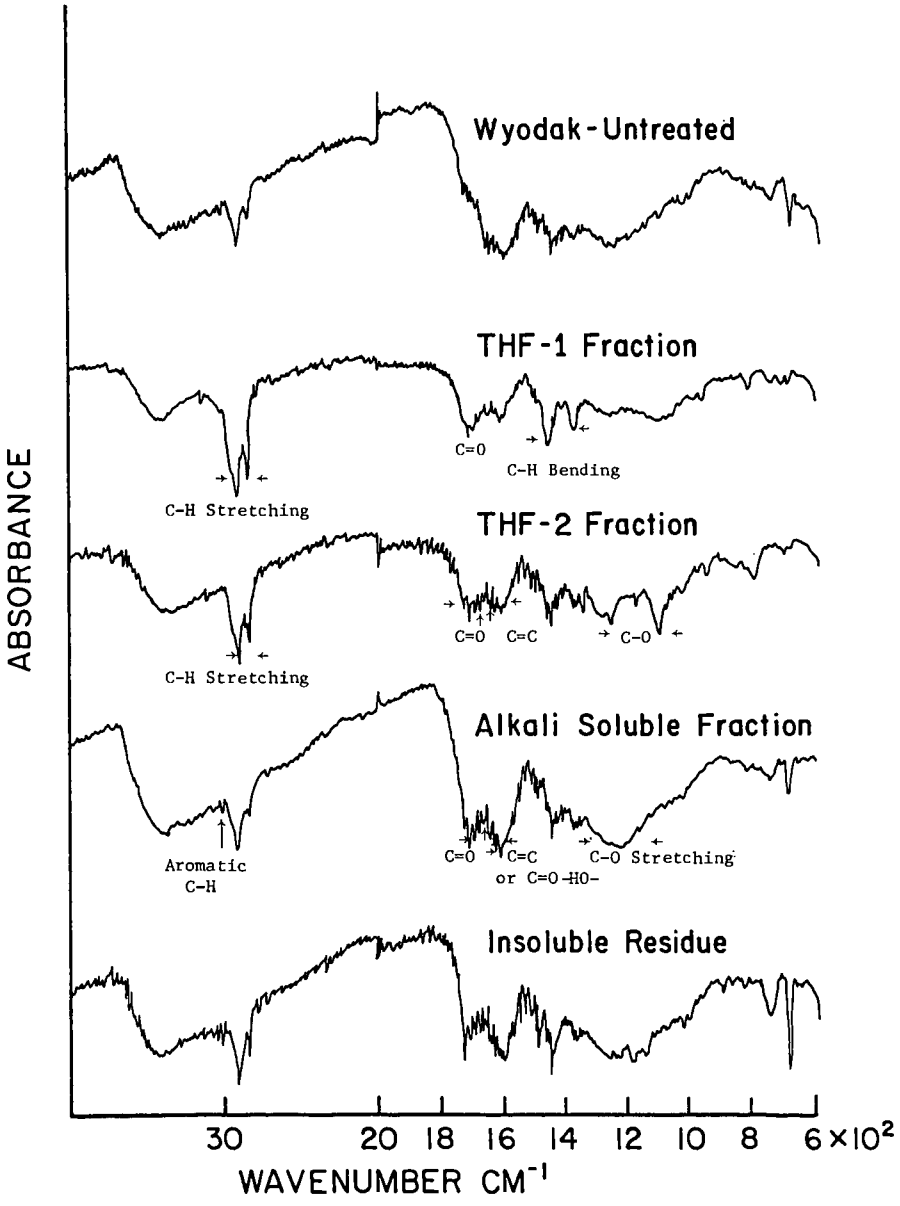

Figure 2. IR spectra of various fractions of K-CE treated Wyodak subbituminous coal.

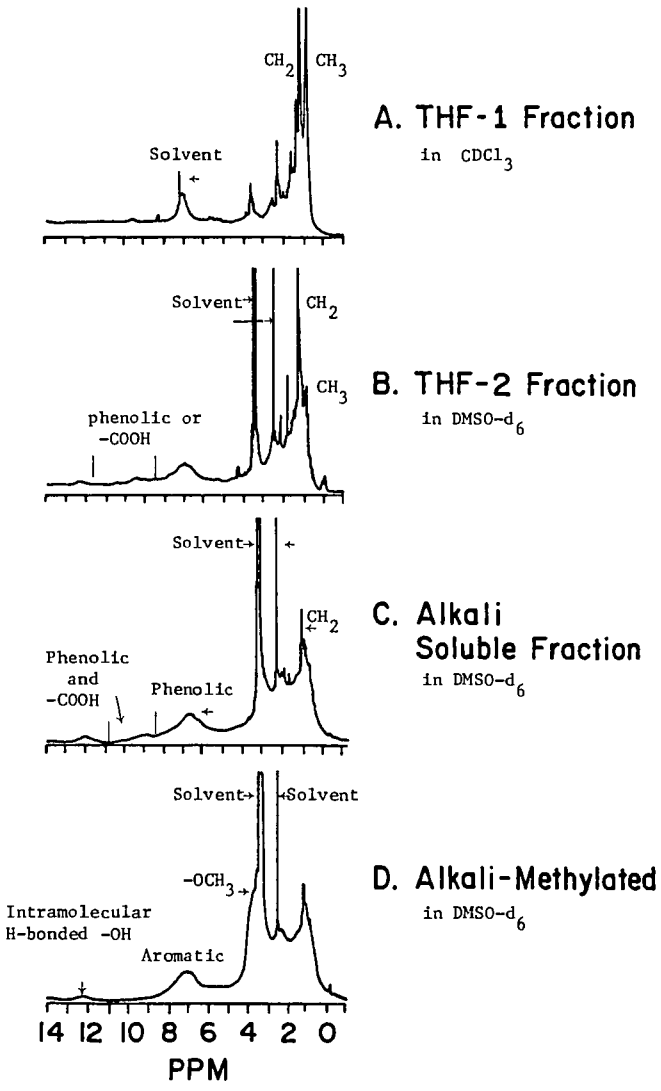

Figure 3. 470 MHz ^{1}H NMR spectra of extracts from reaction of Wyodak coal with K-CE.

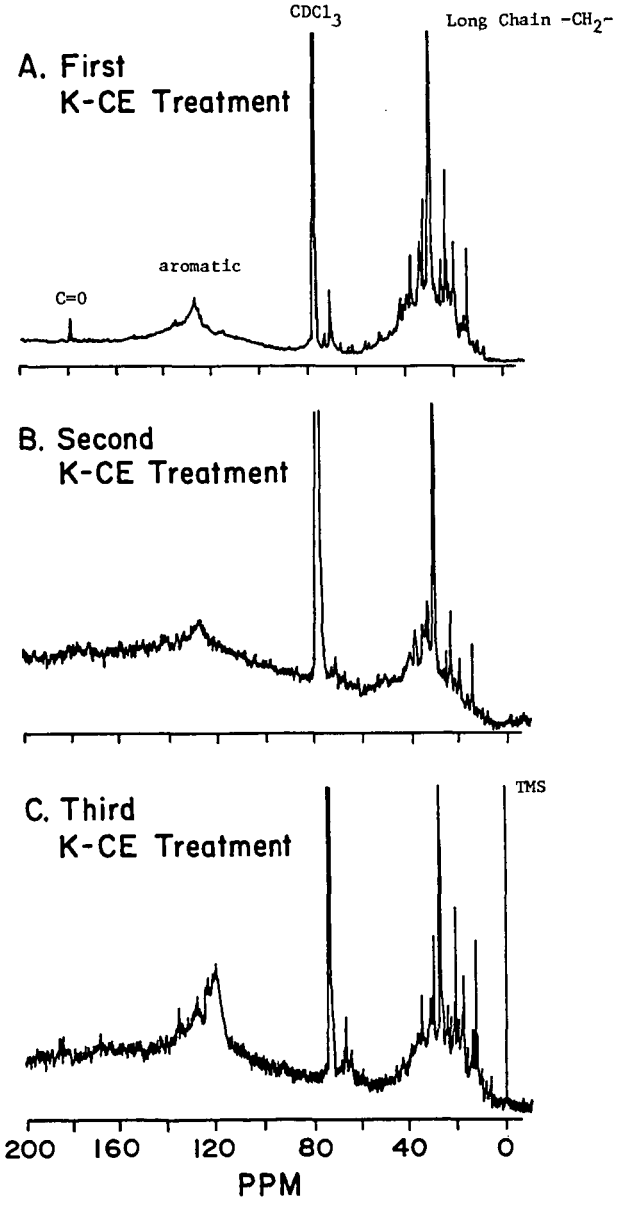

Figure 4. Proton decoupled ^{13}C NMR spectra (50 MHz) of THF-1 in chloroform-d.

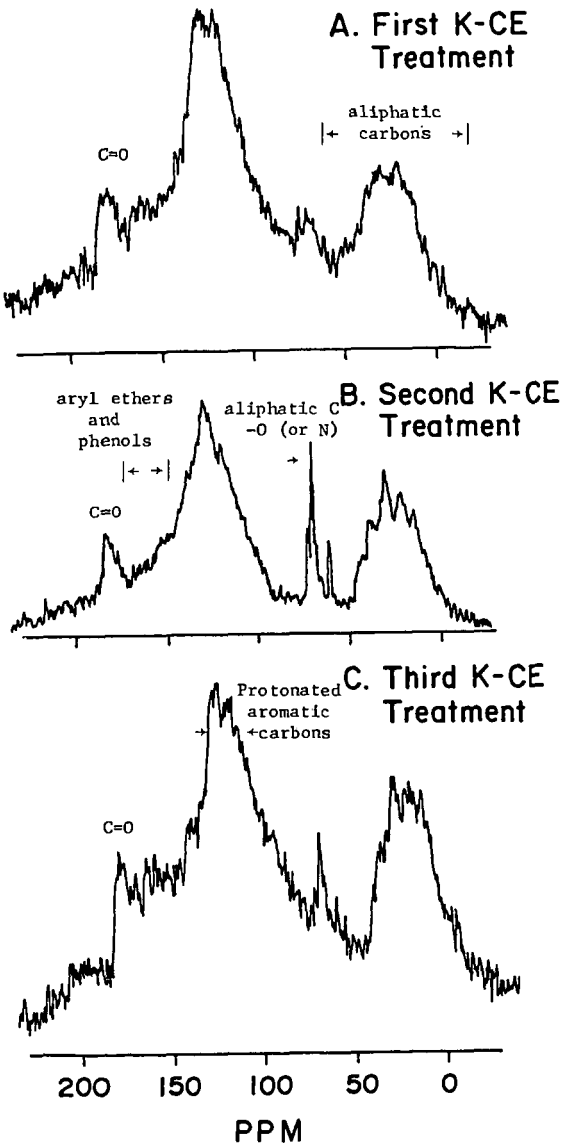

Figure 5. Proton decoupled ^{13}C NMR spectra (50 MHz) of alkali-solubles in $NaOD/D_2O$.

RELATIONSHIPS BETWEEN INORGANIC CONSTITUENTS AND ORGANIC MATTER IN A NORTHERN ONTARIO LIGNITE

E. Van der Flier-Keller
Department of Geography
University of Victoria
Victoria, British Columbia, Canada V8W 2Y2

W.S. Fyfe
Department of Geology
University of Western Ontario
London, Ontario
Canada N6A 5C2

INTRODUCTION

Coal is a complex substance which is composed of organic material and variable quantities of inorganic matter in the form of minerals and trace elements. The presence of these inorganic constituents normally requires that cleaning or modifying procedures must be implemented prior to or during utilization of the coal, so that problems such as boiler fouling, slagging, corrosion; catalyst poisoning; or environmentally hazardous emission may be avoided. To facilitate this, the location and form, in addition to the concentration, of the inorganic substances must be known and understood. This is particularly important where an intimate relationship exists between the organics and the inorganics, making separation using conventional techniques more difficult. This paper examines the relationship between organic matter and the minerals and trace elements in a northern Ontario lignite.

A large number of minerals have been identified in coal. These include a rapidly increasing number of accessory minerals (1) and ultrafine grains (2) including silicates, sulphides, carbonates, oxides and rare earth minerals. Mineral matter in coal has traditionally been examined by X-Ray Diffraction (XRD) following Low Temperature Ashing (LTA) (3), however this method precludes examination of minerals in situ. More recently Scanning Electron Microscopy (SEM) (4) and Scanning Transmission Electron Microscopy (STEM) (2) coupled with Energy Dispersive X-Ray analysis (EDX) are being utilised to determine the mineral distribution and relationship to the organic matter.

A variety of mineral suites, reflecting the changes in physical and geochemical conditions in the coal during formation, are present in most coals. They commonly include a detrital mineral suite consisting of quartz, feldspar and clay minerals, a syngenetic suite comprising clay minerals and a group of epigenetic minerals including for example carbonates or sulphides. The last two mineral groups are respectively extremely difficult and relatively easy to remove from the coal as a result of their varying modes of occurrence. Epigenetic minerals normally fill cleats and exhibit no relationship to the organic matter, while syngenetic minerals may be intimately associated with the coal macerals.

The concentrations and modes of occurrence of trace elements in coal are extremely variable. Concentrations of most elements are low compared with crustal abundances, however certain elements including U, Ge and V may reach ore grade in some coals. Elements may be associated with the coal macerals, clay minerals, sulphides, rare earth minerals, or they may be present as elemental grains. A variety of geological and hydrological factors, such as depositional environment, depth of burial, chemistry and flow rates of circulating groundwater, rank and other post depositional effects, influence both the concentration and location of the trace elements. Coal rank and clay mineralogy appear to be particularly important influences on the latter (5). Modes of occurrence of trace elements have been examined using a variety of techniques, including analysis of concentrations in float

sink fractions (6) or with varying ash content (7); leaching characteristics (8); correlation coefficients (10), and SEM-EDX (1). The latter two techniques are used in this study.

EXPERIMENTAL

The lignite samples discussed below were obtained from the Lower Cretaceous lignite-bearing succession in the Moose River Basin, located in the James Bay Lowlands of northern Ontario. Outcrop exposures and drillcore were sampled. Sampling intervals in the coal seams varied from 1.0 to 0.5 metres, based on lithotype changes in the coal.

Major mineral phases were identified by X-Ray Diffraction. Minor mineral phases and mineral-organic matter relationships were examined using an ISI DS-130 SEM coupled with a PGT System III EDX. Samples for SEM-EDX were prepared from polished sections, broken sample fragments and grain mounts fixed to aluminum studs using silver paint, and carbon or gold coated prior to analysis.

31 major and trace elements were analysed by X-Ray Fluorescence, Atomic Adsorption, and Neutron Activation Analysis. Modes of occurrence of the trace elements were determined using Pearson correlation coefficients and SEM-EDX. Discreet mineral grains were analysed and element windows were run over larger areas to locate elements randomly distributed throughout the organic material. In this way organically bound elements or those associated with extremely fine grained and dispersed mineral matter were identified.

RESULTS AND DISCUSSION

The Moose River Basin lignite is relatively clean by comparison with United States' and other coals worldwide. Isolated samples show no traces of mineral matter, however most samples contain quartz and kaolinite. Accessory clay minerals are restricted to trace amounts of mixed layer clays, illite and mica. Pyrite occurs in less than half the samples analysed, and gibbsite, gypsum and siderite were noted in isolated samples. Mineral abundance and modes of occurrence are summarised in Table 1.

Much of the mineral matter is detrital, for example quartz, mica and some associated clay minerals (Figure 1). Kaolinite appears to be both detrital and derived from in-situ feldspar degradation. Authigenic (syngenetic) kaolinite is commonly associated with fusinitic lignite (Figure 2). A number of other minerals, including pyrite, are intimately associated with the organic matter. Pyrite occurs as crystals infilling cell hollows (Figures 3 and 4) and replacing cell walls. Pyrite also occurs epigenetically, infilling cracks in the lignite (Figure 5). The soily lignite contains most mineral matter, which is also generally detrital. The woody and fusinitic lignite contain isolated detrital grains, occasional detrital-rich bands, and some authigenic mineralisation.

Trace and major element contents of the lignite are summarised in Table 2. Trace element concentrations are generally low, however Sr, Cd, Mo, Au, and As values are elevated compared with concentrations in the surrounding sediments. Modes of occurrence of the elements, as determined from correlation coefficients (Table 3), vertical distributions in the seams (Figure 6), and SEM-EDX are listed in Table 4. Association with the organic matter is the most common mode of occurrence. Cl, Zn, Mo and possibly Pb occur in this way, while Ni, Sr, W and the platinum group elements are associated to some extent with the organic matter. Cr is associated with the heavy minerals, possibly as chromite grains, while Cu, and in part Co, Ni, Sr, U, and Th are associated with the clay minerals. As, Cd and to some extent Co, Ni, Zr, and W are located in the sulphide minerals.

Humic acids are the main organic sites for trace element adsorption and complexation (11). As coalification proceeds and aromatisation increases, humic acid sites decrease in abundance. Association of trace elements with organic matter in coal therefore appears to be favoured in lower rank coals.

CONCLUSIONS

A strong association between the organic matter and both the minerals and trace elements in the Moose River Basin lignite was established. Minerals are detrital, syngenetic and epigenetic. Detrital and syngenetic minerals are fine grained and occur distributed throughout and intimately associated with the organic matter. Epigenetic pyrite, in contrast, is restricted to crack fills and could be readily removed from the coal.

Trace element concentrations are variable and association with the organic matter is the most common mode of occurrence. Elements are also associated with clay minerals, sulphides and heavy minerals.

REFERENCES

1 Finkelman R.B., 1980. Modes of occurrence of trace elements in coal. Unpublished Ph.D. thesis, University of Maryland, 301 p.

2 Harris L.A., 1982. The determination of mineral distributions in bituminous coals by electron microscopy. American Chemical Society 1982 Meeting, Preprints Division of Fuel Chemistry Vol. 27, No. 1.

3. Gluskoter H.J., Ruch R.R., Miller W.G., Cahill R.A., Dreher G.B. and Kuhn J.K., 1977. Trace elements in coal: occurrence and distribution. Illinois State Geological Survey, Circular 499. 154 p.

4. Mackowsky M-Th., 1982. IN Stach et al, 1982. Stach's Textbook of coal Petrology, 42B p.

5. Van der Flier-Keller E. and Fyfe W.S. Geochemistry of two Cretaceous coal-bearing sequences: James Bay Lowlands, N. Ontario and Peace River Basin, N.E. British Columbia, paper accepted by Canadian Journal of Earth Sciences.

6. Kuhn J.K., Fiene F. and Harvey R., 1978. Geochemical evaluation and characterization of a Pittsburgh No. 8 and a Rosebud seam coal. Department of Energy, Morgantown Energy Technology Center, document METC/CR-78/8, 40+ Xiiip.

7. Nicholls G.D. and Loring D.H., 1962. The geochemistry of some British Carboniferous sediments. Geochimica et Cosmochimica Acta, 26, pp. 181-223.

8. Miller R.N. and Given P.H., 1978. A geochemical study of the inorganic constituents in some low rank coals. Technical Report 1, U.S. Department of Energy Report FE-2494-TR-1, 314 p..

9. Goodarzi F., Foscolos A.E. and Cameron A.R., 1985. Mineral matter and elemental concentrations in Selected Western Canadian coals. Fuel, 64, pp. 1599-1605.

10. Glick D.C. and Davis A., 1985. Inorganic element content of U.S. coals: Geographic variability and statistical evidence for modes of occurrence. Abstract, GSA 1985. Annual Meeting, Orlando, Florida.

11. Szalay A., 1964. Cation exchange properties of humic acids and their importance in the geochemical enrichment of UO_{2+} and other cations. Geochimica et Cosmochimica Acta 1964. 28, p. 1605-1614.

Figure 1 SEM micrograph showing detrital quartz surrounded by clay minerals in woody lignite. Scale bar - 40 microns long.

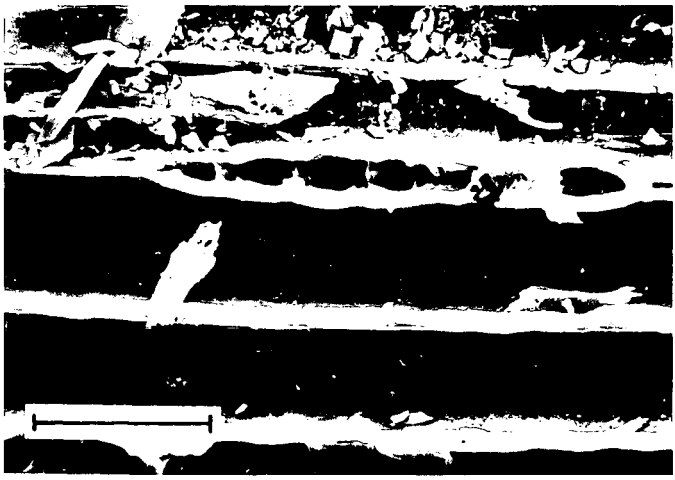

Figure 2 SEM micrograph showing clay minerals in fusinite. Scale bar -40 microns long.

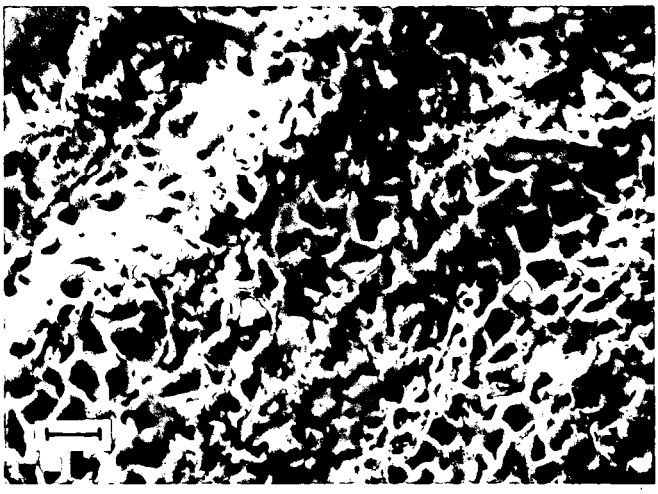

Figure 3 SEM micrograph showing pyrite crystals infilling cells in woody lignite. Scale bar - 40 microns long.

Figure 4 SEM micrograph showing a single pyrite crystal in a cell in woody lignite. Scale bar - 20 microns long.

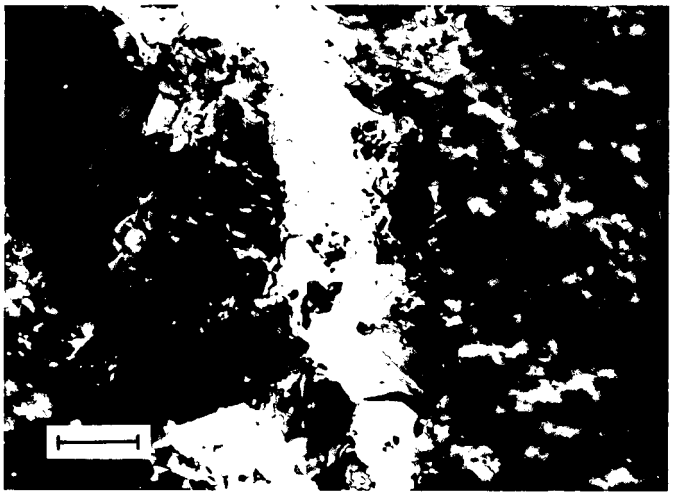

Figure 5 SEM micrograph showing pyrite infilling a crack in woody lignite. Scale bar - 40 microns long.

Table 1: Abundance and Mode of Occurrence of Minerals in the Moose River Basin lignite

	Abundance	Suggested Mode(s) of Occurrence
Quartz	P - ND	detrital infilling cell hollows
Kaolinite	P - ND	detrital authigenic (syngenetic)
Illite	T - ND	detrital
Mica	ND (T)	detrital
Mixed layer clay	T - ND	detrital
Pyrite	T - ND	infilling cell hollows replacing cell walls infilling cracks
Siderite	ND (T)	
Gypsum	ND (T)	recent weathering of pyrite
Gibbsite	ND (T)	authigenic-coating quartz grain surface

P : Major component.
T : Trace component.
ND : Not detected.
() : Mineral present at this level of abundance in only one sample.

Table 2: Summary of major and trace element data for the Moose River Basin lignites

Moose River Basin lignites (17 samples)					
Element %	Mean	Range			
SiO_2	8.57	0.34-30.20	ppm		
Al_2O_3	3.18	0.19-10.30	Cr	65.6	0.0 - 497.5
CaO	1.44	0.57- 3.41	Rb	5.9	0.0 - 20.0
MgO	0.30	0.11- 0.73	Sr	108.7	0.0 - 1000.0
Na_2O	0.02	0.00- 0.07	Zr	93.5	0.0 - 530.0
K_2O	0.06	0.01- 0.21	Cd	0.76	0.0 - 4.77
Fe_2O_3	1.77	0.24- 6.18	Co	35.9	5.0 - 197.5
MnO	0.01	0.00- 0.09	Cu	20.0	2.0 - 44.0
TiO_2	0.17	0.01- 0.80	Pb	25.1	5.0 - 155.0
P_2O_5	0.03	0.00- 0.25	Mo	5.9	5.0 - 15.0
LOI	83.59	55.50-97.40	Ni	47.4	4.2 - 190.7
S	1.44	0.45- 2.47	Zn	159.2	5.2 - 1311.2
ppb (18 ashed samples)			U	1.60	0.14 - 7.20
Au	13.6	1-96	Th	2.74	0.14 - 6.50
Pt	13.3	0-80	Mo	9.1	9.0 - 9.5
Pd	16.1	0-250	As	4.0	3.0 - 6.0
Ir	0.07	0-0.05	W	1.7	1.0 - 3.0

Table 3: Pearson correlation matrix for major and trace elements analysed in the Moose River Basin lignites

	SiO_2	Al_2O_3	CaO	MgO	K_2O	Fe_2O_3	MnO	TiO_2	P_2O_5	LOI	CR	Rb	Sr	Zr	U	Th	Co	Pb	Mo
SiO_2																			
Al_2O_3	.79																		
CaO																			
MgO		.95																	
Na_2O																			
K_2O																			
Fe_2O_3																			
MnO																			
TiO_2	.83	.78	.53	.51			.83												
P_2O_5																			
LOI	-.75	-.68																	
Cr							.54												
Rb		.66						.72											
Sr								.78				.57							
Zr							.68	.75			.57								
Th	.60	.75						.69											
Th/U				.54											-.60				
Cd																			
Co							.51				.94		-.53						
Cu	.52	.79						.60				.61				.85			
Mo																			
Ni											.65						.57		.55
Zn																			
S		-.64						-.57	-.75	.50			-.50		-.65	-.69		.54	

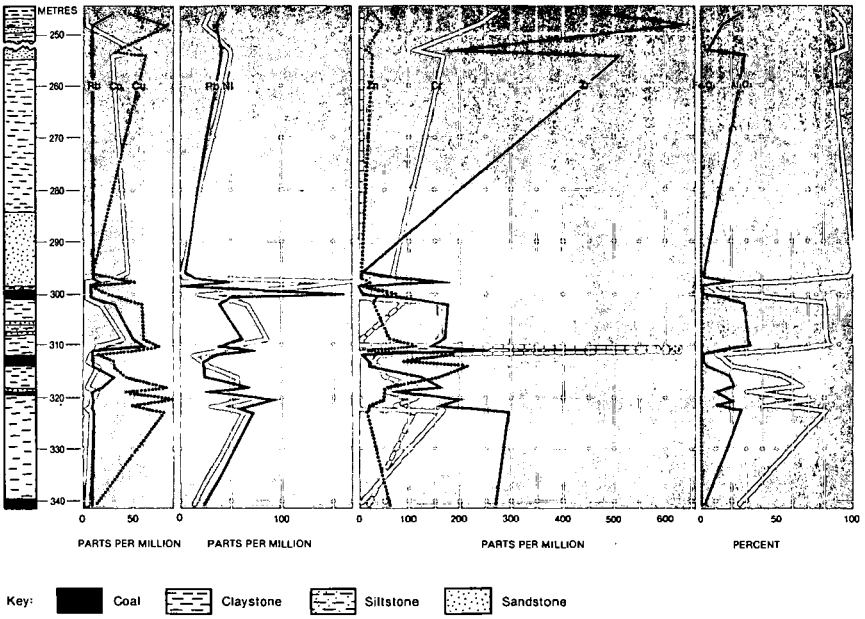

Figure 6 Vertical distributions of trace and major elements in samples from a drill hole (J-1-2) in the Moose River Basin

Table 4: Associations of trace elements in the Moose River Basin lignite

Element	Mode of Occurrence	Element	Mode of Occurrence
Cl	organics	Zr	pyrite
Cr	heavy minerals	Mo	organics
Co	sulphides	Cd	sphalerite
	clay minerals	W	sulphides
Ni	organics		carbonates
	clay minerals	PGE	detrital
	pyrite		organics
Cu	clay minerals	Pb	organics?
Zn	organics	U	clay minerals
As	supphides		carbonate
Rb	detritals	Th	clay minerals
Sr	carbonates		heavy minerals
	clay minerals		
	organics		

QUANTITATIVE ANALYSIS OF COAL AND COAL COMPONENTS BY SCANNING ELECTRON MICROSCOPY AND ELECTRON MICROPROBE ANALYSIS

By

F.R. Karner*!, H.H. Schobert*!!, C.J. Zygarlicke*!, J.L. Hoff*!, T.P. Huber*!

* University of North Dakota Energy Research Center, Grand Forks, ND 58202.
! Department of Geology and Geological Engineering, University of North Dakota, Grand Forks, ND 58202.
!! Department of Material Science and Engineering, Pennsylvania State University, University Park, PA 16802.

Introduction

Quantitative compositional data for coal typically consists of bulk chemical data for organic elements and analyses of the inorganic elements in ash. This paper focusses on bringing together procedures primarily using scanning electron microscopy (SEM) and electron microprobe analysis (EMPA) to obtain:

(1) The inorganic element content of bulk coal samples.

(2) The inorganic element content of specific lithotypes and macerals in coal.

(3) The abundance of macerals in coal (using standard petrographic techniques).

(4) The inorganic element content of specific mineral phases in coal.

(5) The abundance of mineral phases in coal.

SEM/EMPA techniques allow both inorganic analysis of bulk materials and determination of chemistry and abundance of microscopic constituents. This approach provides data on individual components which may be significant in assessing

the origin of a specific coal, its diagenetic and weathering history, and its behavior during utilization.

This paper summarizes a series of procedures which are combined to provide a more complete method of quantitative analysis of coal. Examples are presented that illustrate results of the use of these various procedures in understanding coal origin and utilization.

Methods

Methods summarized in this paper have been developed at the UND Energy Research Center and Department of Geology and Geological Engineering for a variety of applied coal science studies at the Center and academic research and thesis projects at the Department.

Sample Preparation: Sample preparation for analysis of bulk coal by EMPA has been described by Karner and others (1986). Samples were ground to a fine powder, vacuum-dried and compressed under 10 tons pressure to form two flat pellets for each standard and unknown coal. Samples for analysis of minerals in coal have been described by Kleesattel (1985) and Zygarlicke (In Preparation). Vacuum dried samples of low-rank coal were crushed by mortar and pestle to pass a 20 mesh screen. The coal was mixed with epoxy and pressed into cylindrical molds 25 mm in diameter. Vacuum impregnation and/or pressing was used to eliminate air bubbles. After hardening, the epoxy plugs were cut and polished using procedures dependent upon the materials studied. For mineral analysis and abundance determinations, standard procedures using water and oil as fluid media for sawing and grinding were followed (Zygarlicke, In Preparation). For

maceral abundance using light microscopy, standard ASTM techniques were utilized (Kleesattel, 1985). For analysis of inorganic elements in macerals, a series of procedures are being evaluated. Preliminary results show that water should not be used and that grinding and polishing dry or with minimal use of oil is best when Na and other easily removed elements are present. All samples for EMPA were carbon-coated.

Analysis of Bulk Composition by EMPA: A quantitative method for the analysis of the inorganic elements in bulk coal samples is given in Karner and others (1986). A peak-to-continuum (P/C) ratio method is used instead of standard ZAF correction procedures because of the heterogeneous character, low density, and light element composition of coal and other organic materials. Similar procedures have been developed by workers in the biological sciences (Hall, 1968; Russ, 1974; Statham and Pauley, 1978 and Small and others, 1980).

In the P/C method, as an initial approximation, continuum and characteristic radiation are similarly affected by changes in particle size, density and specimen thickness. The ratio of peak intensity; to continuum intensity is approximately constant for a given elemental concentration. A study of nine National Bureau of Standards (NBS) reference standards including four bituminous coals, two subbituminous coals and three dried plant materials was used to evaluate the P/C method (Karner and others, 1986). Operating conditions of a JEOL 35C microprobe system were 15 keV accelerating voltage and 920 picoamperes beam current. The probed area was approximately one square millimeter and the analysis time 400 seconds. A Kevex, lithium-drifted silicon, solid state detector was used with a Tracor-Northern TN2000 x-ray analysis system. The region 2.00

- 5.00 keV was used for measurement of continuum intensity. A reference library of pure element and oxide standard spectra was used with the Tracor-Northern XML least squares fitting routine to generate peak-to-continuum elemental ratios.

Analysis of the standards provided data to calculate the elemental composition of unknowns as well as a means of testing linearity of the plots of determined and expected concentrations for the standards. It was concluded (Karner and others, 1986) that the method performed well for Al, Ca, S and K; that a greater range of composition of standards was necessary to confirm the apparent good fit of Na, Mg, Si, P, Cl and Ti; and that Fe showed considerable scatter. More complete documentation of current standards and additional standards are necessary to improve results for the latter elements.

Analysis of Lithotype and Maceral Composition by EMPA: Early approaches to analysis of macerals by EMPA focussed on organic sulfur, for example studies by Sutherland (1975), Boenteng and Phillips (1976), Harris and others, (1977), Raymond and Gooley (1978) and Markuzewski and others (1981). Recent work is much more diverse and will not be surveyed in this paper. Our quantitative studies are based on the P/C approach outlined above and documented more completely in Karner and others (1986). The analytical procedure for lithotypes and macerals was identical to that for bulk coal except that smaller areas, typically from 20 to 70 square microns were used for analysis. Smaller areas and point analyses may result in observable beam damage to the specimen and larger areas typically are not homogeneous. Specific lithotypes are hand-picked and crushed into chips for analysis. Macerals were identified optically by examining

polished sections with a conventional reflected light microscope. However, macerals, particularly ulminite and vitrinite, were often easily recognized by their characteristic SEM secondary and/or backscattered electron images.

In order to obtain quantitative chemical data for lithotypes and macerals in sections of polished chips we have compared analyses of nearly homogenous materials prepared by two different methods as described above. Vitrain from the Hagel Bed at the Baukol-Noonan Mine near Center, N.D. was obtained from a single piece of fossilized wood about 10 cm in diameter. Megascopically, the vitrain was uncontaminated by extraneous material and came from a small zone in the wood. Part of the material was ground and analyzed as a sample of bulk coal and part was broken into chips and analyzed as the lithotype vitrain consisted essentially of the maceral ulminite. The results comparing bulk analysis and maceral analysis (Table 1) show that:

(1) Average chemical compositions by both methods were very similar particularly for Na, Mg, S, K, Ca and Fe. This observation supports the validity of the use of the technique for epoxy-mounted chips.

(2) Al, Si and Ti averaged 1.5 to 2.6 times as abundant in the powders as the vitrain chips showing that additional aluminosilicate mineral material was incorporated in the powders but was not present in the clear unfractured and unaltered areas of the chips which were selected for analysis. These observed variations suggest that further analysis of the distribution of aluminosilicate material in vitrain should be undertaken. Synthetic, homogeneous material of appropriate chemistry

should be sought to further test the relationship between analyses of powders and chips.

Analysis of Abundance of Macerals: Standard procedures of coal petrography modified for low-rank coals as described by Kleesattel (1985) must be used to determine the abundance of maceral types in low-rank coals.

Analysis of Mineral Phases by EMPA: Conventional microprobe techniques may be used in the study of minerals in coal. In practice, the same epoxy plugs used to analyze macerals are examined for mineral grains using secondary and back-scattered images. Size, shape, chemistry and association with other minerals and with macerals may be determined. Chemistry is determined using the previously described analytical procedures with matrix correction by conventional ZAF or Bence-Albee procedures.

Analysis of Abundance of Minerals: Standard methods of point counting adapted to the characteristics of the SEM/EMPA systems, and to the distribution of minerals in coal fragments were used. The automated stage of the SEM system was programmed to move the epoxy plug in increments of equal length under the stationary electron beam. A grid of analysis points was established so that 500 points on macerals and minerals were obtained over an area of 2.0 - 2.5 cm^2. Points on epoxy ranged up to 30 percent of those on macerals and minerals but were disregarded. An elemental energy spectrum was obtained at each point and used to distinguish between macerals, minerals, and epoxy. Data was recorded on a manual counter. Mineral spectra were acquired over a period of 50 seconds and stored on a floppy disk for detailed examination. Mineral spectra were

recorded separately as specific phases and all maceral spectra were recorded as coal. Low rank coals typically contained 3-4 minerals of major abundance and rarely had more than 10 different minerals. Many minerals had spectral patterns which were easily recognized. Clay minerals were most difficult to identify. Percentages of total oxides present were calculated by correction programs. Notable exceptions were H_2O and CO_2 affecting most strongly the analyses of clay minerals and carbonates. Combinations of maceral and mineral spectra were allotted to minerals if the oxide content exceeded 30 percent.

Application

The procedures described in this paper will enable a major advance in the analysis of coal and coal components, particularly in low-rank coals which contain relatively large amounts of inorganic elements which are organically bound. We have conducted several studies utilizing the recommended methods separately and are combining them in current studies. Two examples of the initial studies are summarized below.

Analysis of Macerals in Low-Rank Coals: The inorganic chemistry of huminite group macerals in four low-rank coals was summarized in Karner and others (1985a, 1985b, 1986). Analyses of ulminite representative of the Beulah-Zap (BZ) and Hagel (HG) lignites, ND, the Martin Lake (ML) lignite, TX, and vitrinite of the Rosebud (RB) subbituminous coal, MT were made using the P/C method (Karner and others, 1986). The results showed that the major huminite group maceral, ulminite or vitrinite, within a specific low-rank coal, has a relatively

high content of inorganic elements. The maceral composition within a coal has a limited range of variability and is distinct from that of other coals. A comparison of the four coals is discussed by Karner and others (1986). BZ ulminites have high Na and Fe and low S and total constituents, HG ulminites have high Ca and low Na and S, ML ulminites have low Na and high Mg, S and total constituents while RB vitrinite has moderate to low values for all elements. Within the coals, BZ and HG ulminites tend to occur as either low or high Na+Mg+Ca types, ML ulminite occurs as a low or high Al+Si type and RB vitrinite types vary from low to high Mg/Al ratio. The chemistry of the huminite group macerals and the bulk compositions of the four coals have striking similarities which are illustrated in Figure 1 (Karner and others, 1985b). BZ is a high Na and low S coal and its ulminite compositions plot relatively high in Na and relatively low in S compared to the other coals. Similarly, HG ulminite has low Na and high Ca and ML ulminite has low Na and high S matching the compositions of the respective coals. The P/C method provides a means to compare and relate the inorganic chemistry of whole coal and macerals. Such geochemical characterization may have great significance for the development of our understanding of coal formation and coal utilization.

Abundance of Minerals in the Harmon Lignite Bed: The SEM/EPMA mineralogy of the Harmon lignite bed from the Gascoyne Mine, ND has been determined by point-count methods by Zygarlicke (In Preparation). Ash, mineralogy and combustion data are given in Table 2. Sodium is the major factor determining fouling in North Dakota lignites. The White Pit and Blue Pit coals have different combustion behaviors and variable sodium contents. Sodium content is not an adequate guide for combustion behavior in this case. Normally one would expect the Blue

pit coal to have the strongest fouling tendency because of its higher sodium content, however, the White pit coal is much more severe in its fouling tendency. The severe fouling of the White Pit coal is thought to be a direct result of the high clay mineral and quartz contents of the coal. The Blue Pit coal which was less severe in its behavior had lower clay mineral and quartz contents. These observations may indicate that the greater availability of aluminosilicate material in the White pit coal allowed for the formation of much harder and more extensive ash fouling deposits. Quantitative information on the abundance of mineral phases is useful in interpreting behavior of coal during utilization.

References

1. Hall, T.A., 1968, Some Aspects of the Microprobe Analysis of Biological Specimens: in Heinrich, K.F.J., ed., Quantitative Electron Probe Microanalysis; N.B.S. Spec. Pub. 298, p. 269-299.

2. Harris, L.A., C.S. Yust, and R.S. Crouse, 1977, Direct Determination of Pyritic and Organic Sulphur by Combined Coal Petrography and Microprobe Analysis (CPMA) - A Feasibility Study: Fuel, v.56, p. 393-396.

3. Karner, F.R., D.R. Kleesattel, H.H. Schobert, and T.P. Huber, 1982a. Inorganic Chemistry of Huminite Group Macerals in Four Low-rank Coals of the Western United States. Geol. Soc. of Am. Abstracts with Programs v. 17, p. 623.

4. Karner, F.R., J.P. Hurley, D.R. Kleesattel, E.N. Steadman, and C.J. Zygarlicke, 1985, Distribution of Inorganics in Low-rank Coals. A.R. and T.D. Direct Utilization Contractors Review Meeting Report, United States Department of Energy, Office of Fossil Energy p. 70-71. (abstract).

5. Karner, F.R., J.L Hoff, T.P. Huber and H.H. Schobert, 1986, Electron Microprobe Technique for Quantitative Analysis of Coal and Coal Macerals. Am. Chem. Soc. Preprints of Papers, v. 31, no. 1. p. 29-34.

6. Kleesattel, D.R., 1985. Petrology of the Beulah-Zap lignite Bed, Sentinel Butte Formation (Paleocene) Mercer County North Dakota. Unpublished Master's Thesis, University of North Dakota. 188 p.

7. Markuszewski, R., L.J. Miller, W.E. Straszheim, C.W. Fan, T.D. Wheelock, and R.T. Greer, 1981, Evaluation of the Removal of Organic Sulfur from Coal: in Blaustein, B.D., B.D. Bockrath, and S. Friedman, eds. New Approaches in Coal Chemistry: Am. Chem. Soc. (Washington, D.C.), p 401-414.

8. Raymond, R., Jr., and R. Gooley, 1978, A Review of Organic Sulfur Analysis in Coal and a New Procedure: Scanning Electron Microscopy/1978/I: SEM Inc; AMF O'Hare (Chicago), p. 93-106.

9. Russ, J.C., 1974, The Direct Element Ratio Model for Quantitative Analysis of Thin Sections: in Hall, T.A., P. Echlin, and R. Kaufmann, Microprobe Analysis as Applied to Cells and Tissues, Academic Press (London), p. 269-276.

10. Small, J.A., K.F.J. Heinrich, D.E. Newburg, R.L. Myklebust, and C.E. Fiori, 1980, Procedure for the Quantitative Analysis of Single Particles with the Electron Probe, in Heinrich, K.F.J., ed., Characterization of Particles, N.B.S. Spc. Pub. 533, p. 29-38.

11. Statham, R.J., and J.B. Pawley, 1978. A New Method for Particle X-ray Microanalysis Based on Peak to Background Measurements: Scanning Electron Microscopy/1978/I; SEM Inc., AMF O'Hare (Chicago), p. 469-478.

Table I. Results of Microprobe Analyses Comparing Weight Percentages of Elements Determined in Ground Samples Versus Epoxy-mounted Chips of Vitrain

ELEMENTS	AVERAGE FOR FOUR AREAS OF GROUND POWDER PELLET	AVERAGE FOR SINGLE AREAS ON EACH OF FIVE GRAINS
Na	0.34	0.39
Mg	0.30	0.26
Al	0.74	0.28
Si	0.14	0.09
S	1.28	1.42
K	0.03	0.03
Ca	1.18	1.16
Ti	0.05	0.02
Fe	0.07	0.07

Table 2. Ash, Mineral and Combustion Data for Gascoyne Mine Lignite

	White Pit	Blue Pit	Red Pit
Quartz	10.06	3.34	2.35
Kaolinite	1.12	0.39	0.39
Montmorillonite	0.70		
Pyrite	1.41	2.23	2.23
Illite	0.77		
Unknown Clay Mineral		0.39	
Gypsum			1.04
Hematite		0.78	
Chlorite			0.44
Total Minerals*	14.07	7.14	6.45
Ash*	17.10	10.12	10.30
Na_2O**	3.50	6.90	2.70
Fouling Tendency	Severe	High	Medium

*Weight percent of coal
**Weight percent of ash

FIGURES

Figure 1. S-Na-Ca Plot of Characteristic Ulminite Types in Beulah-Zap and Hagel Lignites, North Dakota, Martin Lake Lignite, Texas and Vitrinite in the Rosebud Subbituminous Coal Montana.

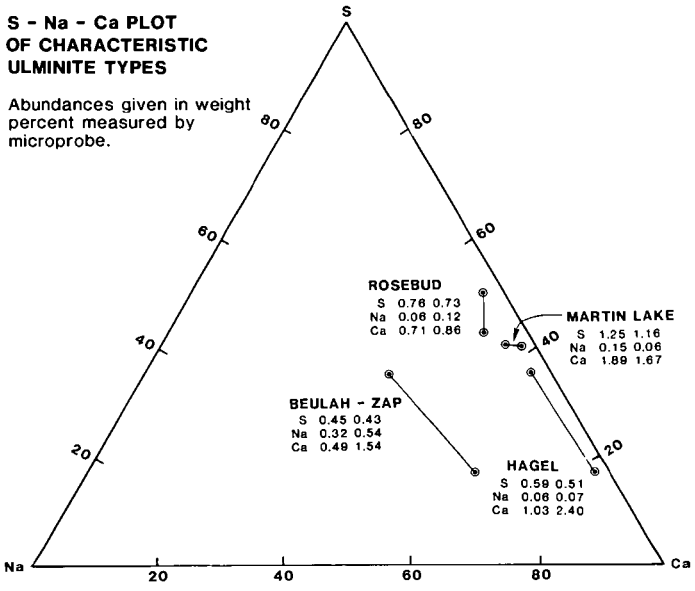

Characterization of Mineral Matter in Sub-bituminous Coals by AIA-SEM

W. E. Straszheim, J. G. Yousling, K. A. Younkin, and R. Markuszewski

Ames Laboratory, Iowa State University, Ames, IA 50011

ABSTRACT

Automated image analysis (AIA) was used with scanning electron microscopy (SEM) and energy-dispersive x-ray spectroscopy to characterize the mineral matter in two western sub-bituminous coals from the Adaville No. 11 seam (Kemmerer, WY) and the Dietz No. 1 & 2 seams (Decker, MT). The samples were ground to -200 mesh and cleaned by float-sink separation at 1.40 and 1.38 sp. gr., respectively. The particles were characterized before and after cleaning for mineral phase and size distributions by classifying them into 6 sizes and 16 mineral categories. Quartz was the dominant mineral in both coals, with the Adaville sample containing primarily quartz and an iron-rich mineral. Traces of apatite were also detected in the Adaville samples. The Dietz coal contained primarily quartz and kaolinite. Preliminary results are also presented for the association of the mineral particles with the coal matrix. These analyses were performed by automatically classifying the composite mineral-coal features into 10 types of particles of increasing specific gravity. The results closely estimated the total mineral matter content, as calculated from the ASTM ash content, and the specific gravity distributions were consistent with data obtained from the cleaning step.

INTRODUCTION

Scanning electron microscopy (SEM) in conjunction with energy-dispersive x-ray spectroscopy can provide in-situ characterization of mineral particles in coal for size, shape, chemical identity, and relation to the coal matrix. Automated image analysis (AIA) techniques are currently available to permit rapid SEM characterization of statistically significant numbers of particles, providing data for the size distribution of individual minerals as well as for the the total mineral matter content. These data can aid in the decision-making process about the extent of grinding needed for effective liberation of mineral matter from coal. AIA-SEM has a decided advantage over other techniques, such as the ASTM ash determinations which provide no information on the original mineral or size distributions, or x-ray diffraction or FTIR analyses which require time-consuming sample preparation but cannot provide size information. Since the AIA data permit cleaning effectiveness to be evaluated with respect to both mineral phase and particle size, problems with the removal of certain particle sizes or phases can be detected and remedied.

AIA-SEM has been used previously at the Ames Laboratory for the characterization of several series of physically and chemically processed bituminous coals (1-3). In this study, AIA-SEM was applied to two sub-bituminous coals before and after physical cleaning. In addition, preliminary results are presented for the direct measurement of the extent of association of mineral particles with coal.

EXPERIMENTAL

Coal Sample Description

Two coals, from the Adaville No. 11 seam (Kemmerer, WY) and from the Dietz No. 1 & 2 seams (Decker, MT), were ground to nominal 200 mesh (~70-80% less than 74 μm), typical of coals introduced into pulverized fuel boilers, and were cleaned in a halogenated hydrocarbon to produce a superclean product with a target ash level of ~3%, using specific gravities of 1.40 and 1.38, respectively. The raw and clean coal fractions were analyzed by standard ASTM techniques for moisture, ash, and sulfur levels (see Table 1). Because both raw coals had low levels of sulfur and moderate levels of ash, typical of western coals, only ~56% of the mineral matter was removed from the Adaville coal, and only ~30% of the mineral matter was removed from the Dietz coal.

Table 1. Analyses of Raw and Cleaned Coals[a]

	Adaville No. 11		Dietz No. 1 & 2	
	Raw	Clean	Raw	Clean
Rank	subB		subA	
Moisture	22.15	11.29	19.82	11.96
Pyritic S	0.03	0.01	0.02	0.02
Sulfate S	0.03	0.01	0.02	0.01
Organic S	0.81	0.70	0.51	0.36
Total S	0.86	0.71	0.56	0.40
Ash	9.20	4.07	5.31	3.70
Mineral Matter[b]	10.41	4.60	6.01	4.19
% MM Removed	---	55.81	----	30.28

[a] Values are expressed as wt. % on a dry basis, except for moisture which is presented on an as-received basis.
[b] Calculated by modified Parr formula, as defined in ref. 4: Mineral matter = 1.13(ash) + 0.47(pyritic sulfur)

Procedures

Since details of the AIA-SEM mineral analyses were described elsewhere (1,2), only the mineral-coal association analysis procedure will be described in this paper. One set of coal-epoxy pellets was prepared using standard petrographic techniques for the AIA mineral study. A second set of pellets was prepared for the association study of the mineral particles with the coal. For these pellets, 2 g. of coal were mixed with 8 g. of melted Carnauba wax, placed in a 1-in. diameter mold under pressure, and allowed to cool. The solid pellets were ground to expose a cross section, polished, and coated with ~50 Å of carbon to provide a conductive surface for SEM examination.

Analysis Hardware. In addition to the AIA-SEM system previously described (1,2) for mineral analyses, a LeMont Scientific OASYS image analyzer system was employed for the mineral-coal association studies. The OASYS image analyzer can process entire images at a time, whether they be from an SEM or a TV camera, and can analyze up to 16 different gray-levels of particles with capabilities for image enhancement and processing.

SEM Conditions. For both types of studies, samples were analyzed in the SEM with an accelerating potential of 25 kV and a beam current of ~4 nA, using the backscattered electron signal since it is especially sensitive to the average atomic number of a phase in a polished cross section. Therefore, mineral particles stand out much brighter than coal particles.

AIA-SEM Association Analyses. The LeMont OASYS image analyzer was used for the preliminary automated association studies. A minimum of 24 fields were digitized for each sample over a range of magnifications from 50x to 300x and recorded on magnetic disk. Thousands of coal and mineral particles were represented by these images.

The intensity of the backscattered electron signal was divided into four segments of increasing brightness to encompass signals from the mounting medium, the coal particles, most minerals, and finally pyrite. The OASYS "Linescan" software package was used to measure the area of associated coal, pyrite, and other mineral particles for each composite feature while keeping track of the association of the individual features. A pixel density of 512 points across the screen was fixed by the OASYS hardware.

Composite coal-mineral features were assigned by the relative abundance of the phases, determined according to gray level, into one of six specific gravity classes (<1.3, 1.3-1.4, 1.4-1.5, 1.5-1.6, 1.6-1.7, and 1.7-1.8) or into four special classes (pure coal, pure pyrite, pure "other" minerals, or a pyrite/mineral mixture). Composites were also classified into the same six size ranges used for the mineral analyses.

RESULTS AND DISCUSSION

Mineral Analyses

The AIA results for the raw and cleaned Adaville and Dietz coals presented in Tables 2a-c and 3a-c, respectively, provide much more insight into the nature of the mineral matter in these samples than do the ASTM results. The data presented are for minerals in the raw coal, minerals in the clean coal, and the percent removal of mineral matter in each size-mineral class. In all cases, the data are presented as weight percent of dry coal.

In Table 2a, results for the raw Adaville coal indicate that the primary mineral phases are quartz and an iron-rich phase. No conclusive identification is presently available for the iron-rich phase, but iron hydroxides are likely candidates. These mineral matter characteristics are in contrast to previous findings for midwestern bituminous coals (1,2), in which the predominant minerals were pyrite, quartz, kaolinite and illite. The particle size distribution of the minerals was notably coarse; about 44% of the mineral matter was larger than 36 μm.

The AIA results also showed the presence of apatite. The amount found was small (0.62% of the dry coal), but it was confirmed by the presence of very small peaks at the appropriate locations in x-ray diffraction patterns. Although this mineral is not unusual for western coals and it does not pose any particular environmental hazard, its detection at such low levels is interesting and demonstrates the utility of the AIA-SEM technique for detecting small amounts of discrete phases as they occur disseminated throughout a matrix. The other minerals in the raw coal were present in smaller amounts and consisted of kaolinite, illite, montmorillonite, pyrite, and other miscellaneous phases.

Table 2a. AIA Results for Raw Adaville Coal (200 mesh x 0), Expressed as Weight Percent of Dry Coal

Mineral Phase	Size, μm <4	<7	<12	<21	<36	>36	TOTALS
PYRITE	0.04	0.00	0.01	0.01	0.01	0.05	0.12
KAOLINITE	0.04	0.11	0.06	0.11	0.09	0.13	0.53
ILLITE	0.00	0.04	0.03	0.02	0.02	0.21	0.32
MONTMORILLONITE	0.00	0.00	0.02	0.02	0.04	0.18	0.26
QUARTZ	0.32	0.42	0.20	0.35	0.47	1.68	3.44
APATITE	0.04	0.04	0.06	0.07	0.07	0.35	0.62
FE-RICH	0.07	0.14	0.09	0.15	0.16	1.57	2.18
SILICATES	0.00	0.00	0.02	0.04	0.03	0.11	0.20
OTHER	0.46	1.30	0.29	0.33	0.14	0.25	2.76
TOTALS	0.95	2.03	0.77	1.10	1.03	4.53	10.41

Table 2b. AIA Results for Clean Adaville Coal (Floated at 1.4 Sp. Gr.), Expressed as Weight Percent of Dry Coal

Mineral Phase	Size, μm <4	<7	<12	<21	<36	>36	TOTALS
PYRITE	0.02	0.02	0.01	0.02	0.01	0.00	0.08
KAOLINITE	0.08	0.11	0.04	0.02	0.02	0.00	0.27
ILLITE	0.02	0.02	0.01	0.01	0.00	0.00	0.05
MONTMORILLONITE	0.01	0.00	0.00	0.00	0.00	0.00	0.01
QUARTZ	0.68	0.94	0.34	0.48	0.37	0.09	2.90
APATITE	0.05	0.14	0.02	0.01	0.00	0.00	0.22
FE-RICH	0.10	0.12	0.04	0.03	0.01	0.00	0.31
SILICATES	0.03	0.04	0.01	0.01	0.01	0.00	0.10
OTHER	0.12	0.30	0.07	0.07	0.06	0.04	0.66
TOTALS	1.10	1.69	0.54	0.66	0.48	0.13	4.60

Table 2c. Percent Removal of Mineral Matter from Adaville Coal

Mineral Phase	Size, μm <4	<7	<12	<21	<36	>36	TOTALS
PYRITE	31	--	45	-242	14	100	33
KAOLINITE	-115	-9	33	78	80	100	48
ILLITE	--	57	62	51	100	100	83
MONTMORILLONITE	--	--	92	93	100	100	95
QUARTZ	-114	-124	-73	-37	23	95	16
APATITE	-29	-295	58	91	100	100	66
FE-RICH	-46	12	54	80	93	100	86
SILICATES	--	--	48	70	60	100	49
OTHER	73	77	77	79	55	84	76
TOTALS	-16	17	30	40	54	97	56

Table 3a. AIA Results for Raw Dietz Coal (200 mesh x 0), Expressed as Weight Percent of Dry Coal

Mineral Phase	Size, μm <4	<7	<12	<21	<36	>36	TOTALS
PYRITE	0.07	0.05	0.10	0.00	0.07	0.07	0.35
KAOLINITE	0.16	0.23	0.28	0.50	0.20	0.00	1.38
ILLITE	0.02	0.01	0.06	0.02	0.15	0.00	0.26
QUARTZ	0.21	0.24	0.22	0.43	0.59	0.36	2.05
CALCITE	0.11	0.09	0.08	0.03	0.00	0.00	0.31
SILICATES	0.04	0.06	0.05	0.01	0.06	0.00	0.22
OTHER	0.46	0.42	0.29	0.20	0.07	0.00	1.44
TOTALS	1.07	1.12	1.07	1.19	1.13	0.43	6.01

Table 3b. AIA Results for Clean Dietz Coal (Floated at 1.38 Sp. Gr.), Expressed as Weight Percent of Dry Coal

Mineral Phase	Size, μm <4	<7	<12	<21	<36	>36	TOTALS
PYRITE	0.04	0.05	0.06	0.10	0.00	0.00	0.25
KAOLINITE	0.06	0.14	0.18	0.23	0.22	0.12	0.95
ILLITE	0.00	0.01	0.02	0.03	0.00	0.00	0.06
QUARTZ	0.27	0.30	0.29	0.28	0.11	0.00	1.24
CALCITE	0.03	0.03	0.03	0.03	0.02	0.00	0.14
SILICATES	0.09	0.05	0.04	0.01	0.00	0.00	0.19
OTHER	0.41	0.46	0.14	0.11	0.17	0.06	1.36
TOTALS	0.90	1.04	0.76	0.80	0.52	0.18	4.19

Table 3c. Percent Removal of Mineral Matter from Dietz Coal

Mineral Phase	Size, μm <4	<7	<12	<21	<36	>36	TOTALS
PYRITE	35	2	30	--	100	100	74
KAOLINITE	60	31	29	48	-23	--	22
ILLITE	75	-15	64	-47	100	--	73
QUARTZ	-44	-39	-49	28	80	100	32
CALCITE	72	66	52	-6	--	--	51
SILICATES	-178	15	12	-14	100	--	4
OTHER	1	-22	46	34	-186	--	-5
TOTALS	6	-4	20	25	49	83	30

For the Adaville coal (Tables 2a-c), little of the mineral matter finer than 36 μm was removed. In the raw coal, 44% of the mineral matter was larger than 36 μm in diameter. From ASTM data (Table 1), only 56% of the mineral matter was removed. Data in Tables 2a-c show that removal of mineral matter from the >36 μm size class accounted for 76% of all the mineral matter removed; the removal was progressively less for the smaller size classes.

The Dietz coal shows similar trends (Tables 3a-c). The mineral matter in the raw coal was dominated by quartz, followed by kaolinite, and then other minerals. However for this coal, the mineral matter was spread over the entire particle size range. Only 26% of the mineral matter was in the two largest size classes (i.e., >21 μm). Of the 30% of the mineral matter was removed during cleaning, 47% was due to the removal of particles larger than 21 μm. Much smaller reductions in mineral matter are noted for the finer size ranges.

It would appear that for both raw coals, the mineral particles were disseminated widely throughout the coal and were intimately associated with the organic matter, so that even at a nominal size of 200 mesh, relatively little mineral matter could be removed by float-sink cleaning. Use of AIA to measure directly the extent of mineral-coal association should help to confirm this.

Association Studies

Preliminary results from the association studies of minerals and coal are given in Table 4. The data are weight fractions of dry coal measured for each particle type. In Table 5, data are presented for comparing ASTM and direct AIA measurements of pyrite and mineral matter content. AIA mineral content was obtained by calculating a weighted area fraction of pyrite and mineral particles as compared to all particles in the cross section. The pyrite estimates of the AIA mineral study were taken from Tables 2a-3b, which were normalized to the mineral matter content calculated from ASTM ash values. The data show reasonable agreement among the measurements, given the preliminary nature of this study, lending credence to the validity of the association results in Table 4. Further work is in progress to improve the agreement.

Summing the weight fractions of the classes of the raw coals (in Table 4) that are lighter than 1.4 sp. gr. should predict the yield for the separation process, that is, 80.41% for the Adaville and 95.28% for the Dietz coal. Actual recovery data are not available for these samples so that direct comparison is not possible. Such data will be secured for future tests. Summing the fractions heavier than 1.4 specific gravity for the clean coals should estimate the amount of minerals misplaced during cleaning. Since less than 1% of the Adaville and less than 2% of the Dietz coals fall in this category, these values appear quite consistent with a float-sink separation for a nominal 200 mesh particle size.

The direct association program appears to have correctly classified the composite mineral particles into specific gravity classes for the Adaville coal. Significant material was found for most particle types in the raw coal, but it was concentrated in the lighter classes for the clean coal.

The results for the Dietz coal were quite different. Virtually the same amount of material was analyzed as being lighter than 1.4 sp.gr. for both the raw and clean coals (95.28% and 98.67%, respectively). In the raw coal, ~2.2% of the dry coal was analyzed as "Mineral matter-rich" (2.08%) plus "(Mineral + Pyrite)-rich" (0.12%). That material alone could account for the reduction of mineral matter from 6.01% to 4.19%, as shown in Table 1. It appears that this level

Table 4. Preliminary Analysis of the Association of Mineral Particles with Coal (Weight Percent of Dry Coal in Each Particle Type Class as Assigned by Gray Level)

Particle Type	Adaville 11 raw	Adaville 11 clean		Dietz 1 & 2 raw	Dietz 1 & 2 clean	
Pure coal	35.06	41.42		76.49	69.70	
<1.3 sp.gr.	31.49	53.00	95.28	13.20	25.48	98.67
1.3-1.4 sp.gr.	13.86	4.99		5.59	3.49	
1.4-1.5 sp.gr.	7.54	0.23		1.60	0.48	
1.5-1.6 sp.gr.	6.47	0.06		0.37	0.19	
1.6-1.7 sp.gr.	0.96	0.05		0.18	0.05	
1.7-1.8 sp.gr.	1.44	0.03	0.59	0.35	0.03	1.31
Mineral matter-rich	2.98	0.19		2.08	0.55	
Pyrite-rich	0.00	0.00		0.00	0.00	
(Mineral + Pyrite)-rich	0.17	0.03		0.12	0.01	
	99.97	100.00		99.98	99.98	

Table 5. Comparison of Direct AIA Measurements of Mineral Matter and Pyrite Content with ASTM Values

	Adaville 11 raw	Adaville 11 clean	Dietz 1 & 2 raw	Dietz 1 & 2 clean
Mineral Matter				
AIA[a]	11.37	2.97	4.00	2.43
ASTM[b]	10.41	4.60	6.01	4.19
Pyrite				
AIA[a]	0.19	0.03	0.13	0.04
AIA[c]	0.12	0.08	0.35	0.25
ASTM[d]	0.06	0.02	0.04	0.04

[a] from OASYS association analyses
[b] from Table 1, as calculated by modified Parr formula
[c] from AIA mineral analyses (Tables 2a-3b)
[d] calculated from ASTM pyritic sulfur content in Table 1

of mineral matter reduction could also have been achieved if the separation had been conducted at a higher specific gravity.

The distribution of mass over the entire range of densities is noteworthy for the two raw coals. A strong bimodal distribution indicates good liberation. In this sense, the mineral particles in the Dietz coal appear to be more liberated than those of the Adaville coal (76.49% vs. 35.06% pure coal particles, respectively, in Table 4). Also, there is no significant "middlings" material for the raw Dietz coal (i.e., in the 1.4-1.6 density range). It would appear that even though more mineral matter was removed from the Adaville coal, it must have been at a cost of lower recovery.

CONCLUSIONS

AIA-SEM was used to obtain a direct insight into the character of mineral matter with respect to both mineral phase and particle size distribution for two western coals. Significant differences were seen in the mineral phases in the raw Adaville and Dietz coals; also, major differences were observed in the size distributions. For example, minerals in the Adaville sample appeared to be much coarser. This technique permitted characterization of low levels of mineral matter that resulted from deep cleaning and documented the selective removal of mineral matter of certain sizes. Correlation of the mass fraction of larger mineral particles and the amount of mineral matter removed suggests that only the larger mineral particles were liberated.

The AIA-SEM technique was used to measure directly the extent of coal mineral association and to produce a particle type distribution curve, relatable to specific gravity, for both raw and clean coals. The direct measure of mineral matter and pyrite content agreed reasonably well with ASTM results. These results indicate that minerals in the raw Dietz coal were more liberated from the coal matrix than those in the Adaville coal.

ACKNOWLEDGEMENTS

Ames Laboratory is operated for the U. S. Department of Energy by Iowa State University under Contract No. W-7405-Eng-82. This work was supported by the Assistant Secretary for Fossil Energy, Division of Direct Coal Utilization, through the Pittsburgh Energy Technology Center (PETC). The authors wish to thank Professor D. L. Biggs (I.S.U.) for collecting the coal samples and J. Cavallaro (PETC) for cleaning the coal samples by float-sink separation.

LITERATURE CITED

1) W. E. Straszheim and R. Markuszewski, "Application of Scanning Electron Microscopy and Automated Image Analysis for Characterization of Mineral Matter in Coal", Am Chem Soc Div Fuel Chem Preprints, 30(1), 47-55 (1985).

2) W. E. Straszheim, J. G. Yousling, and R. Markuszewski, "Analysis of Ash-Forming Mineral Matter in Raw and Supercleaned Coals by Automated Image Analysis-Scanning Electron Microscopy", in The Chemistry of Mineral Matter and Ash in Coal, K. S. Vorres, ed., American Chemical Society: Washington, D. C., 1986, pp. 449-461.

3) R. Markuszewski, D. R. Mroch, G. A. Norton, and W. E. Straszheim, "Coal Desulfurization and Demineralization by Molten Caustic Mixtures", in Environmental Concerns in Fossil Fuel Utilization, R. Markuszewski and B. D. Blaustein, eds., American Chemical Society: Washington, D. C., 1986, pp. 42-50.

4) P. H. Given and R. F. Yarzab, "Analysis of the Organic Substance of Coals: Problems Posed by the Presence of Mineral Matter", In Analytical Methods for Coal and Coal Products, Karr, C. Jr., ed., Academic Press: New York, 1978, Vol. II, pp. 3-41.

THE ROLE OF HEAT OF IMMERSION CALORIMETRY AND GAS ADSORPTION IN DETERMINING THE SURFACE AREAS OF A THERMALLY TREATED LIGNITE AND SUPERCRITICALLY SOLVENT EXTRACTED LOW-RANK COAL RESIDUES

Charles Tye, Dana J. Maas, Michael L. Swanson

University of North Dakota
Energy Research Center
Box 8213, University Station
Grand Forks, ND 58202

ABSTRACT

Comparative surface area data can be obtained from the exothermic heat liberated when a solid substance is immersed in a suitable liquid penetrant. This heat of immersion is dependent on the heat of wetting plus other effects. The apparent surface of a sample is proportional to the heat of wetting term. The surface areas determined by this method provide an explanation of results of thermal treatment and supercritical solvent extraction of low-rank coal.

The thermally treated samples were prepared by drying Indian Head (North Dakota) lignite at 330°C with hot nitrogen gas at atmospheric pressure or with hot water under pressure. Lignite and subbituminous coal samples were also supercritically solvent extracted in a semicontinuous extraction system at temperatures of 250° to 380°C and reduced pressures between 1.05 and 2.00 in methanol, benzene, and cyclohexane. These samples were then tested in a specially constructed heat of immersion calorimeter. Nitrogen Brunauer Emmett and Teller (BET) gaseous adsorption derived surface areas were also compared with the results from the calorimeter.

INTRODUCTION AND EXPERIMENTAL

The surface areas determined in this study served as a valuable tool with which to explain the results obtained from thermal, and supercritical, low-rank coal treatments. Two techniques were used to determine the surface area of coal before and after processing. Heat of immersion calorimetry was used extensively to obtain coal surface areas and results were compared to those from the more standard gaseous adsorption method for the thermally treated samples.

Determination of Surface Area by Heat of Immersion

Differential heat of immersion calorimetry (1) is a way to find specific surface, in square meters per gram, by measurement of the heat released when the surface is wetted by a liquid. This fairly precise measurement is an indication of the number of molecules needed to coat the surfaces of cracks or pores. Since smaller pores limit the accessibility of molecules of increasing size and complexity, the rate and extent of heat released by the wetting process can be used as a measure of pore size distribution and hence a surface area determination.

The differential heat of immersion calorimeter consists of two Dewar flasks, each with its own stirrer, heater, and temperature sensor. An equal amount of liquid is put into each Dewar flask, both imbedded in a massive aluminum heat sink, and the coal or carbon sample is added to one Dewar only. Temperature is measured by a matched pair of thermistors forming opposing arms of a Wheatstone bridge. The heat liberated when the solid sample is added to the working Dewar produces a current imbalance which is recorded directly. Figure 1 shows a cross-sectional view of one calorimeter.

Determination of Surface Areas by Gaseous Adsorption

Historically, it has been known that a porous solid can take up relatively large volumes of a condensable gas. Freshly calcinated charcoal, cooled under mercury, has the property of adsorbing several times its own volume of various gases. This is because the molecules in the surface layer of a solid are bound on one side to inner molecules of the solid and bound to nothing on the surface side, creating an imbalance of atomic and molecular bonding forces on the surface side. Therefore, surface molecules attract gas, vapor, or liquid molecules in order to satisfy these unbalanced, bonding forces. The attraction may be either physical or chemical, depending on the system involved and the temperature employed.

Physical adsorption (Van der Waal's adsorption) is the result of a relatively weak interaction between a solid and a gas. This type of adsorption has one primary characteristic. Essentially all of a gas adsorbed can be removed by evacuation at the same temperature at which it was adsorbed, but the quantity of physically adsorbed gas at a given pressure increases with decreasing temperature. Consequently, adsorption measurements for the purpose of determining surface area of pore size distributions are made at a low temperature.

The physical adsorption of a gas on a smooth surface will continue as the gas pressure is increased at a constant temperature until a condensed layer, 5 or 6 molecules thick, is formed. If the surface contains cracks, crevices, or pores, the adsorbed layer will fill these as its thickness increases. The smaller pores will be engulfed first and, progressively, the larger ones will fill. Filling occurs because a concave liquid surface has a lower vapor pressure than a flat surface. When a pore fills, its surface area becomes a negligible contribution to the measured surface area. Conversely, the pore surface contribution again comes into play as adsorbed gas layers are removed (desorbed) and pore walls are re-exposed.

Continuing the adsorption by incremental steps as described earlier to, or nearly to, the saturation point yields a complete adsorption isotherm. Reversing the procedure by subjecting the sample to stepwise reductions in pressure while continuing to record volumes and equilibrium pressures permits obtaining the desorption isotherm. Adsorption and desorption isotherms coincide precisely only when the solid is completely nonporous and there are no contact points among particles creating the effect of pores.

Thermal Treatments of Coal

Raw lignite from the Indian Head Mine in North Dakota was thermally dewatered using hot nitrogen at atmospheric pressure and hot water under pressure to investigate the amenability of fuel slurry preparation of the dried product (2, 3). Products dried at 330°C and 340°C were used in the present study. Results of the proximate and ultimate analyses of the raw coal and the thermally dewatered samples are given in Table 1.

The hot-gas-dried sample was prepared by treating the Indian Head lignite, sized to 7mm x 10mm, at 330°C under a nitrogen atmosphere, and was conducted using a laboratory-scale fixed-bed coal dryer at atmospheric pressure. This drying apparatus consisted of a 3.8 cm ID by 152 cm long vertical drying chamber that was jacketed for rapid heat-up and cooldown using steam and cold water, respectively. Experimental details have been published elsewhere (2).

The objective of the hot-water drying process, (HWD) as with the hot-gas drying process, is to increase the energy density of low-rank coal/water slurries by changing the chemical and physical surface characteristics of the coal, allowing significantly higher solids content in a water slurry. Surface area measurements of the raw and treated coals are important, since a decreased coal surface means less water is required to wet the coal during slurry preparation.

TABLE 1

PERTINENT TEST DATA AND ANALYSIS OF RAW AND THERMALLY DEWATERED INDIAN HEAD LIGNITE

Treatment	Raw	Hot Nitrogen	Hot Water
Drying Temperature °C	---	328	340
Drying Pressure, psia	---	4	2400
Drying Apparatus		1.0 lites Fixed Bed	2.2 mt/day Pilot Plant
Equilibrium Moisture Content, Wt %	35.0	27.3	16.2
Proximate Analysis, wt % moisture free (mf) basis			
Ash	14.5	13.0	22.0[2]
Volatile matter	47.5	39.7	34.6
Fixed Carbon (by diff.)	38.0	47.3	43.4
Ultimate Analysis, wt % moisture ash free (maf)			
Carbon	72.1	74.1	75.2
Hydrogen	4.9	4.9	4.8
Nitrogen	1.5	1.4	1.4
Sulfur	1.5	1.4	1.6
Oxygen (by diff)	20.0	18.2	17.0
Heating Value, maf basis			
MJ/kg	28.7	29.1	29.6
Btu/lb	12,350	12,500	12,700

[2] Feed coal for the pilot-plant test was a high ash Indian Head lignite.

Process development unit (PDU) runs, using the HWD principle, were typically 120 hours in duration including start-up and shutdown; three tons of coal were usually processed. A schematic of the PDU is shown in Figure 2. The feed to the PDU was a slurry containing a 50/50 mixture, by weight, of deionized water and pulverized coal (80% less than 75 microns). The products, after treatment for 5 minutes at temperatures between 270° to 340°C and corresponding pressures between 800 and 2400 psig, were concentrated and formulated into fuel slurries containing between 55 and 65 wt% coal solids on a dry basis. The sample used in this study was treated at 330°C. A more detailed description of the PDU operation has been published elsewhere (4).

Supercritical Solvent Extractions

Supercritical solvent extractions were performed using a semicontinuous extraction system in which the HPLC grade solvent, i.e. methanol, benzene, cyclohexane, etc., was passed through a fixed bed of coal while under supercritical conditions. The coals extracted in these experiments were Indian Head lignite and Wyodak subbituminous coal (Campbell Co., WY) which had been sized between -60 and +325 mesh. Proximate and ultimate analyses for these coals are given in Table 2. The flowsheet for this test system is shown in Figure 3. The fixed bed of coal was contained in a 25.4 cm by 1.75 cm ID section of high-pressure tubing which held approximately 50 gm of coal between two one-micron sintered metal frits. Supercritical conditions were achieved in approximately seven minutes by immersing the solvent preheating coils and the fixed bed of coal in a preheated fluidized sand bath in a such manner that no solvent flow through the bed of coal occurred during start-up. A Ruska positive displacement pump and high-pressure piston accumulator were used to provide a pulseless flow of solvent through the system once supercritical conditions were obtained. An extraction time of two hours and a solvent flow rate of 120 cc/hr were typically used in these experiments. The pressure of the supercritical solvent and the extracted material was reduced to atmospheric pressure after passing through a back pressure regulator where the extract and solvent were collected in a chilled sample vessel. The volume of noncondensible product gas was measured and collected for analysis by gas

TABLE 2

PROXIMATE AND ULTIMATE ANALYSES OF COALS USED IN SUPERCRITICAL SOLVENT EXTRACTION EXPERIMENTS

	Sample Name and Location	
	Indian Head Mercer Co., ND	Wyodak Campbell Co., WY
Proximate Analysis, MF, (wt%)		
Volatile Matter	43.8	43.5
Fixed Carbon	48.0	50.0
Ash	8.2	6.5
Ultimate Analysis, MF, (wt%)		
Hydrogen	4.74	4.26
Carbon	66.20	64.62
Nitrogen	0.96	1.01
Sulfur	0.72	0.58
Oxygen (Ind)	19.19	23.04
Ash	8.2	6.5

chromatography. After each experiment, the extracted residue and the solvent extract mixture were rotary vacuum distilled at 0.6 psia and 80°C and weighed. This procedure allowed solvent and moisture-free products to be obtained for material balance purposes.

Table 3 summarizes the operating conditions and results from supercritical solvent extraction experiments performed on Indian Head lignite and Wyodak subbituminous coal using three solvents: methanol, benzene, and cyclohexane. The results indicate that the weight loss of the original coal (and the corresponding extract yield) increased with increasing pressure. This would be expected due to the rapidly increasing solvent density experienced by solvents in the supercritical region. However, the increasing weight loss of the coal observed with increasing temperature resulted in spite of a decreasing solvent density. This indicates that temperature has a larger effect on conversions than on solvent densities, particularly at temperatures between 300° to 350°C. Thus, in this temperature range, thermal decomposition of the coal becomes significant, resulting in the liberation of smaller and more soluble fractions from the coal.

RESULTS AND DISCUSSION

Thermally Treated Samples

Table 4 shows the results of the surface area determinations by heat of immersion calorimetry for raw Indian Head lignite and the two thermally treated samples.

TABLE 4

Sample	Heat of Immersion (cal/gm)	Surface Area (m^2/gm)
As-mined Coal	14.3	153
340°C Hot-water-dried Coal[a]	9.2	98
330°C Hot-nitrogen-dried Coal	24.5	263
340°C Hot-water-dried (freeze dried)	16.0	171

[a] The HWD coal was separated from slurry by filtration; the filter cake was then air dried to remove surface moisture.

The surface area for the raw lignite sample was determined to be 153 sq. meters/gram. A similar determination on the 340°C HWD Indian Head coal showed a surface area of 98 sq. meters/gram. The hot-nitrogen-dried (HND) sample (evaporatively dried) showed a surface area value of 263 sq. meters/gram.

Evaporatively drying the coal with nitrogen at 330°C, but at atmospheric pressure, increased the apparent surface area of the coal. This increase was probably due to the volatilization and removal of coal tars and waxes which otherwise may have been filling or sealing some of the coal micropores. This explanation is in accordance with observations made during the drying experiments. Accumulations of waxes and tars were apparent in the outlet piping of the fixed-bed coal dryer, and in the condensate recovered when the hot-nitrogen was quenched (5). Therefore, drying low-rank coal with 330°C nitrogen increased the coal surface areas because tars were extracted with the hot-gas stream. Vacuum freeze drying and air drying were both used for sample preparation on the HWD coal.

TABLE 3

OPERATING CONDITIONS AND RESULTS FROM SUPERCRITICAL EXTRACTION EXPERIMENTS ON INDIAN HEAD AND WYODAK COALS USING SELECTED SOLVENTS

Coal	Temp. (°C)	T_r[a]	Pressure (psia)	P_r[b]	Calc. Solvent Density (g/ml)[c]	Pct. Conv. (maf)[d]	Pct Yield, maf	
							Extract	Gas
Solvent: Methanol								
Indian Head	250	1.021	1760	1.50	0.368	4.17	3.05	1.36
Indian Head	250	1.021	2350	2.00	0.412	5.49	3.80	1.66
Indian Head	250	1.021	2935	2.50	0.434	6.13	4.43	2.23
Indian Head	300	1.118	2350	2.00	0.224	9.55	4.74	6.91
Indian Head	350	1.216	2350	2.00	0.144	23.30	12.43	22.04
Solvent: Cyclohexane								
Indian Head	291	1.020	885	1.50	0.421	6.7	2.14	4.7
Indian Head	291	1.020	1180	2.00	0.465	9.1	2.50	4.6
Indian Head	291	1.020	1480	2.50	0.489	9.1	2.68	4.9
Indian Head	307	1.048	1180	2.00	0.425	10.8	2.64	4.6
Solvent: Benzene								
Wyodak	300	1.020	745	1.05	0.185	10.8	4.62	2.0
Wyodak	300	1.020	1420	2.00	0.511	11.1	7.57	1.8
Wyodak	350	1.109	745	1.05	0.112	15.9	6.31	4.0
Wyodak	350	1.109	1420	2.00	0.345	17.2	10.8	4.4

[a] $T_r = \frac{\text{operating temperature of solvent (°K)}}{\text{critical temperature of solvent (°K)}}$;

[b] $P_r = \frac{\text{operating pressure of solvent (psia)}}{\text{critical pressure of solvent (psia)}}$

[c] Calculated using Lee-Kesler generalization of the Benedict-Webb-Rubin Equation of state.

[d] % conversion $\frac{\text{wt maf coal} - \text{wt maf residue}}{\text{wt maf coal}}$ (100); % yield = $\frac{\text{wt maf product}}{\text{wt maf coal}}$ (100)

The process of vacuum freeze drying was found to increase the surface area of the HWD coal; and in fact, the surface area determined was found to be in excess of that determined for the raw coal (171 sq meters/gram versus 153 sq meters/gram). This last result indicates that the tars and waxes evolved during hot-water coal drying migrate out of the pores to the coal surface where they plug or cap micropore entrances when cooled and resolidified. Freeze drying the HWD coal in a vacuum, as compared to air dyring, removes at least some of these tars and exposes the pore entrances. This is believed to occur because the gases and water trapped in the pores expand and push tar away from the pore entrance when the sample is put in a vacuum. The volume of the newly exposed pores includes the added volume vacated when the tars migrated to the surface of the coal. Additional pore volume is also created when carboxyl groups in the coal matrix decompose and liberate carbon dioxide.

Measurements of the coal surface area before and after hot-water drying at 340°C have shown that the surface area is decreased by 50% due to the hydrothermal treatment and the subsequent capping of pores. The discovery that pore capping by the exuded coal tars was occurring helped to explain the mechanism of increased energy density after hot-water drying of low-rank coal. Until this discovery, pore collapse was believed to produce the decreased surface area in the treated coal particles.

Supercritically Solvent Extracted Samples

Supercritically solvent extracting Indian Head lignite with methanol produced two major results. First, increasing the extraction pressure while keeping the temperature constant, increases the surface area of the supercritically extracted lignite residues. Secondly, an increase in the extraction temperature, while keeping the pressure constant, decreases the surface area. The data listed in Table 5 shows the effect of changing the methanol extraction pressure while keeping the temperature constant. The effect of changes in the methanol extraction temperature at a constant pressure are shown by the data listed in Table 6.

TABLE 5

EXTRACTION OF INDIAN HEAD LIGNITE WITH METHANOL

Extraction Parameters		Surface Area By Heat of Immersion, m^2/gm
Temperature, C°	Pressure, psig	
250	1761	105.6
250	2348	120.7
250	2935	138.4

TABLE 6

EXTRACTION OF INDIAN HEAD LIGNITE WITH METHANOL

Extraction Parameters		Surface Area by Heat of Immersion, m^2/gm
Pressure, psig	Temperature, °C	
250	2348	120.7
300	2348	110.5
350	2348	97.5

As presented in Table 7, the use of cyclohexane to extract Indian Head lignite at constant temperature and increasing extraction pressure increased the measured surface area. The data in Table 8 show that changes in the surface area of a subbituminous coal, after extraction with benzene, were similar to those exhibited by lignite. As extract pressure is increased at a constant temperature, the surface area increased and as extract temperature was increased at constant pressures the measured surface area decreased.

TABLE 7

EXTRACTION OF INDIAN HEAD LIGNITE WITH CYCLOHEXANE

Extraction Parameters		Surface Area By Heat of Immersion, m^2/gm
Temperature °C	Pressure, psig	
291	887	86.1
291	1182	97.7
291	1478	118.9
307	1182	97.2

TABLE 8

EXTRACTION OF WYODAK SUBBITUMINOUS COAL WITH BENZENE

Extraction Parameters		Surface Area by Heat of Immersion, m^2/gm
Pressure, psig	Temperature, °C	
300	746	109.9
300	1420	129.4
350	746	95.7
350	1420	111.8

Finally, a comparison of the heat of immersion calorimetry results was made with the gas adsorption results. The surface areas (BET) for Indian Head lignite extracted in methanol are listed in Table 9. The BET surface areas obtained by nitrogen gas adsorption correlate with the heat of immersion calorimetry-derived surface areas, but are two orders of magnitude lower in value. The higher measured coal surface areas determined by heat of wetting of methanol compared to values obtained by the BET method is a common phenomenon (8).

TABLE 9

COMPARISON BETWEEN NITROGEN GAS ADSORPTION: BRUNAUER, EMMETT AND TELLER (BET) AND HEAT OF IMMERSION DERIVED SURFACE AREAS

EXTRACTION OF INDIAN HEAD LIGNITE WITH METHANOL

Extraction Parameters		Surface Area	
Temperature, °C	Pressure, psig	(BET), m^2/gm	Heat of Immersion, m^2/gm
250	1761	1.36	105.6
250	2348	1.56	120.7
250	2935	2.07	138.4
300	2348	1.47	110.5
350	2348	1.12	97.5

SUMMARY AND CONCLUSIONS

Surface area determinations of supercritical residues indicate that increasing extraction pressure increases the surface area of the extracted residues. For a solvent under supercritical conditions, solvent density increases rapidly with increasing pressure, thus the solubility of larger molecular species can be greatly enhanced with increasing pressure. The increase in surface area which occurs with pressure is probably due to the ability of the supercritical solvents to extract significantly larger molecules from the coal, opening more of the micropores to access by the penetrant. Conversely, a decrease in the residue surface area was observed with increasing extraction temperatures. Increasing methanol extraction temperatures has been shown to alter the surface functional groups left in the residue (6,7). Thus, some of this decreasing surface area could be due to the decrease in functional groups with which the penetrant can hydrogen bond. However, the nitrogen adsorption surface area determinations (which are unaffected by surface-penetrant interactions) also decreased with increasing temperature, indicating that these interactions are a small part of the measured heat of immersion. The decreased surface area is probably due to the extraction temperatures approaching the temperature where the coal tars become plastic and partially obstruct some of the micropores of the coal.

ACKNOWLEDGEMENTS

The supercritical solvent extraction work and the pilot-scale hot-water drying work were supported by the U.S. Department of Energy under Cooperative Agreement No. DE/FC21/83FE60181. The hot-nitrogen drying work was supported by the Electric Power Research Institute under project no. 2470-1.

REFERENCES

1. Tye, C, Neuman, R. and Schobert H.H. The Uses of Dielectic Spectra and Immersional Calorimetry in the Characterization of Low-Rank Coals. ACS National meeting Division of Fuel Chemistry, Miami Beach, Fl., May 1985.

2. Low-Rank Coal-Water Slurries For Gasification. EPRI AP-4262, Project 2470-1, Final Report, November 1984.

3. Sears, R.E., et. al., Production and Combustion of Hot-Water-Dried Low-Rank Slurries, Proceedings of 13th Biennial Lignite Symposium, Bismarck ND, May 21-23, 1985.

4. Potas, T. A., et. al., Pilot Scale Preparation of Lignite and Subbituminous Coal/Water Fuels. Eighth International Symposium on Coal Slurry Fuels Preparation and Utilization, Orlando, FL, May 1986.

5. Low-Rank Coal-Water Slurries For Gasification, Phase II. Project 2470-1, Final Report, June 1986, to be published.

6. Olson, E.S., Swanson, M.L., Olson, S.H. and Diehl, J.W. Reactions of Low-Rank Coals in Supercritical Methanol. A.C.S. Division of Fuel Chemistry Preprints, Anaheim, CA, Sept. 1986, p. 64-69.

7. Swanson, M.L., Olson, E.S. and Diehl, J.W. Supercritical Solvent Extraction. Final Report. OOE/FE/60181-2095, June 1986.

8. Malherbe, P. LCR. Fuel, Lond. 30 (1951) p. 97.

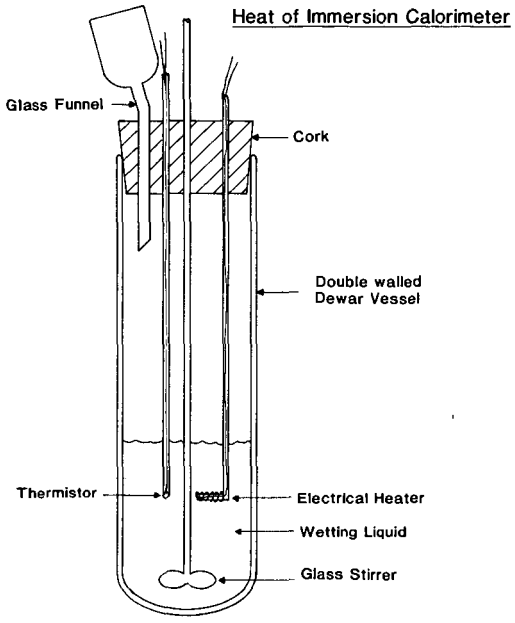

Figure 1. Heat of Immersion Calorimeter.

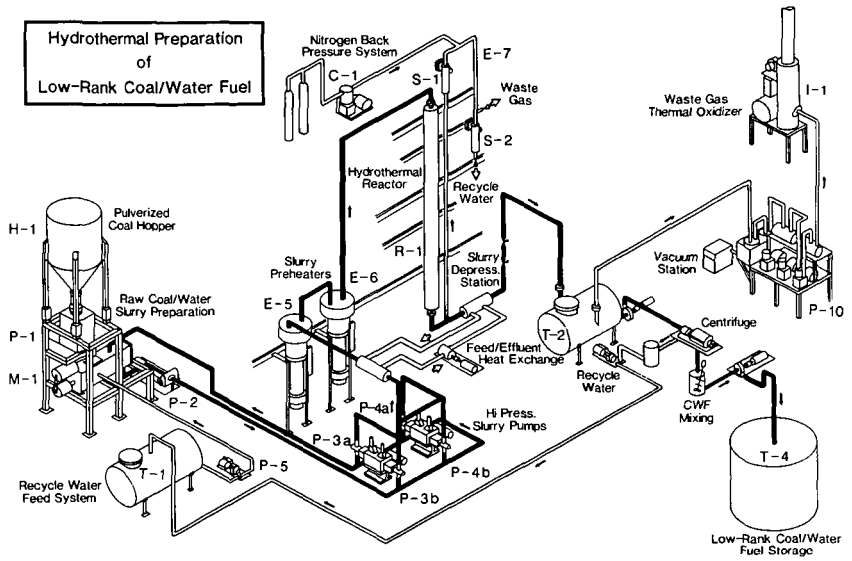

Figure 2. Hyrothermal Preparation of Low-Rank Coal/Water Fuel.

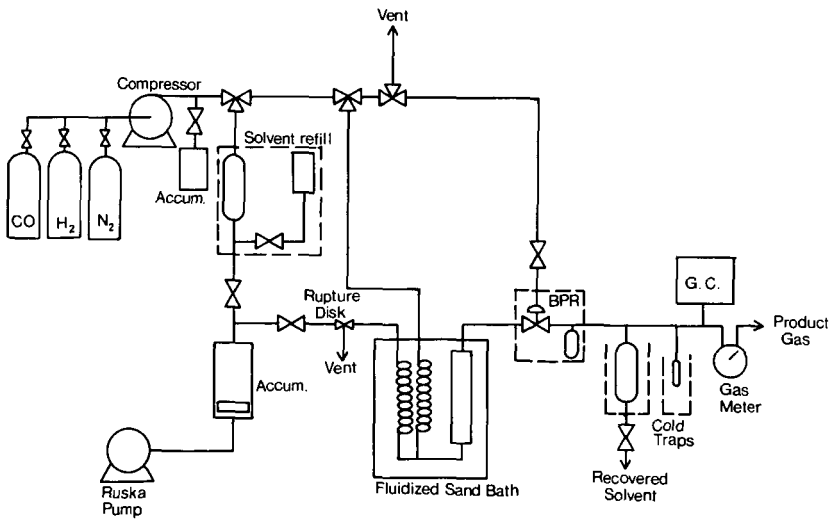

Figure 3. Supercritical Solvent Extraction Apparatus.

SMALL ANGLE X-RAY SCATTERING FROM BROWN COAL

M. REICH, I.K. SNOOK AND H.K. WAGENFELD

Department of Applied Physics
Royal Melbourne Institute of Technology,
124 Latrobe Street, Melbourne, Victoria, 3000, Australia.

Small angle X-ray scattering has been widely used in the past to study the structure of porous materials. The interpretation of the scattering data has been usually been in terms of models based upon discrete pores (1). As it is now recognized, such models are inadequate to describe a complex system such as coal and in this paper we propose to interpret the X-ray scattering from brown coal in terms of fractal concepts.

The use of fractals to describe naturally occurring geometric forms (2) has led to the recent introduction of fractal theory to describe the scattering from porous substances. A fractal interface displays self-similarity at different scales. Electron micrographs at different magnifications show that brown coal appears to be predominantly fractal in structure (the exceptions being the occasional large fossilized skeletal remnant). As parameters such as the surface area are not uniquely defined for a fractal interface it is necessary to use more relevant parameters such as the fractal or Hausdorff dimension to characterize a fractal interface. The Hausdorff dimension is a measure of the irregularity of the interface and varies between 2 for a smooth interface to 3 for a rough convoluted interface. Various scattering studies of coal and other porous materials exhibit a power law dependence upon angle and this has been interpreted as being a result of the material's fractal properties. The fractal dimension can be calculated directly from the power law dependence and the extent of the interface can be determined from the intensity of the scattering.

Figures 1 and 2 show the scattering curves for solar dried brown coal slurries which have undergone two different sample preparation procedures. The 1mm thick samples have been embedded in plastic and polished until the coal surface has been exposed. From the best fit to the scattering data in the angular range 0.4 to 6 mrad we have derived values for the Hausdorff dimension of 2.35 and 2.44. This is somewhat lower than the value of 2.56 reported for North America lignite (3) and suggests that the structure of Victorian brown coal is less convoluted and more "graphitic" than North American lignite. It was also found that the intensity of scattering for two samples of compacted solar dried slurries differed by a factor of 10 procedures. This suggests that the extent of the interface differs by approximately 10 even though the Hausdorff dimensionality derived from the scattering curves for the two samples are not markedly different.

The correlation of the measured Hausdorff dimensions with physical properties of coal will be an interesting avenue for exploration in the future.

References

1. Setek,M., Wagenfeld,H.K., Stacy,W.O. and Kiss,L. Fuel 1983, 62, No.4, 480.

2. Mandlebrot,B.B., The Fractal Geometry of Nature (Freeman, New York, 1982).

3. Bale,H.D. and Schmidt,P.W., Phys. Rev. Letts., 1984, 53, No.6, 596.

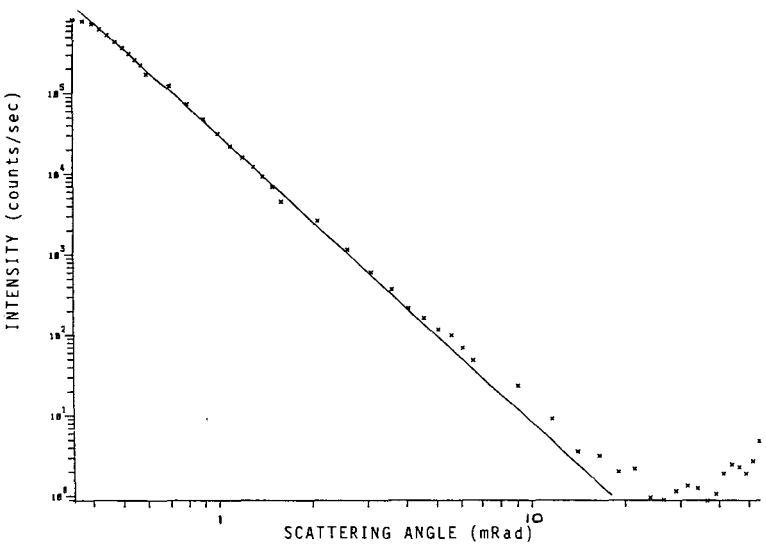

Fig. 1 The scattering curve for ultra-fine ground solar dried coal slurry. The line of best fit corresponds to a Hausdorff dimension of 2.44.

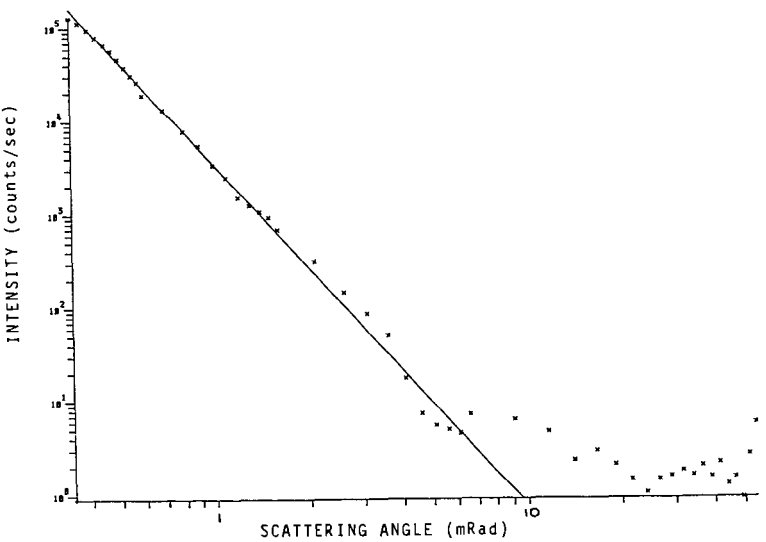

Fig. 2 The scattering curve for alkali-digested solar dried coal slurry. The line of best fit corresponds to a Hausdorff dimension of 2.35.

PYROLYSIS/GAS CHROMATOGRAPHY/MASS SPECTROMETRY OF A SERIES OF BURIED WOODS AND COALIFIED LOGS THAT INCREASE IN RANK FROM PEAT TO SUBBITUMINOUS COAL.

by

Patrick G. Hatcher
Harry E. Lerch, III
Rama K. Kotra
U.S. Geological Survey, 923 National Center
Reston, Virginia 22092
and
T. Vincent Verheyen
Coal Corporation of Victoria, Switchback Road,
Churchill, Victoria, Australia 3842

INTRODUCTION

To better understand the coalification process, we have conducted numerous studies (1-4) of the chemical structural composition of xylem tissue from gymnosperm wood and related woods that has been coalified to varying degrees. These previous studies have relied primarily on use of solid-state ^{13}C nuclear magnetic resonance methods to obtain average chemical structural information as wood is buried in peat and then transformed to coal. The samples included xylem tissue from modern wood buried in peat, xylite brown coal, lignitic wood, subbituminous coalified logs, and from several logs of high volatile bituminous coal rank.

The studies presented here, a continuation of the above studies, examine the chemical nature of buried and coalified xylem tissue at the molecular level. To achieve this, we employed pyrolysis/gas chromatography (py/gc) and pyrolysis/gas chromotography/mass spectrometry (py/gc/ms). Pyrolysis techniques have been used to examine peat, coal, coalified wood, and related substances (5-7). However, the technique has not been previously applied to a systematic and histologically-related series of coalified woods. It is particularly useful to compare the results from pyrolytic studies with the data obtained from solid-state ^{13}C NMR (1-4,8).

METHODS

Approximately 0.2 mg of dry, powdered sample of modern buried wood and coalified xylem tissue, whose nature and rank were described in earlier reports (2-4), were weighed into a quartz capillary tube and placed in the coil of a Chemical Data Systems Model 120 Pyroprobe.* The probe, with sample, was inserted into the injection port of either a Perkin-Elmer Sigma 3B or a Varian 2700 gas chromatograph. The injection port temperature was maintained at 280°C. The Perkin-Elmer gas chromatograph, fitted with a 25 m x 0.25 mm i.d fused silica column (HP-17) coated with a crosslinked 50 percent phenylmethyl-silicone liquid phase, was used strictly for py/gc using a flame ionization detector (FID) whose output was recorded with a Perkin-Elmer Sigma 15 recording

* Any use of trade names is for descriptive purposes and does not imply indorsement by the U.S. Geological Survey.

integrator. The Varian gas chromatograph was fitted with the same column but the effluent stream was split. One part of the effluent was swept by means of a helium make-up gas into a jet separator and into the source of a DuPont 490B mass spectrometer. The other part of the effluent was routed to an FID interfaced to a Perkin-Elmer Sigma 10 recording integrator.

Following insertion of the pyroprobe into the injection port, the gas chromatograph was heated at 8°C/min to 300°C to sweep out compounds volatile at injection-port temperatures. After cooling to room temperature and applying liquid nitrogen to the front end of a portion of the fused-silica column, the sample was pyrolyzed at 610°C for 10 sec. The column was immediately temperature-programmed from 40°C to 300°C at 4°C/min.

Further py/gc/ms analyses were performed on a Hewlett-Packard 5970B/5890 gc/ms system equipped with an identical Chemical Data Systems pyroprobe and similar column as above (25m x 0.25mm SGE, BP-5). Samples were flash pyrolyzed at a filament temperature of 710°C for 20 sec. Prior to temperature-programming (20°-80°C at 8°C/min) the column was held at 20°C for 5 min. After reaching 80°, the column was programmed to 310°C at 4°C/min. Compounds were identified by comparing relative retention times with pyrolysis data in the literature (9) and by comparison to mass spectra from the EPA/NIH library as well as from published data (10). Gas chromatographic peak areas for identified compounds were measured as a percentage of the total peak area calculated by summing areas for all peaks. No corrections were made for FID response factors.

RESULTS

Peat and Brown Coal

Representative py/gc chromatograms for gymnosperm xylem tissue buried in peat and brown coal xylite are shown in Figure 1. The solid-state ^{13}C NMR spectra for these samples are shown in Figure 2. The buried gymnosperm xylem tissue was shown to be essentially lignin-like in composition (3) as indicated by the NMR peaks at 56, 120, 135, and 148 ppm. The peaks at 72 and 106 ppm, minor contributors to the total peak area, indicate that much of the cellulosic material originally present in the unaltered wood has been degraded and lost during burial, as shown by Hedges *et al.* (9), Hatcher *et al.* (11), and Spiker and Hatcher (12). The py/gc data confirm this as the peaks identified are essentially those characteristic of softwood lignin (13). Guaiacol, 4-methyl guaiacol, 4-ethylguaiacol, 4-vinyl guaiacol, *trans*-isoeugenol, acetoguaiacone, and *trans*-coniferyl alcohol are the major py/gc components. The low amounts of phenol, cresol, and catechol as well as the relatively large amounts of coniferyl alcohol attest to the fact that the lignin is relatively undegraded (13). Peaks directly related to lignin-derived products (*e.g.* methoxyphenols) account for about 95% of the total peak areas in buried wood. The broad peak tentatively identified as that of levoglucosan indicates that some carbohydrate-like material is present, consistent with the NMR data.

Brown coal xylite, a log belonging to the *Podocarpacea* family collected from the Yallourn seam, Morwell, Victoria, Australia, shows an NMR spectrum that is only slightly different from that of modern buried wood (Figure 2). The principal differences are for the intensity of methoxyl carbons at 56 ppm and the peak at 115 ppm for protonated aromatic carbons *ortho* and *para* to aryl-O carbons. The smaller amount of methoxyl carbons relative to total aromatic carbons (100-160 ppm) for the brown coal xylite, compared to the modern buried wood, is an indication that methoxyl groups have been lost from lignin structures. This assumes that the lignin of coniferous wood originally had approximately the same amounts of methoxyl groups per aromatic ring as

lignin from modern buried wood. The peak at 72 ppm, mostly that of carbohydrate carbon, is significantly reduced in relative intensity compared to that in the spectrum of buried wood.

The py/gc data for the xylite brown coal (Figure 1) confirm that methoxylated phenols are still major components. Guaiacol, 4-methylguaiacol, 4-vinylguaiacol, and trans-isoeugenol are the four largest components like in the pyrogram for modern buried wood. Other lignin-derived methoxyphenols found in buried wood are also present; however, the yield of these lignin phenols normalized to total phenols is 88 percent, slightly less than that of buried wood. Phenol and the cresols are relatively larger peaks in pyrograms of brown coal xylite compared to buried wood (Figure 1). This is evident from the ratio of lignin phenols to simple phenols. In the modern buried wood this ratio is high but in the brown coal xylite sample it drops to approximately half of the value for the modern buried wood. The methoxyl content determined by NMR and normalized to total aromatic carbon intensity also decreases by half. This indicates that either aromatic rings in lignin are losing methoxyl groups or that methoxylated phenols are being selectively lost during coalification. Either way, the end result is that lignin phenols are becoming smaller contributors to total phenol yields on pyrolysis.

Lignites

Gymnosperm wood coalified to a rank of lignite displays an NMR spectrum that shows a progressive loss of methoxyl carbon when compared to spectra of lignin or brown coal xylite. The samples examined are lignitic logs collected from various locales along the eastern United States (2,4), and a representative NMR spectrum is shown in Figure 3 for a sample collected from the Patapsco Formation (Cretaceous) near Landsdowne, Maryland. The aryl-O carbons at 150 ppm are major contributors, and the area for the peak at 56 ppm for methoxyl carbon is small compared to the area for aryl-O carbons at 146 ppm. This indicates that methoxylated phenols are minor compared to other phenols.

Intensity of the peak at 146 ppm, compared to total aromatic intensity, is nearly the same for lignite logs as it is in the modern buried wood. A ratio of the area for the peak of 146 ppm to the total aromatic carbon area (100-160ppm) shows that approximately 2 aryl-O carbons are present per aromatic ring. This indicates that the proportion of aromatic carbons having an attached oxygen (1/3 of aromatic carbons) does not change from buried wood to lignite even though a precipitous decline in methoxyl groups is observed. This loss of methoxyl groups and retention of aryl-O most likely involves a demethylation reaction rather than demethoxylation and the resultant chemical structures would resemble catechol-like structures.

The pyrolysis data for lignitic gymnosperm woods is consistent with the NMR data showing loss of lignin-like components (Figure 4). Peaks for guaiacol, 4-methylguaiacol, 4-vinylguaiacol, and trans-isoeugenol are significant peaks but phenol, the cresols, and dimethylphenols are much more significant components than they are in buried wood or brown coal xylite. The presence of eugenol and isoeugenols in lignitic logs is evidence that lignin exists in nearly unaltered form with the propyl side chain preserved.

Though methoxyphenols account for about half of total phenols, the presence of simple phenols such as phenol, the cresols, and dimethylphenols indicates that coalification leads to the production of phenolic structures and these most likely originate from methoxyphenols. As discussed above, the NMR data suggest the formation of catechol-like structures from the guaiacyl units in gymnosperm lignin via demethylation. The pyrolysis data show evidence for the presence of catechol, as has been reported in other lignitic logs (14).

The presence of significant amounts of catechol only in lignitic logs indicates it might be diagnostic of specific structural intermediates in the conversion of lignin phenols to the aromatic structures that are dominant in most coals.

Subbituminous Coal

Gymnosperm xylem tissue of subbituminous coal rank from several samples shows a characteristic ^{13}C NMR spectrum, and Figure 3 depicts a representative NMR spectrum for a sample collected from the Doswell Formation (Triassic) near Taylorsville, Virginia. The primary peak is for aromatic carbons at 130 ppm, but aryl-O carbons appear as a small peak at about 150 ppm. The intensity of this aryl-O peak is significantly less than in lignite samples described above. The calculated intensities suggest that approximately one in six aromatic carbons have an attached oxygen, a strong indication that simple phenols are primary chemical structural elements. The exact chemical shift of this aryl-O carbon is also characteristic of specific structural arrangements. In lignitic logs the peak is at 146 ppm, a chemical shift characteristic of two aryl-O carbons adjacent to each other as in methoxyphenols and catechols. For logs of subbituminous coal rank this peak shifts to 153 ppm which is characteristic of aryl-O carbons having no adjacent aryl-O carbons such as simple phenols. The lack of significant intensity in the NMR region of 50 to 100 ppm suggests that few oxygen-substituted aliphatic carbons are present and that methoxyl groups are gone. This suggests that the propyl side chain of lignin has been modified and that methoxyphenols are no longer present.

The py/gc data (Figure 4) confirm the above NMR observations as the primary pyrolysis products (greater than 50 percent of total pyrolysis products) are phenol, the cresols, dimethyl phenols, C_3-phenols, and C_4-phenols. Using py/gc/ms we were unable to detect the presence of methoxyphenols characteristic of lignin or the catechols as observed in lignite. It is likely that the phenols originate from lignin structural units, but these have been modified by loss of methoxyl groups. The lack of catechol in pyrolysis products of subbituminous logs suggests that the catechol-like structures thought to be in lignite have been converted to phenol-like structures via loss of one hydroxyl group per aromatic ring. This is entirely consistent with the NMR data which show an average of 1 aryl-O carbon per aromatic ring.

The major pyrolysis products are phenol and the cresols, but an intense peak in the pyrogram of subbituminous logs is identified as an unresolved mixture of 2,4-dimethylphenol and 2,5-dimethylphenol. The py/gc/ms data suggest that the major contributor to this peak is 2,4-dimethylphenol. The overwhelming amount of 2,4-dimethylphenol, compared with other dimethylphenol isomers, indicates that a specific structural arrangement is retained during alteration of catechol-like structures to phenol-like structures.

DISCUSSION

Py/gc and py/gc/ms have proven to be valuable techniques for characterizing the chemical composition of coal and coal macerals (5,6,9,14-16). Applying this technique to a series of histologically-related coalified logs that increase progressively in rank has allowed us to chart the evolution of lignin from modern buried wood to subbituminous coal. Because the xylem tissue from each of the samples is from gymnosperm wood, we can be reasonably certain that each sample has organic matter derived from a common component, namely lignin composed primarily of guaiacyl structural units. Accordingly, we can make comparisons among the samples and speculate on the chemical transformations that must have occurred during coalification of this gymnosperm lignin. Of course, we must assume that extraneous substances derived from non-lignin sources have not been incorporated to any significant extent.

Both the pyrolysis data and the NMR data shown here and recent studies (10,11) convincingly show that wood buried in peat and in sediments has selectively lost most of its cellulosic components and has retained lignin in a relatively intact form. Consequently, we feel that cellulose does not play a major role in coalification, in contrast to recent suggestions that it does (17). Xylem tissue coalified to a rank of brown coal contains relatively large amounts of lignin, whereas cellulose is not present to any great extent. A gradual change in the lignin can be discerned. This change primarily involves alteration of lignin structural units such that the average number of methoxyl groups per aromatic ring decreases by half, and peaks for lignin pyrolysis products diminish relative to total pyrolysis products. Examination of xylem tissue coalified to a higher rank of lignite reveals that the most likely mechanism for removing methoxyl groups is by demethylation. The lignin is eventually transformed to catechol-like structures. Such a transformation would be consistent with pyrolysis studies showing a decrease in methoxylated lignin phenols and an increase in phenols, cresols, and catechol. It is also consistent with the NMR data showing a decrease in methoxyl carbon and a constant value for the fraction of aryl-O carbons relative to total aromatic carbons.

As lignin in buried wood is gradually transformed to lignite and the lignin structural units are modified to catechol-like structures, the samples show gradually decreasing proportions of pyrolysis products that are directly of lignin origin (e.g. methoxyphenols) and increasing proportions of phenol and catechol-based products which most likely originated from lignin. If one assumes that this trend is related to increasing degrees of coalification, then the loss of methoxyphenols could be used in a quantitative sense to denote increasing rank. It is particularly noteworthy that some lignite samples of Cretaceous age still have a suite of lignin-derived pyrolysis products that suggest that lignin is not extensively altered. This implies a generally high geochemical stability for lignin.

It is difficult to determine from the pyrolysis data if the catechol-like structures in lignite samples are linked by aryl ether bonds as in lignin which shows such a linkage (β-O-4) between the C-4 phenol and the β-carbon on the propyl side chain. However, the NMR data would imply that the catechol-like structures are, in fact, linked in such a manner. Significant intensity in the range of 60-100 ppm is attributable to aliphatic C-O carbons as would be expected from above linkages.

As the xylem tissue is coalified further, lignin pyrolysis products disappear entirely and the catechol-like structures typical of lignite undergo further modification. The data appear to show that catechol-like structures are losing one hydroxyl group per aromatic ring. Pyrolysis products of xylem tissue having a rank of subbituminous coal are principally phenol, the cresols, dimethylphenols, C_3-phenols, and C_4-phenols. The presence of substantial 2,4-dimethylphenol is indicative of the fact that the carbon linkage at C-4 associated with the three-carbon side-chain of lignin is retained. The lack of ^{13}C NMR signals in the range of 60-100 ppm suggests that the three-carbon side chain of lignin has been modified, probably by cleavage of the β-O-4 linkage.

ACKNOWLEDGEMENTS

We thank our colleagues at the U.S. Geological Survey for kindly making samples available for study, especially Albert J. Froelich, Ronald W. Stanton, Roger Thomas, and Dave Gottfried. We also thank Robert Gaulton (State Electricity Commission of Victoria), and Geoffrey Perry (Coal Corporation of Victoria) for kindly providing us access to samples of Victorian brown coal.

REFERENCES

1. Hatcher, P.G., Breger, I.A., and Earl, W.L., Org. Geochem., 3, 49, (1981).
2. Hatcher, P.G., Breger, I.A., Szeverenyi, N.M., and Maciel, G.E., Org. Geochem., 4, 9, (1982).
3. Hatcher, P.G., Romankiw, L.A., and Evans, J.R., Proc. 1985 International Conf. on Coal Science, 28-31 Oct., 1985, Sydney, Australia, p. 616, (1985).
4. Hatcher, P.G., "Dipolar dephasing ^{13}C NMR studies of buried wood and coalified xylem tissue: Evidence for chemical structural changes associated with defunctionalization of lignin structural units during coalification" manuscript in preparation (1986).
5. van de Meent, D., Brown, S.C., Philp, R.P., and Simoneit, B.R.T., Geochim. Cosmochim. Acta, 44, 999 (1980).
6. Larter, S.R., and Douglas, A.G., J. Anal. Appl. Pyrol., 4, 1, (1982).
7. Sigleo, A.C., Geochim. Cosmochim. Acta, 42, 1397 (1978).
8. Hatcher, P.G. and Romankiw, L.A., In "Proceedings of the Second U.S. Geological Survey Workshop on the Early Mesozoic Basins of the Eastern United States," Robinson, G.R., Jr. and Froelich, A.L. (eds.), U.S. Geological Survey Circular 946, p. 65 (1985).
9. Schenck, P.A., de Leeuw, J.W., Vieto, T.C., and Haverkamp, J., In "Petroleum Geochemistry and Exploration of Europe," Geol., Soc. Spec. Bull. No. 11, p. 267 (1983).
10. Obst, J.R., J. Wood Chem. Technol. 3, 377-397 (1983).
11. Hedges, J.J., Cowie, G.L., Ertel, J.R., Barbour, R.J., and Hatcher, P.G., Geochim. Cosmochim. Acta, 49, 701 (1985).
12. Spiker, E.C., and Hatcher, P.G., manuscript submitted to Geochim. Cosmochim. Acta (1986).
13. Saiz-Jimenez, C., and de Leeuw, J.W., Org. Geochem., 6, 417 (1984).
14. Chaffee, A.L., Johns, R.B., Baerken, M.J., de Leeuw, J.W., Schenck, P.A., Boon, J.J., Org. Geochem., 6, 409 (1984).
15. Philp, R.P., Russell, N.J., Gilbert, T.D., and Fridrich, J.M., J. Anal. Appl. Pyrol., 4, 143 (1982).
16. van Graas, G., de Leeuw, J.W., and Schenck, P.A., In "Advances in Organic Geochemistry 1979," Douglas, A.G., and Maxwell (eds.), Pergamon Press, Oxford, p. 485 (1980).
17. Hayatsu, R., Botto, R.E., Scott, R.G., McBeth, R.L., and Winans, R.E., Fuel, 65, 821 (1986).

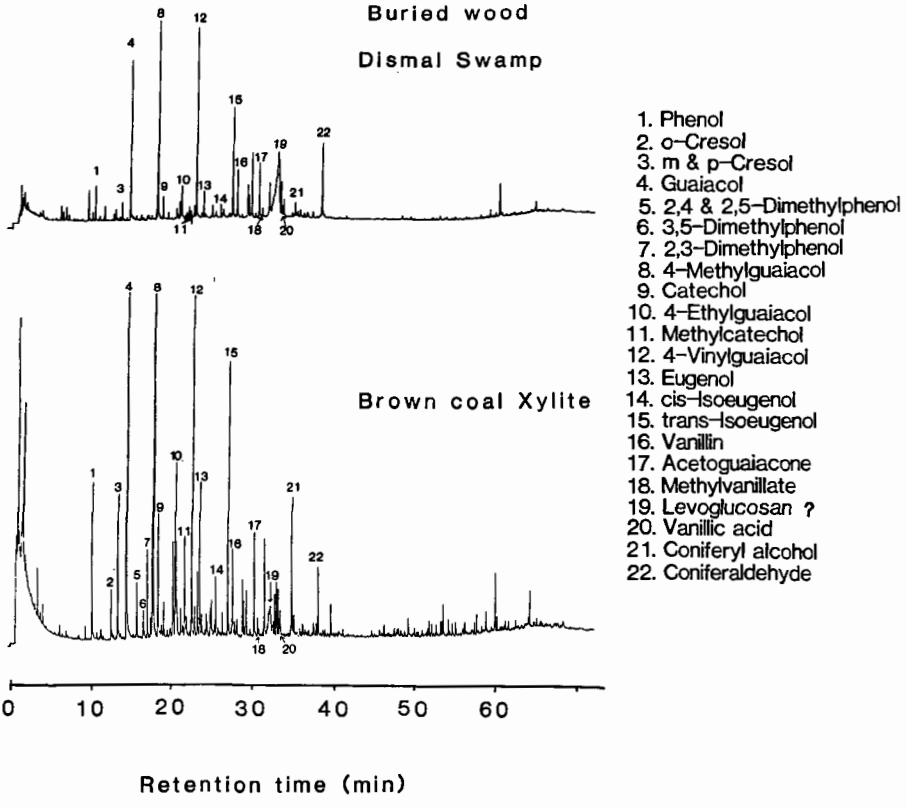

Figure 1. Py/gc-ms traces of buried wood described by Hatcher et al.(3) and a sample of a Podocarpacea log (xylite) described in the text.

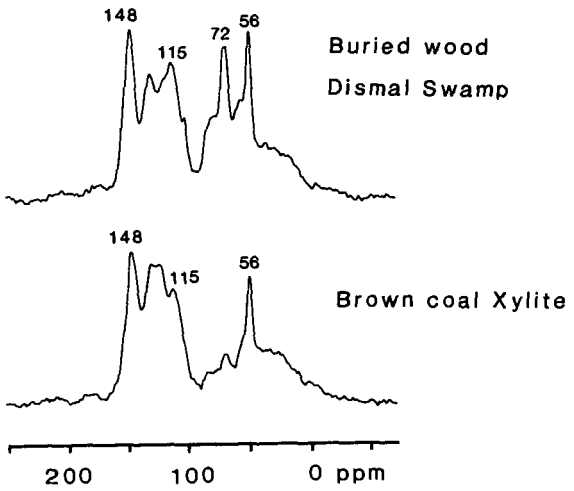

Figure 2. Solid-state ^{13}C NMR spectra of buried wood and Podocarpacea log. Spectra are reproduced from previous publications (4,8).

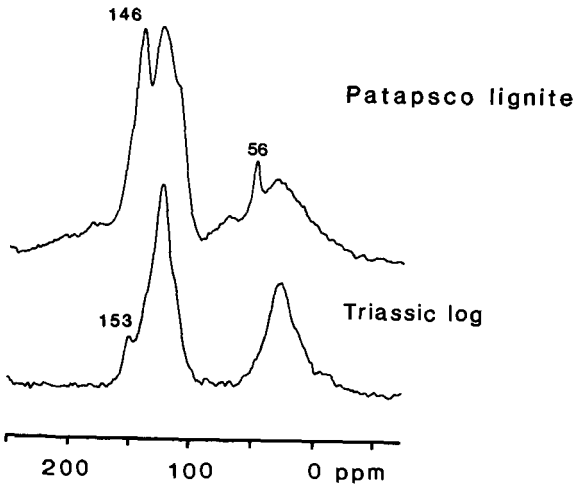

Figure 3. Solid-state ^{13}C NMR spectra of samples described in previous reports (3,8) and in the text.

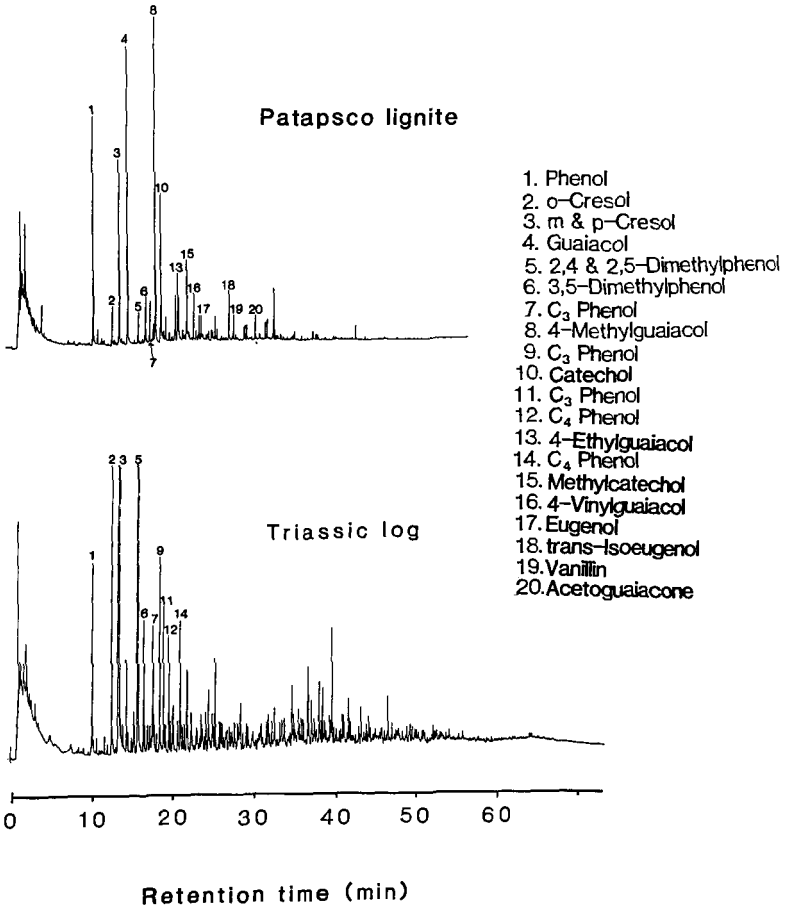

Figure 4. Py/gc-ms traces for the lignite from the Patapsco Formation and for the Triassic log of subbituminous rank.

PREPARATION AND REACTIVITY OF LATEXES FROM LOW-RANK COALS

E.S. OLSON, J.W. DIEHL AND M.L. FROEHLICH

University of North Dakota Energy Research Center
Box 8213, University Station, Grand Forks, ND 58202

INTRODUCTION

The conversion of coals into oils, solutions, or dispersions is of great interest in the production of new liquid fuels. This paper describes our investigations of the conversion of low-rank coals into a stable dispersed form which exhibits altered reactivities toward various alkylating, reducing, and oxidizing reagents. This stable dispersion of a solid in a liquid medium is properly called a latex.

Extraction of coal with aqueous base such as sodium hydroxide followed by precipitation by the addition of acid to the extract yields dark material known as humic acid. Humic acids are defined by van Krevelen (1) as plant-derived "components which can be 'dissolved' in alkaline hydroxide," while others regard humic acids as being the water- or base-extractable material formed from oxidation of coal (2). The term is used both for the products of the decay and gelification of woody material and the products from coal. Since the compositions of neither the oxidized or unoxidized material are well defined, we shall use the term in a general sense to mean the material recovered from acidification of base extracts, although the materials in this report were obtained by base treatments of unoxidized coals carried out in the absence of oxidizing reagents and oxygen. The low-rank coals are hydrophilic in nature owing to their high concentrations of carboxylic acid and hydroxyl groups, consequently they yield significantly greater amounts of humic acids than do the bituminous coals. The yields of humic acids from lignites are known to vary with temperature and base concentration and of course with the degree of oxidation before or during the extraction. Unoxidized North Dakota lignites generally give about 4% yields of humic acids in extractions with 5% sodium hydroxide at ambient temperatures in 12 hours. In contrast, leonardites are highly oxidized lignites and easily convert to humic acids in 80% to 90% yields (3).

The objective of this study was to study the conversion of low-rank coals to humic acids under conditions of high mass flow (under nitrogen) and to investigate the nature of the humate material with regard to solubility and reactivity. The effects of coal type, nature of the base, and added surfactant on the conversion were studied.

EXPERIMENTAL

Coal samples (10 g) were blended with 5% sodium hydroxide or other basic solution (250 ml) in a 1.25 l kitchen-style Osterizer placed in a large glove bag under nitrogen atmosphere. Low conversions were obtained at the medium speed blending for 12 hours, and high conversions were obtained at the high speed for 2 hours. The temperature of the medium rose to about 45°C during the extraction as a result of blade friction. The blended slurry was washed into 250 ml centrifuge bottles and centrifuged at 3000 rpm in an IEC Model K centrifuge. The supernatant latex was then carefully decanted from the residue. Analytical data for the coals are presented in Table 1.

TABLE 1
ANALYTICAL DATA FOR LOW-RANK COALS

Analysis	Beulah Lignite	Wyodak Sub	Big Brown Lignite
Moisture	28.8	30.4	27.8
Volatile Matter	29.0	30.5	32.8
Fixed Carbon	30.8	33.2	30.0
Ash	11.7	5.8	9.5
Carbon, maf	69.5	73.5	69.9
Hydrogen, maf	4.4	5.2	5.2
Nitrogen, maf	1.0	1.1	1.2
Sulfur, maf	2.8	0.7	1.2
Oxygen (dif), maf	22.3	19.5	22.4

RESULTS AND DISCUSSION

Treatment of low-rank coals with aqueous basic solutions in the blender under nitrogen atmosphere and very mild temperatures (45°C) gave high conversions to products which were stable to centrifugation. The residue of larger particles which did separate during centrifugation was examined by photoacoustic FTIR spectroscopy and microscopic petrographic techniques and was found to consist mainly of minerals and liptinite macerals. The black suspension obtained after centrifuging and decanting from the residue resembled the black humate "solution" obtained in 4% yield by the simple sodium hydroxide extraction of lignites. The latex was examined in a static cell of a low-angle laser light scattering photometer. An intense flashing or sparkling characteristic of fine particle or colloidal suspensions (Tyndall effect) was observed. This contrasts with the glowing spot of Raleigh scattered light observed for methyl and acetylated derivatives of the humic acids which are highly soluble in organic solvents such as toluene, tetrahydrofuran, and dimethylformamide (3).

Addition of acid to the latex resulted in precipitation of the humic acid. Conversions were determined from weight yields of the precipitated humic acids after drying and are reported in Table 2. Addition of the acid was presumed to neutralize the negative charges of the carboxylate and phenolate anions of the colloidal coal particles by converting them to the acid and phenol forms. Coagulation of the particles occurred when the pH was lowered to about 4, where repulsive forces of the remaining carboxylate anionic groups no longer overcome the attractive forces between the coal macromolecules.

The highest conversions to the latex were observed for the Beulah (North Dakota) lignite where a 90% yield of humic acids was obtained by blending at high speed with 5% sodium hydroxide. This contrasts with the 28% yield obtained at medium speed blending of the same coal. It is believed that the high-speed stirring is required to increase the mass flow of aqueous base through the coal pore structure.

The effect of the nature of the base used in the blender treatment was investigated. When a 5% sodium carbonate solution was used, a 27% conversion of the Beulah lignite was obtained. The lower yield for this base suggests that high concentrations of hydroxide, as well as the high mass flow, may be essential for effective

TABLE 2
CONVERSIONS OF LOW-RANK COALS TO LAXTEXES

Coal	Blender Speed	Base	Yield of Humic Acid (Wt.% mf)
Beulah	high	NaOH	90
Beulah	med	NaOH	28
Beulah	mag.stir.	NaOH	4
Beulah	high	Na_2CO_3	27
Beulah	high	NH_4OH	11
Beulah	high	pyridine	7
Beulah	high	$NaOCH_3$	3
Wyodak	high	NaOH	65
Big Brown	high	NaOH	81

production of the latex. The use of sodium carbonate offers the possibility of easier recovery of humic acids from the latex using carbon dioxide to lower the pH and then regeneration of the sodium carbonate solution by heating the recovered aqueous phase. The lower conversion to the latex form using sodium carbonate may be compensated by its ease of regeneration and thus may be useful in coal cleaning or liquefaction processing of low-rank coals. Ammonium hydroxide (30%) gave a conversion of 11%. Thus a mechanism involving nucleophilic attack by the base does not seem to be important. Pyridine (neat) gave only a 7% conversion.

When the reaction of dried lignite with sodium methoxide in methanol was carried out with high-speed blending, the conversion was insignificant. Essentially only the waxy acids and some hydrocarbons were solubilized. Photoacoustic spectroscopy of the coal residue showed no incorporation of the methanol as methyl esters or ethers. A nucleophilic role of the base in the blending process again does not seem likely. Since transesterification was not exhibited in this attempted reaction with methoxide in methanol, it is unlikely that hydroxide would act by an equivalent ester hydrolysis mechanism in the aqueous hydroxide medium. No evidence exists for the presence of a significant amount of esters in low-rank coals. A possible mechanism for the aqueous hydroxide reaction is the base-catalyzed guaiacol ether cleavage demonstrated for lignin. The low-rank coals have small amounts of guaiacols and presumably some residual lignin. Cleavage of the alpha (benzyl) ethers of these residual and, therefore, hindered structures may require the high hydroxide concentrations and high mass flow conditions which we know to be important for breakdown to the colloidal state. Breakage of hydrogen bonds may also be important. The creation of a highly charged surface essential to the colloidal formation was clearly not possible in the blending attempt in methanol but was obtainable in water.

Two other coals were investigated for comparison with the Beulah (North Dakota) lignite. Wyodak subbituminous coal gave a conversion of 65% with high-speed blending in 5% sodium hydroxide. A Big Brown (Texas) lignite sample in the same conditions gave a conversion of 81%. The reason for the lower conversions of these two coals is not yet understood, but these two coals are known to be more aliphatic and contain less lignin than the Beulah lignite, which gave a 90% conversion.

The latexes from the Beulah lignite were shown to be quite reactive to alkylating reagents. Dimethyl sulfate was added to the aqueous basic latexes to give the methyl humate derivatives. These products were soluble in organic solvents, but insoluble in water. The molecular weights of these soluble derivatives were determined using low-angle laser light scattering photometry after reduction with zinc metal (4). These results indicate that the more severe blending processing breaks more of the cross-links or branch-points in the coal structure to give the higher yields of humic acids but in a smaller size distribution (Table 3) (5). The reactivities of the latexes in oxidizing and reducing conditions are currently under investigation.

TABLE 3
MOLECULAR WEIGHTS OF REDUCED METHYL HUMATE DERIVATIVES

Source of Humate Derivative	M_w (daltons)
High speed blending (90% yield)	4.3×10^5
Medium speed blending (28% yield)	8.8×10^5
Mag. stirring (4% yield)	1.3×10^6

REFERENCES

1. van Krevelen, D. W. **"Coal,"** Elsevier, Amsterdam (1961) p. 104.
2. Wender, I., Heredy, L.A., Neuworth, M.B. and Dryden, I.G.C. in **"Chemistry of Coal Utilization,"** Sec. Suppl. Vol., M.A. Elliott, ed. Wiley, New York (1981) p. 456.
3. Fowkes, W.W. and Frost, C.M. Bur. of Mines Report of Investig. 5611 (1960).
4. Olson, E.S. and Diehl, J.W., J. Chromatogr. 349 (1985) 337-346.
5. Olson, E.S. Diehl, J.W. and Froehlich, M.L. Coal Characterization for Conversion Processes Symposium, Rolduc, Netherlands (1986), accepted for publication, Fuel Sci. Tech.

DRY CATALYTIC LIQUEFACTION OF A SUBBITUMINOUS COAL: STRUCTURAL INFERENCES

F.J. Derbyshire, M.-T. Terrer, A. Davis and R. Lin

College of Earth and Mineral Sciences
The Pennsylvania State University
University Park, PA 16802

The catalytic liquefaction of a subbituminous coal has been studied in the absence of solvent using an impregnated sulfided Mo catalyst. Reactions were conducted for various times at temperatures from 300-400°C. The yield and composition of gaseous products, chloroform-soluble liquids and insoluble residue were followed as a function of the reaction conditions, using a number of techniques.

The liquefaction process was divided into two distinct regimes typified by low and high liquid yields (< ca. 10% and > ca. 20%, respectively). Compared to the parent coal, at low yields (realized at 300°C), there was little production of C_1-C_4 hydrocarbons, a sharp increase in the aliphatic hydrogen content of the liquids and little change in the oxygen functionality of the liquids and residue.

At high yields, C_1-C_4 production increased and the aliphatic hydrogen content of the liquids was reduced concomitant with an increase in asphaltene content. The oxygen functionality of the liquids and residue also decreased.

Associated changes in the structure and composition of the chloroform-insoluble residue have been further investigated by petrographic analysis and by measurements of swelling in pyridine. The implications are that a large proportion of the coal network structure involves hdyrogen-bonded cross linkages.

INTRODUCTION

In earlier publications, results were presented to describe the application of low-severity catalytic hydrogenation in the absence of added vehicle for providing information on coal structure and liquefaction mechanisms (1-3). In all of these studies the coals were impregnated with a molybdenum disulphide catalyst at a loading of 1% wt Mo (dmmf coal) and reacted at temperatures of 400°C and less, where cracking and condensation reactions will be minimized.

Although the exclusion of solvent undoubtedly creates some disadvantages (e.g. in facilitating catalyst dispersion and eliminating a source of donatable hydrogen) and does not directly relate to liquefaction processing, the past research has shown that this technique offers certain benefits. The derivation of fundamental information is simplified in the absence of solvent and changes in the physical properties of the modified coals and insoluble residues can be measured directly.

The research discussed in this paper describes the results of a study of the low-severity catalytic hydrogenation of a single subbituminous coal at temperatures from 300-400°C. The yield and composition of gaseous, liquid and solid products were followed as a function of reaction time at different temperatures, using several analytical and other techniques. The principal objectives were to provide insight into the two-component coal structural model and the compositional changes associated with liquefaction.

EXPERIMENTAL

Coal preparation

The subbituminous coal was obtained from the Penn State Coal Sample Bank. Properties of the coal are shown in Table 1.

The coal samples were crushed to -60 mesh (250 microns) in a glove box in flowing nitrogen and without drying, and were subsequently stored under nitrogen in sealed vials.

The coal was impregnated with molybdenum to a loading of 1% wt Mo (dmmf) using an aqueous solution of a water-soluble molybdenum salt. In order to introduce the catalyst in its most active form (MoS_2) (4,5), an aqueous solution of ammonium heptamolybdate, $(NH_4)_6Mo_7O_{24}.4H_2O$ was used to produce the thiosalt, $(NH_4)_2MoS_4$, by reaction with H_2S. The thiosalt decomposes to form MoS_2 upon mild heating. The procedure has been previously described in detail (1).

Hydrogenation reaction

Hydrogenation reactions were performed in batch tubing bomb reactors (6). Experiments were conducted at temperatures between 300°C and 400°C for residence times between 5 and 180 min. The bombs were loaded with approximately 3.5-4.5 g of impregnated coal and 0.02 cm^3 of CS_2 to ensure that the molybdenum was maintained in the fully sulphided form. After flushing, the reactors were pressurized to 7MPa of hydrogen (cold). The reactors were heated by immersion in a preheated fluidized sandbath heater which rapidly raised the reactor contents to the desired temperature. Agitation was provided by vertical oscillation of the reactor through a displacement of 2.5 cm at a frequency of 200 min^{-1}. At the end of the reaction period, the reactor was removed from the sandbath and quenched in water.

The gaseous products were collected by venting at room temperature into an evacuated expansion bulb of known volume. Gas samples were analyzed by gas chromatrography to determine the yields of CO, CO_2 and C_1-C_4 hydrocarbons.

The reaction products remaining in the bomb were rinsed into a pre-dried ceramic thimble with chloroform and extracted overnight in a Soxhlet apparatus. The extract was filtered and the recovered solids were added to those in the Soxhlet thimble. The solvent was removed from the filtrate and the total residue by evaporation under reduced pressure. The extract was dried for 3 h at 100°C in vacuum and the residue for 12 h under the same conditions. The experimental reproducibility for conversion to gases and soluble extract was found to be ±3%.

The chloroform-solubles were further separated into hexane-solubles (oils) and hexane-insolubles (asphaltenes).

Product analyses

The liquid products were analyzed for elemental composition, by ^1H NMR spectroscopy (deuterated chloroform solvent; trimethylsilane internal reference), and by Fourier transform infrared spectroscopy (FTIR).

The chloroform-insoluble residues were first derivatized by reaction with acetic anhydride prior to FTIR analysis in order to follow the changes in concentration of -OH groups (7).

The swelling of the residues in pyridine was examined using the procedure described by Liotta et al. (8).

Optical microscopy

The techniques of microscopic examination and petrographic point-count analysis have been used to follow the processes involved in the hydroliquefaction of various ranks of coal, including subbituminous (9,10). In particular, the efficiency of reaction has been monitored by such features as the proportions of undissolved macerals and the production of insoluble intermediates. In this study, the liquefaction residues (both unextracted and chloroform-insoluble) were embedded in an epoxy resin and polished. Examination was undertaken with a polarizing reflected-light microscope under oil immersion at a magnification of 400. Point-count analyses were performed only on the chloroform-insoluble residues at a magnification of 625; 500 points were counted for each analysis.

Mean reflectance determinations were performed on huminite (vitrinite) and high-reflecting vitroplast.

RESULTS AND DISCUSSION

Product yield

The effects of reaction temperature and residence time on the yield of chloroform-solubles produced by dry catalytic hydrogenation is shown in Figure 1.

The extract yields increased with increasing residence time and reaction temperature. At 300°C, the production of chloroform-solubles was low, and even after extended reaction the yield was not much higher than that obtained by Soxhlet extraction of the parent coal (4.4% dmmf). At this temperature, a comparison of catalytic and noncatalytic reactions showed that the presence of the catalyst did not significantly affect the liquid yield.

Higher yields of extract production were measured at 350 and 400°C. After 180 min at 400°C the extract yield was about 65%. Taken together with the gas yield this means that almost 80% of the coal was converted to gaseous and soluble liquid products under these mild reaction conditions. There was little production of light hydrocarbons at low extract yields (< 10%), indicating that there was relatively little cracking at 300°C. The yields of these gases increased at higher conversions.

Composition of liquids

At low liquid yields (< 10%), there was a sharp increase in the hydrogen content and the H/C atomic ratio of the chloroform-solubles compared to that of the parent coal extract, Figure 2. It was also found that there were corresponding changes in the oil to asphaltene ratio. The ratio increased from a value of 0.8 in the parent coal extract to 8.0 at a yield of about 10% before falling to ca. 1.0 at yields above 20%.

Analyses of the liquids by ^{1}H NMR showed that the initial rise in hydrogen content was due to the presence of polymethylene chains. The liberation of long chain alkanes on liquefaction and pyrolysis has been observed by other workers (11-13).

At conversions greater than 20% (liquid yield) the aliphatic hydrogen content was reduced from about 10.5% to 6.5%.

Evidently there is a sharp demarcation between the events which take place at low and at high conversions. In the context of the mobile phase/network concept of coal structure, it can be argued that, for the coal studied here, the observed

boundary represents the limit of the mobile phase, beyond which the additional products derive from the substantial breakdown of the network.

Composition and swelling behavior of residues

Analyses of the acetylated residues by FTIR showed that, at low conversions (< 10%), there was little change in the absorption bands attributed to the derivatized -OH groups. Above, about 20% liquid yield, there was a rapid disappearance of -OH groups with increasing conversion.

The change in the swelling ratio of the residues with conversion to chloroform-soluble liquids is shown in Fig. 3. In parallel with the changes in extract composition in going from low to high conversion (as seen by the results of elemental analysis, ^1H NMR and oil/asphaltene ratio) the swelling ratio increased sharply at low conversion, passed through a maximum and fell to much lower values at conversions greater than 20%. Duplicate experiments confirmed that these data were reproducible.

At low conversions, the FTIR analyses showed that there did not appear to be an appreciable change in the OH content compared to that of the parent coal. The substantial removal of functional groups would be expected to reduce the extent of hydrogen bonding and lower the swelling ratio.

At higher conversions, two factors probably contribute to the reduced swelling, the removal of polar groups and the progressive reduction in the concentration of vitrinite in the residue.

Petrographic analysis of residues

The products from the hydrogenation experiments contained the following organic petrographic entities: unreacted huminite (vitrinite) macerals, unreacted liptinite macerals, unreacted inertinite macerals, low-reflecting vitroplast, and high-reflecting vitroplast. Vitroplast is a pitch-like isotropic material which is derived either directly from the melting of vitrinite and other macerals, mainly from coals of bituminous rank, or from the liquid products of dissolution. Low-reflecting vitroplast was observed to have been formed within disintegrating huminite after hydrogenation for 5 min at 400°C. Such material was observed only in the unextracted whole products and is believed to be part of the extractable liquid products; it was no longer present in the residues of chloroform extraction prepared for petrographic point-count analysis. However, certain of these latter residues did contain high-reflecting vitroplast; this material is thought to have been rendered less soluble as a result of thermal treatment.

Table 2 gives the results of the point-count analyses on the chloroform-insoluble residues. It shows that with increasing severity of reaction conditions, liptinite disappears, huminite decreases substantially, inertinite shows an overall increase, and the high-reflecting vitroplast, which appears when the reaction temperature reaches 400°C, also increases. These results suggest a partial explanation for the change in swelling characteristics of the residues illustrated in Fig. 3. The dotted line in this figure represents the swelling which would be shown by the huminite and huminite-derived fraction; it assumes that the inertinite is non-swelling and that the huminite structure in unaltered. This theoretical curve indicates that for the milder conditions (up to 400°C; 5 min), the swelling of the humitic materials remains high. Only where this material becomes more highly reflecting (Table 2) does the swelling show a substantial decrease (continuous line, Fig. 3). Such residue components together with the inertinite are though to be depleted in polar side groups and it is this paucity of crosslinks which results in a lowering of the swelling properties. Further, the unreacted huminites in the residues from the more severe treatment conditions have been progressively altered, as shown by their reflectances (Fig. 4). Consequently, oxygen-containing functional

groups would have been gradually eliminated from the huminite structure as a result of the reaction, as supported by the FTIR spectra of the residues.

SUMMARY

The results of this research have shown that two regimes of liquefaction can be distinguished.

At low conversion (about 10%) liquids and gases are apparently liberated either through the release of physically trapped materials or through the rupture of weak linakges. Only small quantities of C_1-C_4 hydrocarbons are produced and the extractable liquids are highly paraffinic. There was no significant change in the concentration of functional groups in the chloroform-insoluble products.

At higher conversions (> 20%), there were several notable changes in the composition and properties of the chloroform-soluble liquids and the insoluble residues and an increase in the production of higher hydrocarbon gases. It is considered that the liquids produced at high conversions were substantially derived from the coal network and that the abrupt change in properties between low and high yields is representative of a boundary, based upon behavioral characteristics, between the mobile and network phases.

The results of the swelling experiments suggest that a large proportion of the intra-network cross-linking in this coal involves hydrogen bonding.

Petrographic examination and point-count analysis of the residues shows that huminite (vitrinite) and liptinite are progressively lost as reaction conditions become more severe. This trend is accompanied by increases in the proportions of inertinite and high-reflecting vitroplast, an isotopic pitch-like material generated as a part of the product of dissolution. Although an increase in these latter components would contribute to the decrease in swelling behavior of the residues, it appears that a loss of hydroxyl groups from the huminite is a major factor in this change.

ACKNOWLEDGEMENTS

The authors would like to acknowledge the support provided by U.S. Department of Energy under Grant No. DE-FG22-83PC60811 and the Cooperative Program in Coal Research at The Pennsylvania State University.

REFERENCES

1. Derbyshire, F.J., et al., Fuel Proc. Tech., 1986, 12, 127-141.

2. Davis, A., et al., Fuel, 1986, 65, 500-506.

3. Stansberry, P.G. et al., to be published in Energy and Fuels.

4. Anderson, R.R. and Bockrath, B.C., Fuel, 1984, 63, 329-333.

5. Weller, S.W. Proceedings of the Fourth International Conference on the Chemistry and Use of Molybdenum (Eds. H.F. Barry and P.C.H. Mitchell), 1982, 179-186.

6. Yarzab, R.F., et al., Fuel, 1980, 59, 81-92.

7. Blom, L., et al., Fuel, 1957, 36, 135-153.

8. Liotta, R., et al., Fuel, 1983, 62, 781-791.

9. Mitchell, G.D., et al., Liquid Fuels from Coal (Ed. R.T. Ellington), Academic Press, 1977, 245-270.

10. Walker, P.L., et al., Characterization of Mineral Matter in Coals and Coal Liquefaction Residues, Annu. Rep. Penna. State Univ. to EPRI. EPRI AF-832, Project 366-1, 1978.

11. Snape, C.E., et al., Fuel, 1985, 64, 1394-1400.

12. Youtcheff, J.S. et al., Org. Geochem., 1983, 5, 157-164.

13. Calkins, W.H. and Tyler, R.J., Fuel, 1984, 63, pp. 1119-1124.

TABLE 1

Coal Properties

Penn State Sample Bank No.

Seam - Anderson
County - Campbell Co.
State - Wyoming
Province - Northern Great Plains

ASTM rank class - sub B.

Moisture content, % wt (a.r.) - 23.3
Mineral Matter, % wt dry coal - 11.9*

Elemental Composition	% dmmf
C	73.0
H	4.5
O**	20.4
N	1.2
S	0.9

Maceral Analysis	% vol
Vitrinite	87
Exinite	2
Inertinite	11

Sulfur Forms	(% dry coal)
Organic	1.2
Pyritic	0.3
Sulfate	0.05
Total	1.55

*Reported as ASTM "Ash"
**By Difference

TABLE 2

Petrographic Analyses of Chloroform-insoluble Residues

Temperature °C	Time min.	Yield	Unreacted Huminite, %	Unreacted Liptinite, %	Unreacted Inertinite, %	High-Reflecting Vitroplast, %
300	5	3.37	87	8	5	0
300	60	6.46	86	7	7	0
350	60	34.69	85	6	9	0
400	15	44.47	63	0	10	27
400	30	50.09	55	0	12	33
400	60	60.65	41	0	8	51

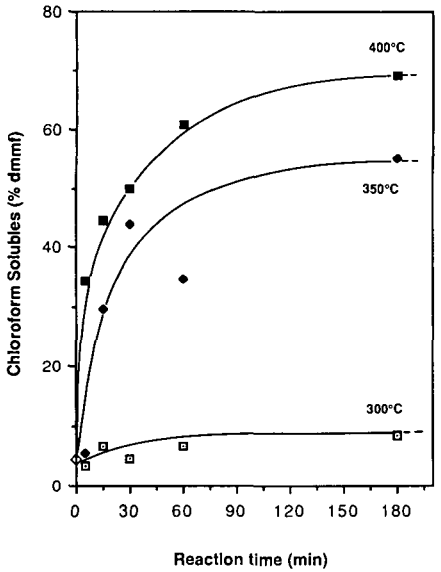

CHLOROFORM-SOLUBLES YIELD AS A FUNCTION OF TEMPERATURE AND REACTION TIME

(SUBBITUMINOUS COAL (PSOC-1403P); 7 MPA H_2, COLD; 1% WT MO)

FIGURE 1

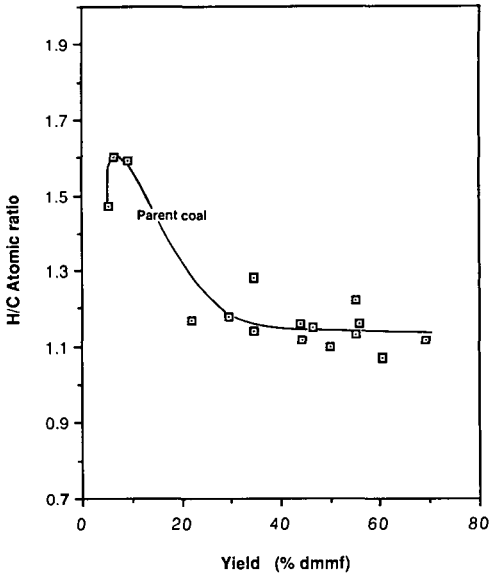

VARIATION OF THE H/C ATOMIC RATIO AS A FUNCTION OF CONVERSION YIELDS

(SUBBITUMINOUS COAL (PSOC-1403P); 7 MPA H_2, COLD; 1% WT MO

FIGURE 2

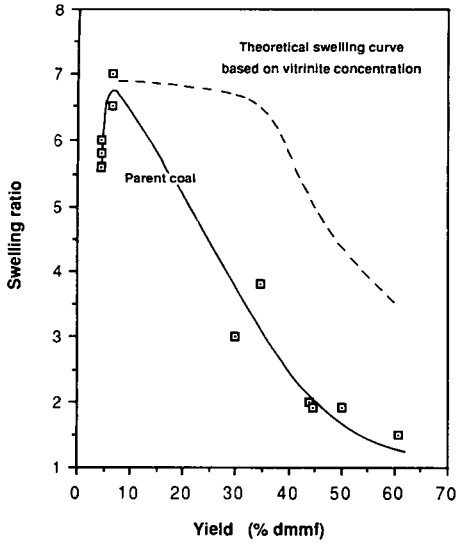

VARIATION OF THE SWELLING RATIO OF CHLOROFORM-EXTRACTED RESIDUES WITH CHLOROFORM-SOLUBLES YIELD

(SUBBITUMINOUS COAL (PSOC-1430P); 7 MPA H_2, COLD; 1% WT MO)

FIGURE 3

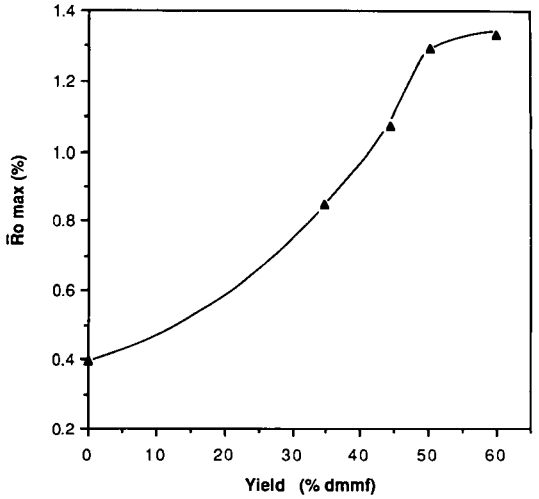

VARIATION IN MEAN MAXIMUM REFLECTANCE OF HUMINITE (VITRINITE) AND VITROPLAST RESIDUE COMPONENTS WITH CHLOROFORM-SOLUBLES YIELD

FIGURE 4

INVESTIGATIONS OF ANODICALLY OXIDISED COAL

Shashi B. Lalvani

Dept. of Mechanical Engineering & Energy Processes
Southern Illinois University - Carbondale
Carbondale, Illinois 62901
Telephone: (618) 536 - 2396

A number of studies carried out on the electrolysis of coal in basic media(1-7) support the conclusion that electroxidation of coal in NaOH forms soluble products similar to humic acids. Upon further electrolysis the humic acids - like material decomposes to liberate CO_2 at the anode. Hydrogen is liberated at the cathode with high efficiency and, depending upon the electrode potential and other conditions, relatively small amounts of O_2 and traces of CH_4 and C_2H_2 form at the anode. Different cell geometries have been explored, ranging from a stirred - cell reactor(1-5) to a reactor with an anode made of anthracite coal(6); other electrodes which have been used include Pt, graphite, Pb and Ni. The effect of catalysts, such as vanadium pentoxide and cobalt chloride, on the oxidation rates have also been studied(3). Some researchers(3) reported that horizontal electrodes caused higher rates of coal conversion than vertical electrodes. Belcher(4) characterized the various coal electrolysis products by separating them into acetone - soluble and acetone - insoluble products. Khundkar(5) showed that peat displays higher electrochemical activity than coal under similar conditions. Excepting recently reported work(7) coal electrolysis has usually been done galvanostatically. Senftle and coworkers(6) argued that $OH^{\cdot}$ radicals are the most probable agents for hydrogen abstraction and/or addition to aromatic rings. In addition to containing an excellent review of the oxidising species formed during the electrolysis of water, this paper(6) also gives some experimental data as to the products of coal electrolysis.

The present study reports more details as to products formed during coal electrolysis in basic media and considers various possible reaction pathways for electrochemical oxidation of coal. Constant potentials were employed in this work and the reaction products were analysed by FTIR, and for elemental compositions.

Reaction mechanisms of coal oxidation by electrolysis are neither very well understood nor widely studied. Guidance may be gleaned, however, from a number of experimental investigations of the mechanism of the oxidation of coal by chemical reagents. It has been reasoned

from such results that free radicals formed during the early stages combine to form larger entities; then this is followed by an essentially oxidative - hydrolytic process in later stages(8). For example, air - oxidation makes coal increasingly soluble in alkali during the later stages with ultimate conversion of about 20 - 30% (wt) of the carbon to carbon - oxides and about 40 - 50% of the hydrogen to water(8). The solubilised portion of the coal, considered to be "humic acid" is spectroscopically similar to the parent coal molecule except for increased concentrations of oxygen - rich functional groups, including phenolic -OH, -COOH and =CO (ketone and/or quinone). The limiting elemental compositions of these humic acids depend strongly on the temperature of oxidation and vary slightly with the rank of the coal.

Humic acid is a term usually applied to certain dark amorphous substances which occur in soil, peat and low - rank coal. Humic acid are alkali - soluble, can be precipitated by acids, and have molecular weights in the range of 20,000 - 50,000 daltons(9). A "typical" humic acid has a "core" which is partly aromatic in nature with other structural features derived from lignin, e.g. phenols and resorcinols(9). In addition, alcohol, carboxyl, carbonyl and quinoid groups and heterocyclic nitrogen are present in humic acids.

The humic acids formed by oxidising coal can be oxidised further to produce low molecular weight water - soluble acids. All the aromatic carboxylic acids (with the exception of benzoic acid), oxalic, succinic and acetic acids have been identified(9) in the products. Intense oxidation of coal if carried out for a sufficiently long time, consumes intermediate products such as humic acids and yields CO_2 and H_2O as ultimate products(9). Rates of coal oxidation are accelerated by higher temperatures and higher oxygen partial pressures. At even higher temperatures above 250 ^{o}C in air, a virtual low - temperature combustion sets in. Humic acids are used as drilling muds, boiler scale removers, pigments for printing inks, carriers of fertilizers and growth hormones for plants, transporters of trace minerals in soil and soil conditioners.

The rate of oxidation of coal is enhanced by the presence of alkali. When coal is slurried with aqueous sodium hdroxide and reacted with oxygen under pressure, and at temperatures up to 200 ^{o}C, the organic portion of the coal is completely solubilized and large amounts of aromatic carboxylic acids(11,12) are formed. Thirty to forty - five percent of the total carbon is recovered as carboxylic acids, and the remainder is converted to carbon dioxide. Jensen et al.(13) proposed that with coal in air, the predominant primary process is rapid generation of humic acids followed by decomposition of the carboxyl groups. In wet oxidation, the humic acids are presumed to form at the outer regions of the particles. The humic acids then dissolve and get further oxidised in the homogeneous solution phase, thereby exposing fresh reactive surface on the shrinking coal particle for continuing "primary" oxidation. This mechanism for the oxidation of coals in aqueous NaOH at 50 to 100 ^{o}C is discussed in detail by Deno and coworkers(14).

EXPERIMENTAL

North Dakota lignite of particle size less than 77 um was electrolysed in 1M NaOH at room temperature in a stirred reactor made of Pyrex, using Pt electrodes. Experimental details and properties of the lignite are given elsewhere(7).

The lignite was weighed before and after the electrolysis. After electrolysis, the solid residue was filtered from the slurry, washed with distilled water and dried under vacuum at 40 ^{o}C. The aqueous filterate was acidified therby causing a precipitate to form and gases to evolve. The gases produced during this operation were collected and analysed. The two solid products (solid electrolysed lignite residue and precipitate from acidified electrolyte) were characterized by transmission measurements using a Nicolet 7199 Fourier Transform Infrared Spectrometer (FTIR); these samples were also subjected to elemental analysis using a Perkin Elmer Model 240 analyzer. The parent lignite was similarly subjected to FTIR investiagations and elemental analysis.

RESULTS AND DISCUSSIONS

When lignite was electrolysed in 1M NaOH slurries using Pt electrodes, products similar to humic acid were produced in addition to CO_2, H_2, relatively small amounts of O_2 and traces of CH_4 and C_2H_2. The potential applied to the cell influences the production distribution; for example, increasing the electrode potential from 1.2 V to 2.5 V vs. SCE gave correspondingly greater humic acid production(7). Increasing the potential still further, however, lowers the amount of humic acid formed.

Elemental Analysis of Reacted Coal

Table I provides a comparison of the elemental analyses of electrolysed lignites with those of a virgin lignite and a lignite that had been treated with 1M NaOH for 24 hours but not electrolysed. The most striking feature of the data seems to be the monotonic decrease of the oxygen content of the residual particulate material as electrode potential is increased. The decrease of oxygen content of the partially reacted lignite particles with increasing electrode potential may well be related to the greater solubility of the more oxygen - rich fragments produced during electrolysis. The outermost oxidised portions of the coal particles may be viewed as possessing large populations of carboxylic groups which render them potentially alkali - soluble. As these oxidised outer portions dissolve in the basic electrolytes, the inner coal residue would become relatively richer in carbon and poorer in oxygen. Figure 1 shows one hypothetical course of such a reaction in basic electrolytes in which nucleophilic addition of OH^{-} at an aliphatic carbonyl causes an adjacent C-C bond to rupture, thereby

producing a soluble carboxylic fragment and an insoluble residue richer in C and H than the intial composition. The result is that a molecule near the surface of the coal particle breaks along an aliphatic linkage to leave a relatively oxygen - poor residue on the coal particle while contributing a soluble, oxygen - rich, humic - acid - like fragment to the electrolyte solution. The larger population densities of carboxylic groups produced at higher potentials will have a greater tendency to decarboxylate. Such behavior probably underlies the increasing production of CO_2 with potential(7).

FTIR Results

Transmission infrared spectra of the parent lignite and its reaction production were obtained using a Nicolet Model 7199 Fourier Transform Infrared Spectrophotometer. The i.r. beam was passed through pellets prepared from a dry, finely ground (20 minutes in a "Wig-L-Bug") coal sample (10 mg) mixed with 300 mg of KBr. Thirteen - mm diameter pellets were pressed in an evacuated die under 20,000 lbs pressure for one minute and dried overnight at 105 ^{o}C. The spectra of the samples were corrected by subtracting background absorption in the 2000 - 4000 cm^{-1} region.

In the i.r. spectrum of virgin NDL coal in Figure 2 various peaks are assigned as shown based on the work of Bouwman(15). A very low signal/noise ratio is observed for wave numbers greater than about 3600 cm^{-1}. This is attributed to scattering and low intentsity of the i.r. source in this region. The broad band at 3400 cm^{-1} arises from hydrogen bonding involving hydroxyl groups in free or bound H_2O. Bands at 2920 and 2860 cm^{-1} (due to -CH stretching vibrations), indicate the presence of aliphatic hydrocarbon species. The band at 2360 cm^{-1} is attributed to the presence of CO_2 and that at 1700 cm^{-1} can be assigned to the carbonyl C=O stretching vibration of, e.g., carboxylic acids; the latter is a relatively small peak in most coals including the NDL used here. The band at about 1600 cm^{-1} in Figure 2 (and which can occur anywhere between 1580 - 1620 cm^{-1}) is characteristic of solid carbonaceous system and is usually attributed to the ring vibrations in poly-nuclear condensed aromatic carbon structures. Contributions can also occur in this region from attenuated carbonyl vibrations of compounds in which intramolecular H-bonding bridge formation takes place between the -OH and the -C=O group, e.g.,

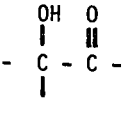

The bands at 1440 and 1380 cm^{-1} correspond respectively to the presence of CH_2 and CH_3 groups (C-H bonding vibrations). Aromatic structures (C-H in-plane bending) can also contribute to 1440 cm^{-1} band. The 1250 cm^{-1} band can be assigned to the C-O-C ether group. The bands at 910, 800 and 750 cm^{-1} are difficult to assign but are believed to arise from

minerals in the coal samples and out-of-plane C-H bending in aromatic structures. The most notable observations from a comparison of the i.r. spectra of: (1) lignite contacted with NaOH but not electrolysed, (2) residual lignite particles after electrolysis at 3.1 V vs. SCE and (3) of the humic acid - like products formed from the coal and later precipitated from the electrolyte is the large intensity in the 1700 cm^{-1} region (carbonyl band) for the dissolved residue compared to much lower intensities for both the residual lignite particles and the parent lignite. This indicates that the oxidised portion of the coal gets dissolved from the coal particles into the basic electrolyte. The 1700 cm^{-1} band is also enhanced for the solid residue after electrolysis but not nearly as much as for the soluble residue. The insoluble solid residues from electrolysed lignite were also Soxhlet extracted with an equivolumetric mixture of benzene and ethanol(16). The i.r. spectra of these residual solids after extraction showed greater oxygen functionality than the corresponding solids remaining after the parent lignite was extracted in the same way.

Using the 1580 - 1620 cm^{-1} band as an internal standard representative of the aromatic portion of the coal, the I_{1700}/I_{1600} intensity ratio gives a qualitative measure of the extent of the carbonyl functionality in the coal. The intensity ratio I_{1380}/I_{1600} and, to some extent the I_{1440}/I_{1600} ratio, are indicative of the content of alkane groups(15). Figures 3 and 4 show the variation of these intensity ratios of the solid residue after electrolysis as a function of electrode potential. The curve for the I_{1700}/I_{1600} ratio suggests that the oxygen content increases with an increase in the electrode potential, reaches a maximum due to the formation of carbonyl groups and then declines with further increase in potential. The later decrease in the ratio could be attributed to the dissolution of carboxylic material in NaOH where it reacts via Kolbe's mechanism to form CO_2; Figure 5 shows a monotonic dependence of CO_2 production on the applied electrode potential. The variation of the I_{1380}/I_{1600}, and I_{1440}/I_{1600} ratios with the electrode potential permit speculation that at the lower potentials the soluble products that dissolve away from the solid particles are more aromatic than the lignite; this dissolution process then leaves behind solid particles, the surfaces of which get relatively higher in alkane concentrations as the electrode potential increases. Increase of electrode potential beyond the maxima of Figures 3 and 4 may cause additional oxidation of the surface alkane groups to soluble products or CO_2, thereby reducing the relative alkane intensity observed at higher potentials.

CONCLUSIONS

The nature of coal oxidation products is a strong function of the applied elctrode potential. As the oxidising power is increased, oxygen containing functional groups are formed on the surface of coal, however, a further increase in the electrode potential results in formation of alkali - soluble carboxylic groups leaving behind an oxygen - poor reacted coal particle. The research work to date suggests that by selectively controlling the electrode potential, desirable coal oxidation products may be obtained.

ACKNOWLEDGEMENTS

We gratefully acknowledge the help of Dr. J. D. Freihaut of United Technologies Research Center, East Hartford, Connecticut for his help in preparing FTIR spectra of various coal samples. The financial support for this research was provided by the Coal Technology Labs at Southern Illinois University and the U. S. Dept. of Energy.

REFERENCES

1. Beer Sohne, C. F., D.R.P., 380, 387 (1923).

2. Lynch, C. S. and Collett, A. R., Fuel, 11, 408-415 (1932).

3. Eddinger, R. T. and Demorset, D. J., Fuel, 26, 157-159 (1947).

4. Belcher, R., J. Soc. Chem. Ind. Long., 67, 213, 217, 218, 265 and 267 (1948).

5. Khundkar, M. H. and Kamal, M. M., Fuel, 45, 9-15 (1966).

6. Senftle, F. E., Keith, M. P. and Irvin, H., Fuel, 60 (1981).

7. Lalvani, S. B., "Electrochemical Oxidation of Coal in Aqueous Electrolytes," Ph. D. Dissertation, University of Connecticut, August 1982.

8. Kikharenko, T. A., Solid Fuel Chemistry, Vol.10, No. 3 (1977).

9. Steelink, C., J. Chem. Ed., Vol. 40, No. 7 (1963).

10. Chakrabartty, S. J., ACS: Div. of Fuel Chemistry, Vol. 26, No. 1 (1981).

11. Montgomery, R. S. and Holly, E. D., Fuel, 36, 63, 493 (1957).

14. Montgomery, R. S. and Holly, E. D., Fuel, 37, 181 (1958).

13. Jensen, E. J., Melnyk, N., Wood, J. C. and Berkowitz, N., Adv. Chem. Ser. 55, 621 (1966).

14. Deno, N. C., Greigter, B. A. and Stroud, S. G., Fuel, 57, 455 (1978).

15. Bouwman, R. and Feriks, I. L. C., Fuel, 58 (1979).

16. Lalvani, S. B. and Coughlin, R. W., "Solubility Enhancement of Electrolysed Coal," Fuel processing Technology, 11, 37-46, 1985.

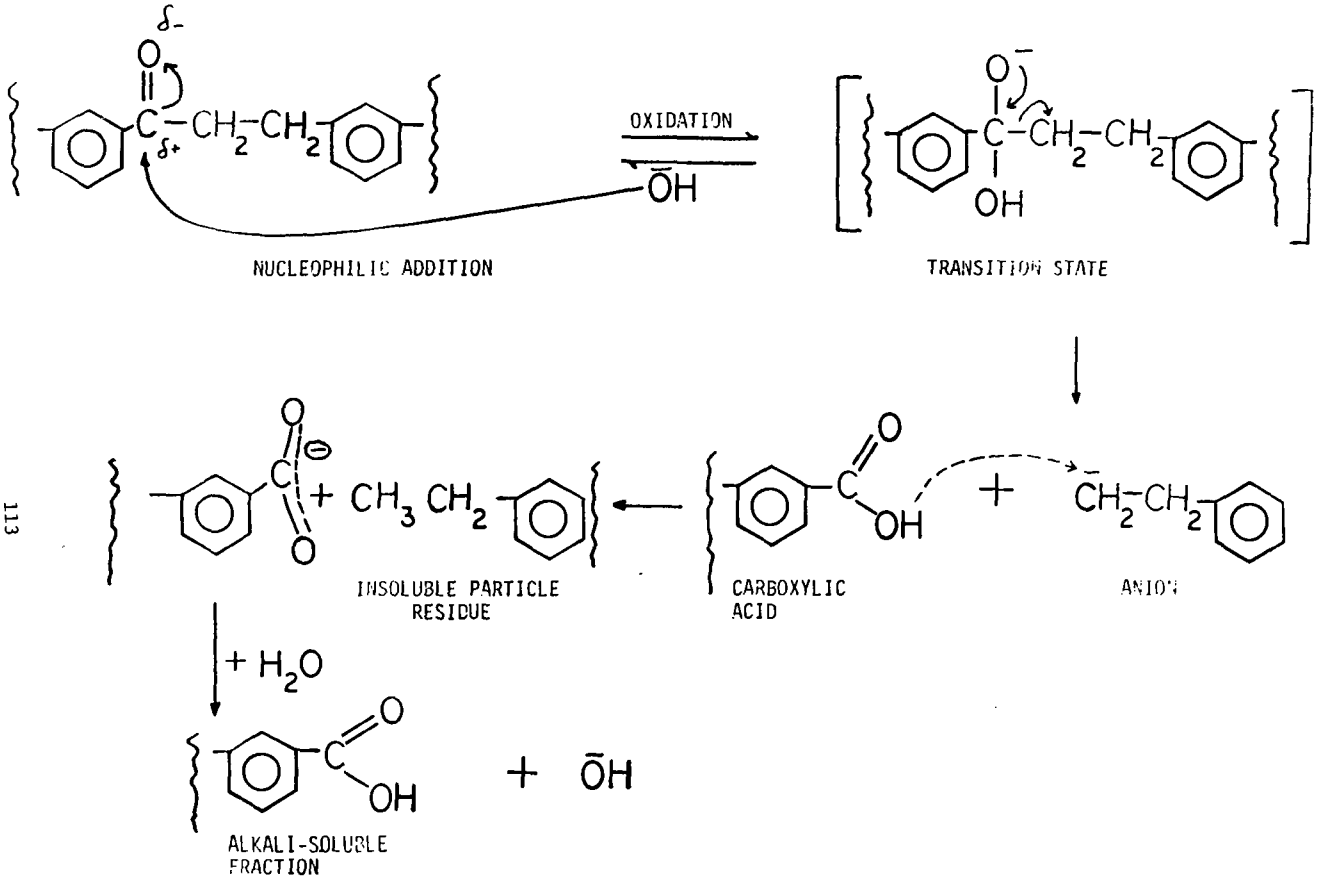

Figure 1. A proposed overall mechanism for coal oxidation.

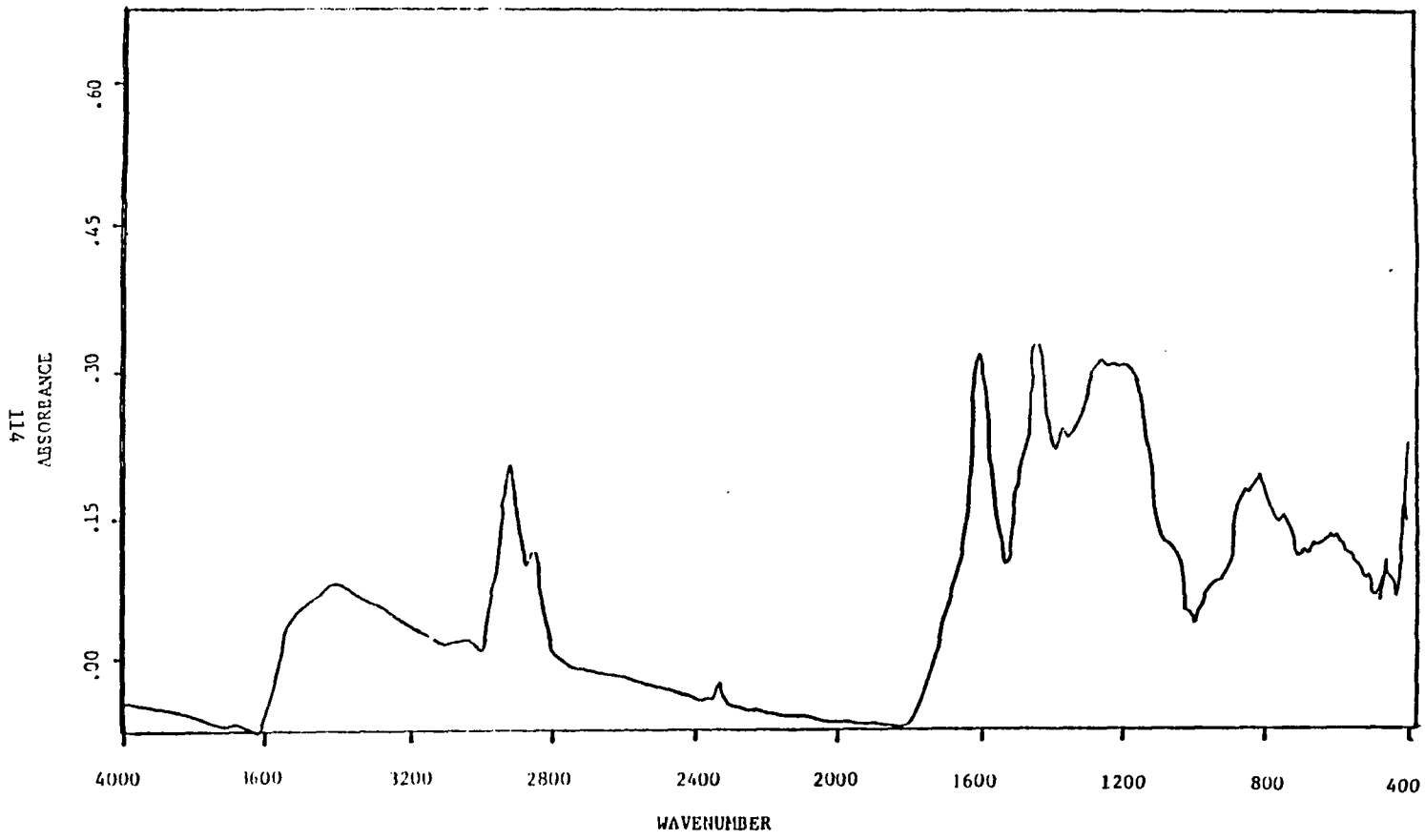

Figure 2. FTIR spectrum of virgin NDL coal.

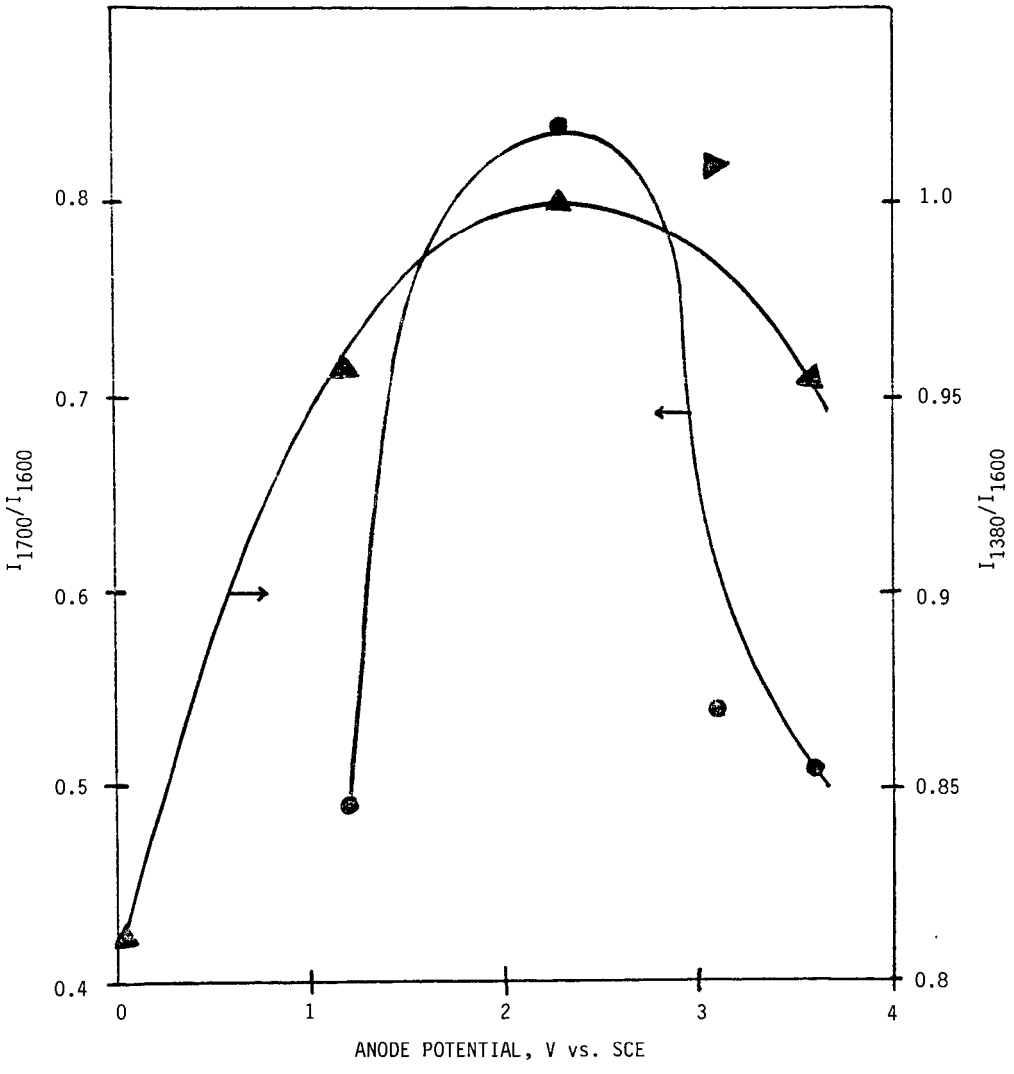

Figure 3. FTIR band intensity ratios of insoluble lignite residues as a function of electrode potential. Experimental conditions as in Table 1.

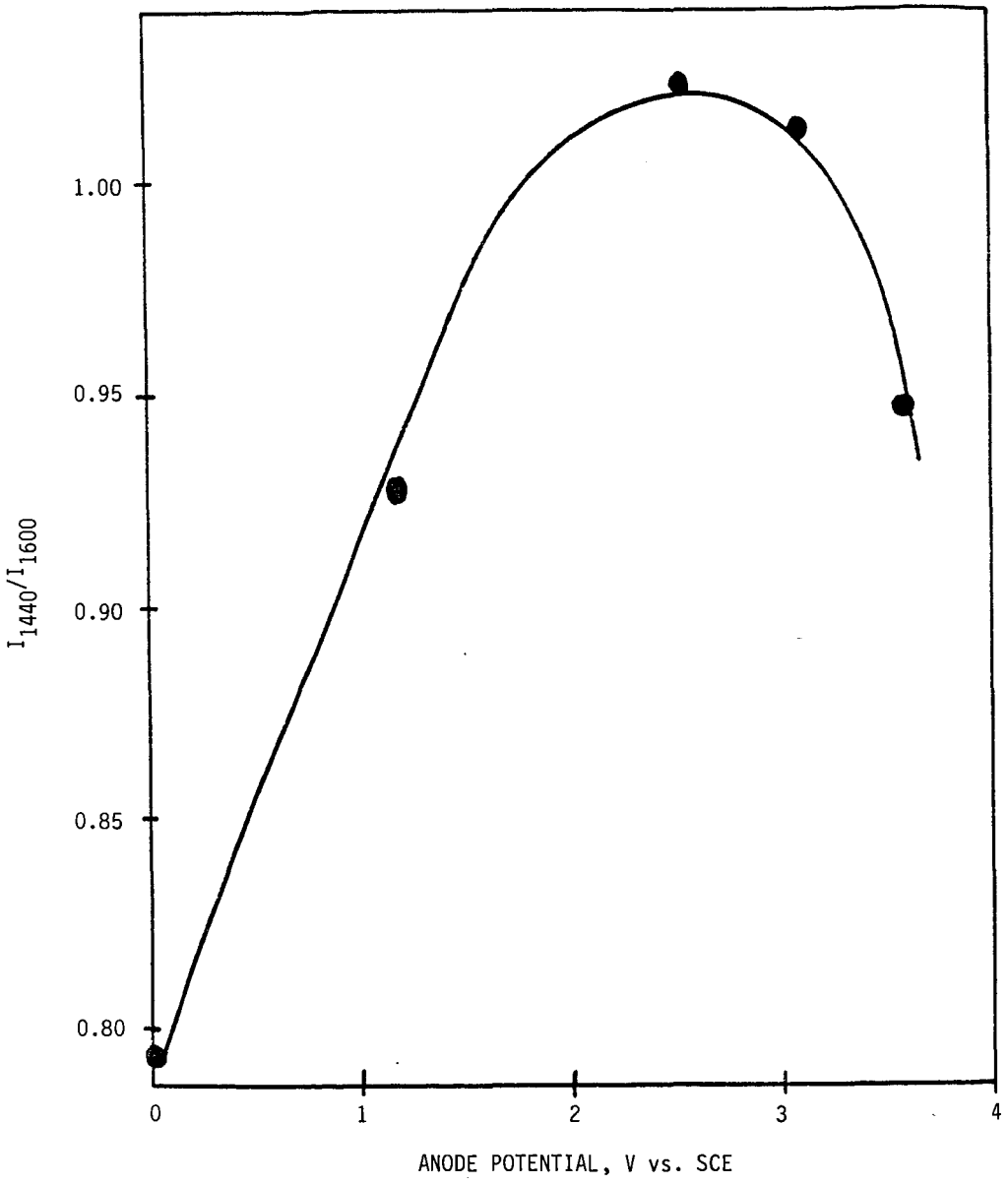

Figure 4. FTIR band intensity ratios of insoluble lignite residues as a function of electrode potential. Experimental conditions as in Table 1.

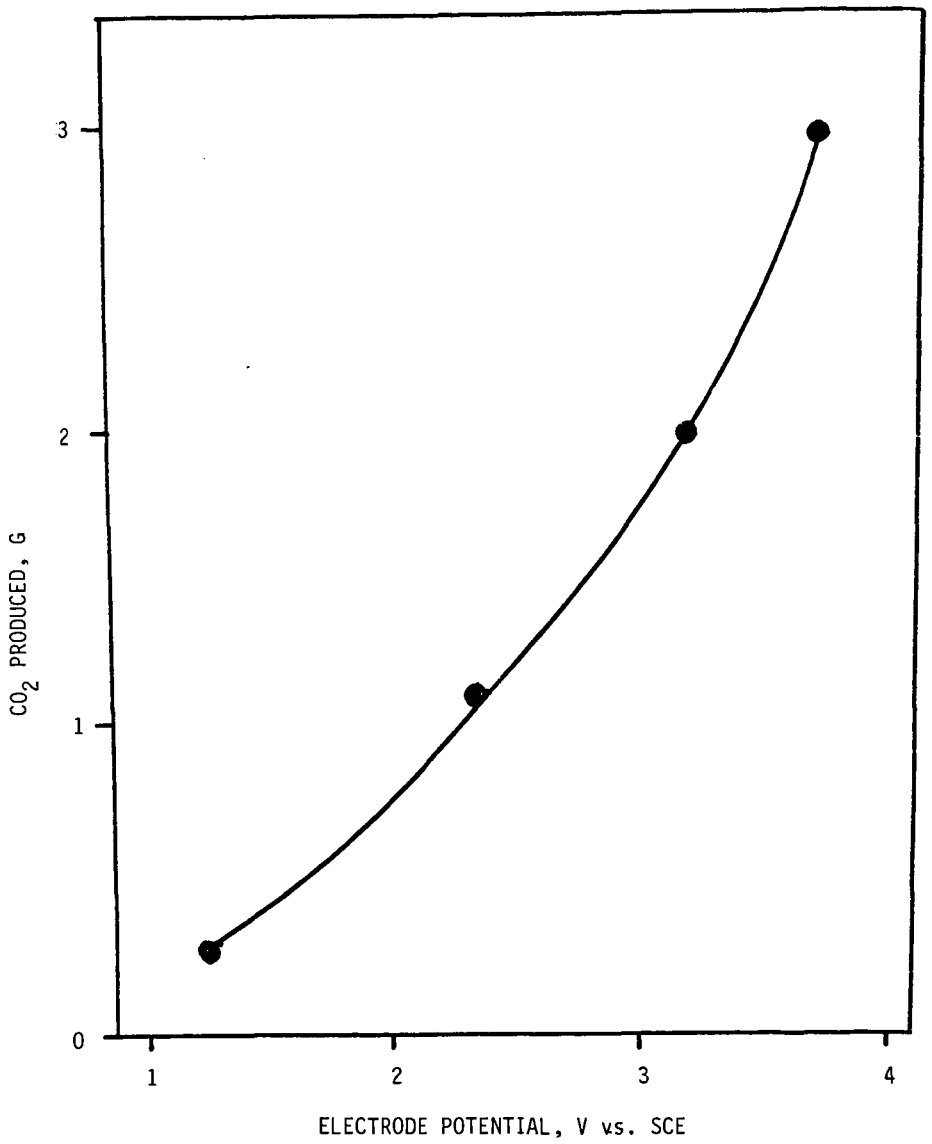

Figure 5. Influence of potential on amount of CO_2 liberated after acidificaiton of electrolyte. Experimental conditions as in Table 1.

EXPLOSIBILITY OF VICTORIAN BROWN COAL DUST

F WOSKOBOENKO

STATE ELECTRICITY COMMISSION OF VICTORIA
HOWARD STREET, RICHMOND, 3121, VICTORIA, AUSTRALIA

ABSTRACT

The explosibility of Victorian brown coal dusts has been investigated in a wide range of equipment, including the 1.2 dm^3 Hartmann bomb and the 20 litre spherical bomb. The Hartmann bomb seriously underestimates the severity of brown coal dust explosions and empirical relations between Hartmann bomb and Spherical bomb results cited in the literature are not valid for brown coal. Explosibility increases with decreasing moisture content and particle size and increases with increasing volatile matter content.

1 INTRODUCTION

Dust explosions can occur in any industry that handles fine-particulate combustible material and the coal industry is no exception. In the period 1972 to 1977 there were 39 major coal mine explosions throughout the world and these caused 1901 deaths (1).

In Victoria, Australia, brown coal is mined at a rate of about 38 million tonnes per annum, about 90% of this is used to generate power and about 10% is briquetted. There have been many examples of minor brown coal dust explosions (2), fortunately, so far there has been only one fatality.

For a dust explosion to occur the following conditions must prevail:

- The dust must be combustible and be suspended in an atmosphere capable of supporting flame.
- The dust must have a particle size distribution capable of propagating flame.
- The concentration of dust must be within its explosible range.
- An ignition source of sufficient energy to initiate flame propagation must be present.

The only explosibility work previously reported for Victorian brown coal was carried out by Allardice (3) who used a modified Hartmann apparatus (1.2 dm^3 bomb). This work was of a preliminary nature and was necessarily limited in scope. More importantly, it has since been demonstrated that small explosibility-testing apparatus, such as the Hartmann bomb, significantly underestimate explosion severity (4). Therefore, this investigation was undertaken to obtain sufficient quantitative explosibility data to design and operate plant for handling Victorian brown coal.

2 EXPERIMENTAL

A wide range of explosibility tests were carried out on dusts prepared from Morwell run-of-mine coal and the two extremes in coal type from the Yallourn field, viz.,

Yallourn pale and dark lithotypes. Air-dry samples were exhaustively ground to yield dust at least as fine as that which accumulates on ledges in coal preparation plant. Standard SECV procedures were employed to obtain complete proximate, ultimate, minerals-inorganics, physico-chemical and particle size analyses for all dust samples. Some of the key analytical data are shown in Table 1, whilst complete analyses are available elsewhere (2).

The apparatus used in the explosibility tests included : 1.2 dm^3 vertical tube (VT), modified Godbert-Greenwald furnace (GGF), 1.2 dm^3 Hartmann bomb (HB) and 20 dm^3 spherical bomb (SB) (Figure 1).

The explosibility parameters measured and the apparatus used were : Tmin - minimum ignition temperature (GGF), Emin - minimum ignition energy (VT), Cmax - maximum explosible concentration (SB), $[O_2]$lim - limiting oxygen concentration to prevent ignition (VT), Pmax - maximum explosion pressure (HB and SB) and (dP/dt)max - maximum rate of pressure rise (HB and SB). Most of these parameters are self explanatory, however, full details of the apparatus, procedures and parameter definitions are available in the literature (2, 5, 6). Many of the pressure rise tests were carried out both in the HB and SB in order to establish whether for brown coal there is a quantitative relationship between the results obtained from these bombs.

3 RESULTS AND DISCUSSION

The two parameters used to measure explosion severity (Pmax and (dP/dt)max) are readily obtained from a preasure-time curve as in Figure 2. The bulk of the results of this investigation are discussed in terms of these two parameters and the explosibility dust constant (K_{St}).

3.1 Explosibility Dust Constant

From extensive gas and dust cloud explosibility tests carried out in vessels ranging in volume from 1 x 10^{-3} to 60 m^3, Bartknecht (4) has shown that, provided conditions such as concentration, pressure and ignition characteristics remain constant, as the volume of the bomb increases the maximum explosion pressure is essentially constant, but the maximum rate of pressure rise is related to bomb volume by the following equation:

$$(dP/dt)max.V^{1/3} = K_{St} \qquad 1)$$

where V = volume of vessel (m^3)
K_{St} = explosibility dust constant ($bar.m.s^{-1}$)

Equation 1 is known as the cube-root law and it applies to spherical vessels that have a capacity of at least 16 dm^3 and a strong ignition source. The German dust explosibility classification system is based on K_{St} values as follows:

K_{St} ($bar.m.s^{-1}$)	Duat Explosion Class (St)	
0	St 0	Non-explosive
0 - 200	St 1	Explosive
200 - 300	St 2	Strongly explosive
> 300	St 3	Extremely explosive

3.2 The Model

A quantitative model of the combustion process in a brown coal dust explosion is beyond the scope of this study. However, the following simplified sequence of events in a coal dust explosion, which is based on a model proposed by Hertzberg (7, 10), will be used to rationalise the results obtained in this study:

- Removal of adsorbed water from surface.
- Devolatilisation of the particle.
- Mixing of volatiles with air.
- Combustion of air/volatile mixture.
- Oxidation of char substrate.

The processes which quench propogation are a complex combination of convective, conductive and radiative heat transfer from the burnt products to the unburnt particles and the surrounding gases.

3.3 The Effect of Coal Dust Concentration on Explosibility

Dust/air mixtures, like gas/air mixtures, are only explosible within a certain concentration range, i.e. there is a minimum and a maximum explosible concentration. The values of the explosibility limits for a dust depend mainly on its chemical composition, but also on the particle size distribution, ignition energy, moisture content and particle structure - porosity, surface area and shape. The effect of dust concentration on Pmax and (dP/dt)max for air-dry Morwell coal is shown in Figure 3.

At concentrations below Cmin, the heat liberated from the combustion of the particles near the ignition source is not sufficient to ignite adjacent particles; consequently flame propagation does not occur. For the dusts tested, Cmin ranged between 0.09 and 0.20 kg m^{-3} for the pale (60% volatiles) and dark (51% volatiles) lithotypes respectively (Table 3). Once the dust concentration exceeds Cmin, flame propagation is favoured and the flame speed increases with coal dust concentration (Figure 3). The explosion severity peaks at a dust concentration (Cex) of 0.50 kg m^{-3}. The stoichiometric ratios of total fuel/oxygen and volatile matter*/ oxygen are 0.15 and 0.20 kg m^{-3} respectively, i.e. a significant quantity of fuel is not consumed in the explosion. With gas mixtures, which are homogeneous at a molecular level, the explosion severity peaks at the stoichiometric ratio. However, for the two phase dust dispersions the rate of oxidation is limited by the rate at which the particles are heated and devolatilised, thus Cex occurs at a concentration above the stoichiometric ratio.

At fuel concentrations above Cex the severity of the explosion decreases since the excess fuel acts as a heat sink and reduces the maximum temperature rise. The quenching effect of the excess fuel increases as the dust concentration increases until at the upper explosible limit no flame propagation occurs. In practice it is very difficult to measure Cmax owing to the difficulty of obtaining a uniform, dust concentration throughout the vessel. Agglomeration of the dust inhibits dispersion, whilst turbulence results in concentration stratification (9). Therefore, the upper explosibility limit should be regarded as a guide to Cmax and not an absolute measurement. For air-dry Morwell coal Cmax was found to be 7.0 kg m^{-3}, whilst the zero moisture coal was still explosible at the maximum concentration achievable in the apparatus (10 kg m^{-3}).

---

* For rapid heating rates ($\sim 10^4$ °C s^{-1}), such as these experienced in a dust explosion, Victorian brown coal produces about 70% volatile matter (8).

3.4 Ignition of Brown Coal Dust Clouds

Ignition and flame propagation in a dust cloud may take place if the temperature of the cloud is raised above Tmin or if there is a local input of high energy, for example a spark with an energy greater than Emin. For air-dry Morwell coal Tmin and Emin were determined to be 390°C and 50 mJ respectively.

Since explosibility is dependent upon the type of ignition source and its energy the HB tests were carried out with high energy spark ignition ($\sim$ 10 J) and hot coil ignition. The results shown in Figure 4 are typical for the HB tests; it is clear that within the experimental scatter the two types of ignition yield the same results. With the SB two 5 KJ chemical igniters were used since it has been demonstrated that this yields the same results as high energy spark ignition (4).

A technique commonly employed in industry to prevent dust cloud ignition is gas inertion. With brown coal this may be achieved by the introduction of N_2 or CO_2 or by self-inertion in a sealed silo. For Morwell air-dry coal $[O_2]$lim is 13% Vol.

3.5 The Effects of Moisture Content, Particle Size

It is clearly established from the literature that explosibility increases as the dust particle size or moisture content decreases. These tests were carried out with ultrafine dust, mass-median diameters (Dm) of 13 and 21 μm, in order to obtain the data for the most hazardous industrial situation. Moisture contents were varied between the equilibrium (14% H_2O) and 0% H_2O. The results of the HB and SB explosibility tests are shown in Figure 5 and Table 3.

The following conclusions can be drawn:

- The HB seriously underestimates the severity of brown coal dust explosions. Over the moisture range tested Pmax is underestimated by 2.0 to 2.5 bar, whilst the "apparent" HB K_{St} is under-estimated by factors of 6 to 13.

- Pmax increases marginally as the moisture content decreases.

- The explosion severity increases linearly with decreasing moisture content. The transition from the explosive (St1) to the strongly explosive (St2) category occurs at about 4% moisture.

- The explosion severity increases marginally when Dm is reduced from 21.4 to 13.2 μm, i.e. for these very small particle sizes moisture content has a much greater impact on explosibility than does particle size.

The rate of devolatilisation and combustion of brown coal is dependent on the effective surface area of the dust, which in turn is dependent on particle size, porosity, moisture content and internal surface area. For these extremely fine dusts the moisture content is the dominant factor. Hertzberg (7, 10) claims that for mass-median diameters of less than 40 μm the explosibility-particle size dependence disappears and that the gas phase combustion of the volatiles is the rate controlling step. The coal moisture reduces flammability in a number of ways, it acts as a fuel dilutant and as an inertant, but more importantly it reduces the effective solid-air interfacial surface area. The dry Morwell coal has a porosity of 41% and a surface area of 213 m^2g^{-1}, however, at equilibrium moisture content the coal has an adsorbed multilayer of water which is 3-4 molecules thick, i.e. the micropores are completely water filled. Clearly this water has to be desorbed prior to devolatilisation and oxidation and will thus reduce the coal flammability.

Complete removal of the equilibrium moisture was found to increase the explosible concentration range from 0.16 - 7.0 to 0.10 - >10 kg m^{-3}. The fuel dilution effect only accounts for 0.01 kg m^{-3} of the difference in Cmin and only about 3% of the heat liberated in combustion is absorbed by the water vapour. Since the equilibrium moisture does not significantly alter the dust dispersion characteristics the major impact of the moisture is to reduce ignition sensitivity.

3.6 Effect of Bomb Size

From Equation 1 it can be seen that for vessels larger than 16 dm^3 explosion severity (dP/dt)max) decreases as the bomb size increases. Small bombs, such as the Hartmann apparatus, have a large surface area to volume ratio and there are large heat losses at the walls of the bomb. Consequently, small bombs underestimate explosion severity. The data obtained from the HB are frequently used to determine explosion relief vent areas by the vent ratio method (10). However, in recent times there have been a number of attempts to obtain a quantitative relationship between 1.2 and 20 dm^3 bomb data (e.g. References 11 and 12). The ultimate objective of such studies is to develop procedures which allow the Nomograph method of venting (11) to be applied to Hartmann bomb data. The relationship proposed in References 11 and 12 is shown in Figure 6. From this figure it can be seen that for the various moisture content Morwell coal dusts there is a linear relationship between (dP/dt)max HB and K_{St} SB, however it is clear that the more explosible brown coal dusts do not conform to the proposed (11, 12) limit.

The brown coal results show that for a single material of the same particle size the "apparent" K_{St} HB is underestimated by factors of ranging from 13 to 6 as the moisture content decreases (i.e. as the explosibility increases). However, at this stage, there is insufficient brown coal data to establish a reliable correlation between SB and HB results. These brown coal results highlight the fact that there is no one simple correlation between 1.2 and 20 dm^3 bomb results for dusts of different chemical or physical composition. It should be stressed that the proposed St1 explosibility limit based on the Hartmann data (11, 12) are not valid for Victorian brown coal. Moreover, extrapolation of the brown coal data shown in Figure 6 suggests that a more explosible brown coal (e.g. zero moisture pale lithotype) may in actual fact fall into the upper St2 or lower St3 range and yet the proposed HB limit could classify such a dust as St1; an incorrect classification such as this could have catastrophic consequences in an industrial application.

3.7 Effect of Coal Type

Owing to differences in hardness, porosity, and equilibrium moisture content (Table 1) it was not possible, or desirable, to test the different air-dry coal types at precisely the same conditions. Despite the above differences it was found that the differences in the explosibility parameters were too large to be attributed to the effects of moisture and particle size alone. In terms of each of the parameters Cmin, Pmax, (dP/dt)max and K_{St}, the explosibility increased going from dark lithotype to ROM to pale lithotype coal. This trend can be attributed to a combination of physico-chemical factors, however, the major factor is high liptinite content of the pale lithotype. The liptinite content of the pale and dark lithotypes is 26.4 and 2.2% respectively, consequently the pale lithotype coal has a high volatile matter content and specific energy (Table 2). Furthermore, although the dark lithotype coal has the highest surface area, it has the lowest porosity and the highest equilibrium moisture content. This increase in explosibility with increasing volatile matter content is consistent with the literature (e.g. 13) and this is the keystone to many of the postulated dust

explosibility models. In these models (e.g. 7, 10) it is presumed that only the volatile matter is consumed in an explosion and that the role of the less reactive material, the char, is that of a heat sink. Such models fail to recognise the importance of the phyaical structure of the particle. The physical structure of the coal has two main effects on combustion. Firstly, the rate of devolatilisation, and ultimately the rate of combustion, is dependent upon the pore size distribution of the coal. For example, combustion ignition tests on single particles of brown coal have shown that for a single coal sample the ignition time is inversely related to porosity (14). Secondly, the reactivity of the char substrate to direct oxidation increases markedly as the porosity or surface area increases. For example, both the brown coal char and anthracite listed in Table 3 are essentially composed of carbon (> 90% C, ∿ 1% volatiles) and yet in all respects the char is much more explosible. The reactivity of the char is much higher than that of the anthracite because of its higher porosity (∿ 40% cf 10%) and surface area (∿ 600 cf 400). It is therefore not unreasonable to suppose that oxidation of the char is the initial flame front may contribute to the explosibility of brown coal. However, this has yet to be experimentally verified. It is concluded that the explosibility of brown coal increases as the porosity increases due to the enhanced rate of volatile release and the possibility of an increase in the rate of oxidation of the resulting char in the flame front.

3.8 Hazard Rating of Victorian Brown Coals

The explosibility parameters for a wide range of coal based dusts are as given in Table 3, the dusts have been ranked in terms of their explosibility dust constants K_{St} or their Hartmann (dP/dt)max values. In terms of these explosion severity parameters the Victorian brown coal dusts are the most hazardous of the dusts listed.

The US Bureau of Mines has developed a series of empirical explosibility indices based on the explosibility parameters of Standard Pittsburgh Coal (SPC) (Table 3). These indices take into account both ignition sensitivity and explosion severity. The indices enable qualitative comparisons of explosibility hazards to be made, however, they are limited in their usefulness since they are based on HB data. The indices for air-dry Morwell and Yallourn pale lithotype* coal are given below.

	MORWELL ROM	YALLOURN PALE LITHOTYPE
Ignition sensitivity	Weak	Moderate
Explosion severity	Moderate	Severe
Explosibility index	Moderate	Moderate

It is concluded that at equilibrium moisture content Morwell brown coal is at least as hazardous as SPC and German brown coals, whilst the pale lithotype or oven dried coals are significantly more hazardous than SPC.

ACKNOWLEDGEMENTS

All the explosibility tests were carried out at the Fire Research Station, Borehamwood, Hertfordshire, UK, under the supervision of Messrs A R Abrahamsen and P Field. This paper is published with the permission of the SECV.

---

* Emin and Tmin assumed to be the same as that for Morwell coal.

REFERENCES

1 Reinke, D. K., and Meerbach, H., Gluckauf and Translation, 117, No 12, 324 (1981).

2 Woskoboenko, F., Research and Development Department Report No SC/86/105, State Electricity Commission of Victoria, Australia (1986).

3 Allardice, D. J., Planning and Investigations Department Report No 292, State Electricity Commission of Victoria, Australia (1974).

4 Bartknecht, W., Explosions - Course and Prevention, Springer-Verlag, Berlin, Ch 2 (1981).

5 Field, P., Dust Explosions, Elsevier, Amsterdam (1982).

6 Field, P., Explosibility Assessment of Industrial Powders and Dusts, HMSO, London (1983).

7 Hertzberg, M., Cashdollar, K. L., Ng, D. L., and Conti, R. S., Proc. 19th Symposium (International) on Combustion, 1169 (1982).

8 Brockway, D. J., and Stacy, W. O., Research and Development Department Report No SO/82/53, State Electricity Commission of Victoria, Australia (1982).

9 Deguingand, B., and Galant, S., Proc. 18th Symposium (International) on Combustion, 705 (1980).

10 Hertzberb, M., Cashdollar, K. L., and Lazzara, C. P., Proc. 18th Symposium (International) on Combustion, 717 (1981).

11 United States, ANSI/NFPA 68, National Fire Protection Association, Batterymarch Park, Quincy, MA, USA (1978).

12 Abrahamsen, A. R., and Field, P., Proc. Solidex 84, Harrogate, UK, C-97 (1984).

13 Nagy, J., and Verakis, H. C., Development and Control of Dust Explosions, Marcel Dekker, NY, Ch 4 (1983).

14 Woskoboenko, F., and Stacy, W. O., Proc. International Coal Science Conference, Sydney, Australia, p 505 (1985).

15 Kuhnen, G., Beck, H., Glienke, N., Scholl, E. W., Reeh, D., Wiemann, W., and Faber, M., "Brenn-und Explosions - KenngroBen von Stauben". Hauptverband der gewerblichen Berufsgenossens chaften eV, Bonn (1980).

16 Nagy, J., Dorsett, H. G., and Cooper, A. R., US Bureau of Mines Report No RI 6597 (1965).

TABLE 1 : EXTRACT OF PHYSICO-CHEMICAL ANALYSES

Sample Designation	EMC	Dm (μm)	Ash (% d.b.)	HI	P (% Vol)	S (m^2/g)	I
Morwell - ROM (1)	14.1	21.7	2.8	113	40.9	213	1.3
Yallourn - PL	11.4	19.5	1.4	97	50.1	175	1.5
Yallourn - DL	14.8	36.4	0.9	47	35.8	304	3.9

EMC - Equilibrium moisture content, HI - Hardgrove index, P - Total porosity, S - Surface area, I - Ignition index, ROM (1) - Morwell Run Of Mine Coal Sample 1, PL - Pale Lithotype, DL - Dark Lithotype.

TABLE 2 : EXTRACT OF CHEMICAL ANALYSES (DRY MINERAL AND INORGANIC FREE BASIS)

Sample Designation	Volatile Matter (%)	Specific Energy (MJ/kg)	C	H	So	N	O
Morwell - ROM (1)	49.5	27.6	69.9	5.0	0.28	0.66	24.2
Yallourn - PL	59.7	28.8	70.2	6.0	0.25	0.51	23.0
Yallourn - DL	50.6	26.7	68.2	4.8	0.25	0.49	26.3

So - organic sulphur.

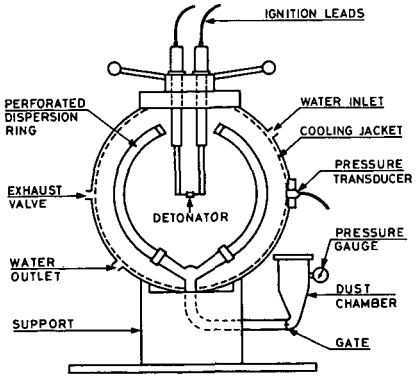

Figure 1 - Twenty litre spherical bomb.

TABLE 3 : SUMMARY OF COAL EXPLOSIBILITY RESULTS

Coal Classification	% H_2O	Dm (μm) or %<x μm	Bomb Size (dm^3)	Cmin ($kg\ m^{-3}$)	Tmin (°C)	Emin (mJ)	$[O_2]$lim % Vol	Pmax (bar)	$(dP/dt)max$ ($bar.s^{-1}$)	¶ K_{St} $bar.m\ s^{-1}$	Ref No
Morwell brown coal	0	22	20 1.2	$1.0x10^{-1}$	-	-	-	7.62 5.82	812 351	220 NA	PS PS
Yallourn pale	11.4	19.5	1.2	$9.0x10^{-2}$	-	-	-	5.61	225	NA	PS
Morwell brown#	14.1	22	20 1.2	$1.6x10^{-1}$	390	190	13	7.47 5.19	598 167	162	PS PS
Peat	15	58	$1x10^3$	$6.0x10^{-2}$	480	-	-	10.9	157	157	15
Standard Pittsburgh Coal, 37% Volatiles	2.0	100% < 74 μm	1.2	$5.5x10^{-2}$	610	60	-	5.7	159	NA	16
Brown coal	∿10*	32	$1x10^3$	$6.0x10^{-2}$	380	-	-	10.0	151	151	15
Brown coal 5% Ash, 44% Volatiles	11	57% < 90 μm	$1x10^3$	$6.0x10^{-2}$	450	-	12	9.0	150	150	15
Bituminous/ coking coal	-	24	$1x10^3$	$6.0x10^{-2}$	590	-	∿14	9.2	129	129	15
Yallourn dark lithotype	14.8	36.4	20 1.2	$2.0x10^{-1}$	-	-	-	6.67 4.95	337 69	91 NA	PS PS
Brown-coal char	∿2*	16	$1x10^3$	$3.0x10^{-2}$	680	-	-	8.4	64	64	15
Anthracite	-	30	$1x10^3$	$2.0x10^{-1}$	710	-	-	0.6	<1	1	15

¶ - coals listed in order of decreasing explosion severity; # - more hazardous result of two series of tests cited; * - moisture contents not given in original reference approximate values estimated; NA - not applicable to 1.2 dm^3 bomb data; PS - present study.

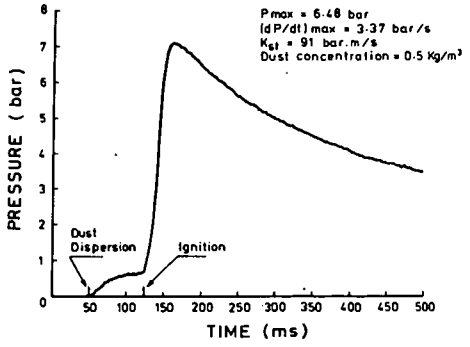

Figure 2 - Typical pressure-time curve for Yallourn dark lithotype coal dust.

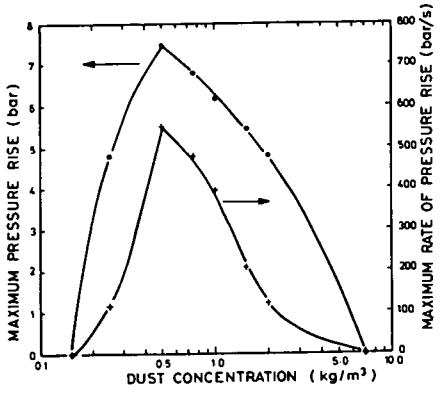

Figure 3 - The dependence of explosibility on coal dust concentration.

(Morwell air-dry coal, Dm = 21.4 μm, 20 dm^3 bomb data.)

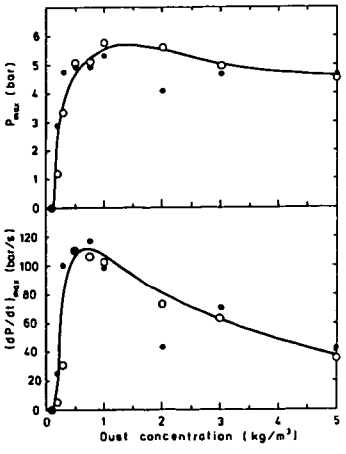

Figure 4 - The effect of ignition source on dust explosibility. (Air-dry Morwell coal, 1.2 dm^3 bomb.)

o spark ignition
● hot coil ignition

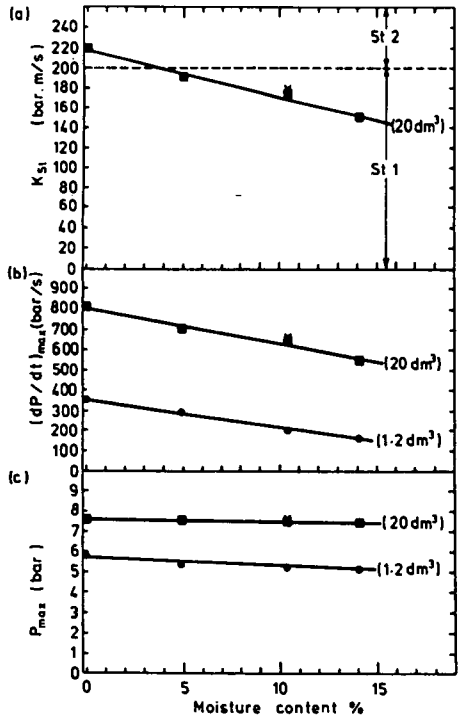

Figure 5 - The effect of moisture content on the explosibility of Morwell coal dust.

- o Dm = 21.4 μm, 1.2 dm³ bomb
- ■ Dm = 21.4 μm, 20 dm³ bomb
- x Dm = 13.2 μm, 20 dm³ bomb

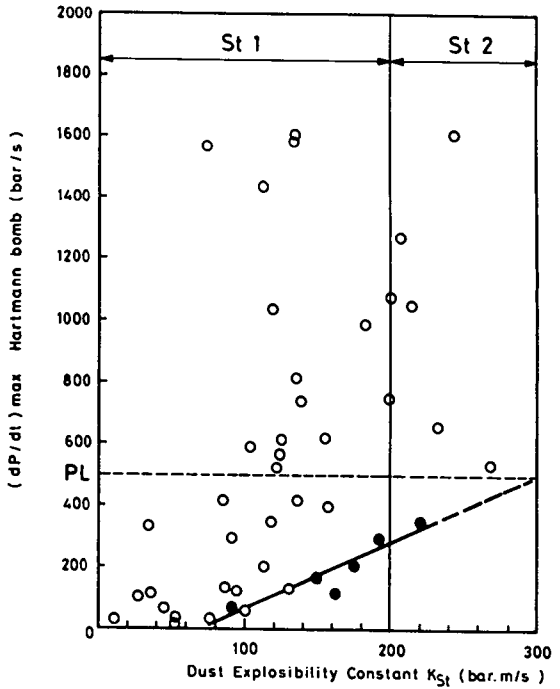

Figure 6 - Relation between SB K_{St} values and HB (dP/dt)max results.

PL Hartmann bomb St1 limit proposed in Refs 11 & 12
- • Brown coal data from present study
- o Non-coal data from Ref 12